University of Szeged

Faculty of Pharmacy

Institute of Pharmaceutical Chemistry

APPLICATION OF A NOVEL HETEROGENEOUS SILVER CATALYST FOR DIVERSE SYNTHESIS METHODS UNDER BATCH AND CONTINUOUS-FLOW CONDITIONS

Ph.D. Thesis

Rebeka Ildikó Mészáros

Supervisors:

Prof. Dr. Ferenc Fülöp

Dr. Sándor B. Ötvös

2021

† This work is dedicated to the memory of our mentor, friend and colleague, ***Prof. István Pálinkó****, who passed away a few months before the completion of this work. Many thanks for your permanent support and guidance.*

"To improve is to change; to be perfect is to change often."
Winston Churchill

† This work also dedicated to the memory of our mentor and supervisor ***Prof. Ferenc Fülöp****. I wanted to take a moment to thank you for your help, guidance and support throughout my PhD work.*

"The scientist is not a person who gives the right answers, he's one who asks the right questions."
Claude Levi-Strauss

Table of contents

List of publications and lectures

Papers related to the thesis

I. Sándor B. Ötvös, Rebeka Mészáros, Gábor Varga, Marianna Kocsis, Zoltán Kónya, Ákos Kukovecz, Péter Pusztai, Pál Sipos, István Pálinkó, Ferenc Fülöp
A mineralogically-inspired silver–bismuth hybrid material: an efficient heterogeneous catalyst for the direct synthesis of nitriles from terminal alkynes
Green Chemistry, **2018**, *20*, 1007-1019. IF.: 9.405

II. Rebeka Mészáros, Sándor B. Ötvös, Gábor Varga, Éva Böszörményi, Marianna Kocsis, Krisztina Karádi, Zoltán Kónya, Ákos Kukovecz, István Pálinkó, Ferenc Fülöp
A mineralogically-inspired silver–bismuth hybrid material: Structure, stability and application for catalytic benzyl alcohol dehydrogenations under continuous flow conditions
Molecular Catalysis, **2020**, *498*, 111263. IF.: 5.062

III. Rebeka Mészáros, András Márton, Márton Szabados, Gábor Varga, Zoltán Kónya, Ákos Kukovecz, Ferenc Fülöp, István Pálinkó, Sándor B. Ötvös
Exploiting a Silver–Bismuth Hybrid Material as Heterogeneous Noble Metal Catalyst for Decarboxylations and Decarboxylative Deuterations of Carboxylic Acids under Batch and Continuous Flow Conditions
Green Chemistry, **2021**, 23, 4685-4696. IF.: 10.182 (2020)

Other papers

IV. Sándor B. Ötvös, Ádám Georgiádes, Mónika Ádok-Sipiczki, Rebeka Mészáros, István Pálinkó, Pál Sipos, Ferenc Fülöp
A layered double hydroxide, a synthetically useful heterogeneous catalyst for azide−alkyne cycloadditions in a continuous-flow reactor
Applied Catalysis A: General, **2015**, *501*, 63–73. IF.: 4.012

V. Márton Szabados, Rebeka Mészáros, Szabolcs Erdei, Zoltán Kónya, Ákos Kukovecz, Pál Sipos, István Pálinkó
Ultrasonically-enhanced mechanochemical synthesis of CaAl-layered double

hydroxides intercalated by a variety of inorganic anions
Ultrasonics Sonochemistry, **2016**, *31*, 409–416. IF.: 4.218

VI. Rebeka Mészáros, Sándor B. Ötvös, Zoltán Kónya, Ákos Kukovecz, Pál Sipos, Ferenc Fülöp, István Pálinkó
Potential solvents in coupling reactions catalyzed by Cu(II)Fe(III)-layered double hydroxide in a continuous-flow reactor
Reaction Kinetics, Mechanisms and Catalysis, **2017**, *121*, 345–351. IF.: 1.515

VII. Sándor B. Ötvös, Ádám Georgiádes, Rebeka Mészáros, Koppány Kis, István Pálinkó, Ferenc Fülöp
Continuous-flow oxidative homocouplings without auxiliary substances: Exploiting a solid base catalyst
Journal of Catalysis, **2017**, *348*, 90-99. IF.: 6.759

VIII. Rebeka Mészáros, Bai-Jing Peng, Sándor B. Ötvös, Shyh-Chyun Yang, Ferenc Fülöp
Continuous-Flow Hydrogenation and Reductive Deuteration of Nitriles: a Simple Access to α,α-Dideutero Amines
ChemPlusChem, **2019**, *84*, 1508–1511. IF.: 2.753

Cumulative impact factor: 43.906

Scientific lectures related to the thesis

1. Mészáros Rebeka, Ötvös Sándor Balázs, Varga Gábor, Kocsis Marianna, Pálinkó István, Fülöp Ferenc:
Terminális alkinek közvetlen nitrillé alakítása újfajta heterogén ezüstkatalizátorral
Heterociklusos és Elemorganikus Kémiai Munkabizottság ülése, Balatonszemes, 2017. május 15-17.

2. Mészáros Rebeka:
Újfajta heterogén ezüst katalizátor alkalmazása terminális alkinek közvetlen nitrillé alakítására
A Szegedi Ifjú Szerves Kémikusok Támogatásáért Alapítvány tudományos előadóülése, Szeged, 2017. május 26.

3. Rebeka Mészáros, Sándor B. Ötvös, Gábor Varga, Marianna Kocsis, István Pálinkó, Ferenc Fülöp:
Characterization and a potential catalytic application of a novel silver-bismuth

composite

International Conference on Coordination and Bioinorganic Chemistry, Smolenice, Slovakia, June 4-9, 2017

4. Rebeka Mészáros, Sándor B. Ötvös, Marianna Kocsis, Gábor Varga, István Pálinkó, Ferenc Fülöp:
A novel silver-bismuth nanocomposite, an effective and reusable catalyst for nitrogenation and hydration of alkynes
18th Tetrahedron Symposium, Budapest, Hungary, June 27–30, 2017

5. Mészáros Rebeka, Ötvös Sándor Balázs, Varga Gábor, Kocsis Marianna, Pálinkó István, Fülöp Ferenc:
Hatékony heterogén ezüst katalizátor fejlesztése terminális alkinek közvetlen nitrillé alakításához
Katalízis Munkabizottsági Ülés, Szeged, 2017. december 18.

6. Mészáros Rebeka Ildikó:
Újfajta heterogén ezüst katalizátor alkalmazása terminális alkinek közvetlen nitrillé alakítására
Pillich Lajos Miniszimpózium, Budapest, 2018. február 14.

7. Mészáros Rebeka, Ötvös Sándor Balázs, Varga Gábor, Kocsis Marianna, Pálinkó István, Fülöp Ferenc:
Terminális alkinek közvetlen nitrillé alakítása újfajta heterogén ezüstkatalizátorral
Nano&Kat Nap, Budapest, 2018. május 15.

8. Mészáros Rebeka Ildikó:
Nitrilek és vinil-azidok előállítása heterogén ezüst katalizátorral szakaszos és áramlásos szintézis módszerekkel
ÚNKP előadónap - GYTK, Szeged, 2018. május 17.

9. Rebeka Mészáros, Sándor B. Ötvös, Marianna Kocsis, Gábor Varga, István Pálinkó, Ferenc Fülöp:
A silver–bismuth hybrid material, an efficient catalyst for the direct synthesis of nitriles from terminal alkynes
16th Belgian Organic Synthesis Symposium, Brussels, Belgium, July 8-13, 2018

10. Rebeka Mészáros, Sándor B. Ötvös, István Pálinkó, Ferenc Fülöp:
Application of a heterogeneous silver catalyst in dehydrogenation and multicomponent coupling reactions in a continuous-flow system
14th Pannonian International Symposium on Catalysis, 3-7. September 2018, Starý Smokovec, Slovakia

11. Mészáros Rebeka Ildikó:
Terminális alkinek közvetlen nitrillé alakítása hatékony heterogén ezüstkatalizátorral
Patonay Tamás-díj pályázat, 2019. március 13., Budapest

12. Mészáros Rebeka Ildikó:
Szelektív áramlásos kémiai szintézisek heterogén ezüst katalizátorral
GYTK ÚNKP előadóülés, 2019. május 7., Szeged

13. Rebeka Mészáros, Sándor B. Ötvös, István Pálinkó, Ferenc Fülöp:
Application of a heterogeneous silver catalyst in dehydrogenation reactions in a continuous-flow system
International Conference on Coordination and Bioinorganic Chemistry, Smolenice, Slovakia, June 2-7, 2019

14. Rebeka Mészáros, Sándor B. Ötvös, István Pálinkó, Ferenc Fülöp:
A Continuous Flow Process For Silver Catalyzed Alcohol Dehydrogenation
International 18th Blue Danube Symposium on Heterocyclic Chemistry, Ljubljana, Slovenia, September 18-21, 2019

Other scientific lectures

15. Rebeka Mészáros, Márton Szabados, Pál Sipos, István Pálinkó:
Phenolate anions intercalated into CaAl-layered double hidroxide by mechano-hydrotreatment technique combinate with ultrasonic irradiation
18th International Symposium on Intercalation Compounds, Strasbourg, France, May 31-June 4, 2015

16. Rebeka Mészáros, Sándor B. Ötvös, Zoltán Kónya, Ákos Kukovecz, Pál Sipos, Ferenc Fülöp, István Pálinkó:
Potential solvents in coupling reactions catalyzed by CuFe-layered double hydroxide in a continuous-flow reactor

13th Pannonian International Symposium on Catalysis, Siófok, Hungary, 19-23, September, 2016

17. Mészáros Rebeka, Ötvös Sándor Balázs, Pálinkó István, Fülöp Ferenc:
Nitrilek hidrogénezése és reduktív deuterálása egyszerű és fenntartható áramlásos módszerrel
MTA Gyógyszerkémiai és Gyógyszertechnológiai Szimpózium, Kecskemét, 2019. szeptember 5-6.

Abbreviations

DTBP	di-*tert*-butyl peroxide
DEAD	diethyl azodicarboxylate
^{t}BuOOH	*tert*-butyl hydroperoxide
dppm(AuBr)$_2$	bis(bromogold(I))bis(diphenylphosphino)methane
PhI(OAc)$_2$	(diacetoxyiodo)benzene
IPrAuCl	chloro[1,3-bis(2,6-diisopropylphenyl)imidazol-2-ylidene]gold(I)
DCE	1,2-dichloroethane
TMSCN	trimethylsilyl cyanide
phen	1,10-phenanthroline
Py	pyridine
bipy	2,2′-bipyridine
PPh$_3$	triphenylphosphine
BINAP	2,2′-bis(diphenylphosphino)-1,1′-binaphthyl
t-BuOCl	*tert*-butyl hypochlorite
KOtBu	potassium *tert*-butoxide
TBDMS	*tert*-butyldimethylsilyl
PANF-NHC-Ag	*N*-heterocyclic carbene stabilized silver NPs supported on polyacrylonitrile fiber
CF	continuous-flow
TMEDA	*N,N,N′,N′*-tetramethylethane-1,2-diamine
TMOF	trimethyl orthoformate
NMR	nuclear magnetic resonance
GC-MS	gas chromatography–mass spectrometry

UV/VIS/NIR	ultraviolet/visible near infrared spectroscopy
DRS	diffuse reflectance spectroscopy
ICP–AES	inductively coupled plasma atomic emission spectroscopy
XPS	X-ray photoelectron spectroscopy
AFM	atomic force microscope
BET	Brunauer-Emmett-Teller (BET) surface area analysis
SEM-EDX	scanning electron microscopy - energy dispersive X-ray analysis

1. INTRODUCTION AND AIMS

Silver-catalyzed reactions are of significant importance in organic synthesis.[1] Soluble salts are typically employed as catalyst sources in these transformations. However, silver-containing catalytic systems with efficient reusability features are scarce.[2] Importantly, silver-containing catalysts are more economical and environmentally benign than other commonly used transition metal catalysts such as platinum, palladium or gold. As concerns sustainability and simplicity, the reusability of heterogeneous silver catalysts are highly beneficial. However, in most cases, active silver species are immobilized via weak forces which, particularly under demanding reaction condition, often involves inadequate catalyst stability.[3, 4]

In our work we first synthesized a novel silver–bismuth hybrid material (AgBi-HM) as solid catalyst to apply it in different silver-catalyzed synthesis methods. Our aim was to create a solid material with structurally-bound silver catalytic centers and with the layered structure of a naturally occurring mineral. The catalyst synthesis was successfully carried out by means of urea-mediated homogeneous precipitation of the corresponding metal nitrates. Furthermore, the solid catalyst was characterized by means of various complementary techniques. After the promising catalyst synthesis, our aim was to apply the material in silver-mediated synthesis processes under batch and continuous-flow conditions. Before detailed the flow experiments, we planned to test the stability of the hybrid material in different solvents under a variety of continuous-flow conditions.

Alkynes are significant molecules in several catalytic transformations, such as diverse coupling and cyclization reactions.[5] Nitriles are effective building blocks in the synthesis of pharmaceuticals and natural products. On the other hand, most of their classical synthesis methods involve the use of hazardous reaction partners.[6, 7] Besides, alkynes can be directly converted into nitriles through a silver-mediated nitrogenation approach.[8] Our aim was to apply the prepared AgBi-HM as a solid catalyst for nitrogenation of alkynes with $TMSN_3$ as nitrogen source. During a thorough optimization procedure, we intended to explore the role of temperature and reaction time, as well as the effects of various solvents and additives. The scope of the reaction with different aliphatic and aromatic alkynes was in the focus of our experiments as well. Furthermore, we intended to examine the reusability and robustness of the catalyst, and planned an extended characterization of the used/reused catalyst.

The oxidation of diverse alcohols to their appropriate carbonyl compounds is one of the most fundamental functional group transformations in organic chemistry and it is a

conventional method in academic and industrial areas.[9, 10] On the other hand, these synthesis methods have several drawbacks. Therefore, there is a high demand for new, additive-free, simple, and environmentally benign processes in this research field. We proposed to explore a novel flow-chemistry method for the dehydrogenation of benzyl alcohols to the corresponding carbonyl compounds in the presence of the AgBi-HM catalyst. Our goal was to investigate the main reaction parameters: flow rate (residence time), temperature, and concentration of the substrate, as well as the examination of the scope of the reaction.

Carboxylic acids are inexpensive and useful starting materials for several transformations, such as protodecarboxylations and related decarboxylative couplings (formation of C–C, C–X, and C–H bonds). However, the most common catalysts for protodecarboxylations are typically homogeneous preparations (copper or silver salts, etc.) in combination with various ligands or bases.[11–13] We intended to explore the heterogeneous decarboxylation and decarboxylative deuteration method catalyzed by our heterogeneous AgBi-HM preparation under batch and flow conditions. Before the chemically intensified continuous-flow process was developed, an initial batch method was established. We intended to explore the applicability and the scope of the batch and flow methods through decarboxylations of a diverse set of aromatic and fused heteroaromatic carboxylic acids. Finally, we aimed to explore the silver-catalyzed decarboxylative deuteration using D_2O as a readily available deuterium source.

2. LITERATURE SURVEY

2.1 Syntheses catalyzed by coinage metals

Synthesis methods mediated and catalyzed by transition metals developed for decades are widely used in industry and academic research.[14–17] The coinage metals (copper, gold, and silver) are extensively applied for various organic transformations.[18–20] Silver and gold catalysis has only recently become the focus of organic chemistry. Copper chemistry, in contrast, has been studied extensively for decades. Copper is an earth-abundant metal and its chemistry is extremely diverse. The application of copper-based materials is more cost effective and they are used prolifically compared to catalysts containing precious transition metals such as rhodium, palladium or ruthenium.[21–23]

Lei and co-workers demonstrated the first copper-catalyzed oxidative alkenylation reaction of simple ethers to synthetize allylic ethers. To achieve the appropriate alkenylation products, they cross-coupled different substituted olefins and simple ethers with good yields including open-chain ethers as well.[24]

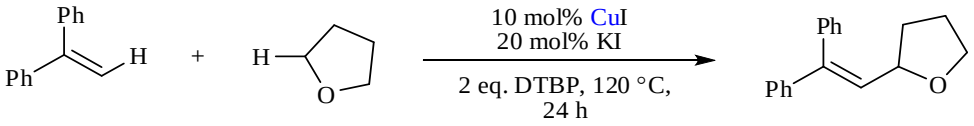

Scheme 1. *Copper-catalyzed oxidative C–H/C–H coupling between olefins and simple ethers*[24]

Zhang and co-workers reported an easy-to-handle and mild method to form propargylamines with terminal alkynes through catalytic cross-coupling of tertiary amines in the presence of copper catalyst and inexpensive/renewable calcium carbide. In the scope of the reaction, they received the corresponding propargylamines with good to excellent yields, and they also observed good results in the case of aliphatic compounds.[25]

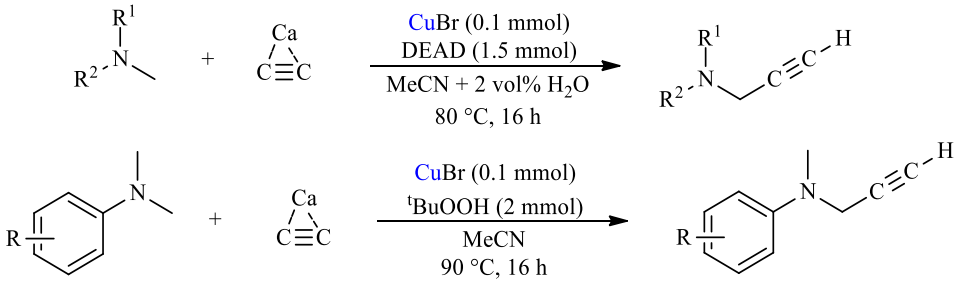

Scheme 2. *Copper-catalyzed alkynylation of tertiary amines with CaC_2 via sp^3 C–H activation*[25]

Liu and co-workers reported a copper-catalyzed general stereoconvergent Sonogashira C(sp3)–C(sp) cross-coupling reaction of a wide variety of terminal alkynes and racemic alkyl

halides in the presence of a chiral cinchona alkaloid-based P,N-ligand. This method is a potential synthetic process for the synthesis of stereoenriched functional or bioactive derivatives, natural products, and medicinal compounds possessing a range of chiral C(sp3)–C(sp/sp2/sp3) bonds.[26]

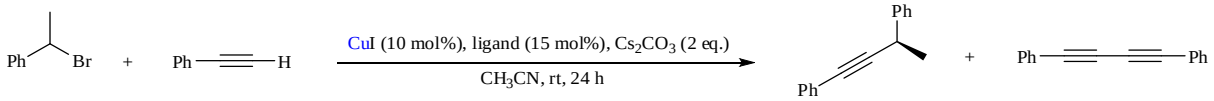

Scheme 3. *A general asymmetric copper-catalyzed Sonogashira C(sp3)–C(sp) coupling*[26]

In contrast, gold was considered to be catalytically inactive for decades. In early reports the use of gold as a catalyst did not show higher potentials than other metals.[30, 31] However, this changed when Bond and co-workers developed the hydrogenation of olefins over supported gold catalysts in 1973.[32] More than a decade later, in some studies, gold proved to be the best catalyst in contrast to previous reports, for example in the low-temperature oxidation of CO[33] or hydrochlorination of ethyne to vinyl chloride[34] (both are heterogeneous reactions). Nowadays, gold has rich organometallic and coordination chemistry,[27–29] as well as gold catalysts are widely used in various reactions[35–39] and they have important industrial applications.[40]

Shi and co-workers demonstrated the first example of a gold-catalyzed alkyne oxidative cross-coupling for the synthesis of unsymmetrical conjugated diynes. This approach is highly selective, simple, and efficient. Furthermore, it does not require the prefunctionalization of the alkyne or a large excess of one of the coupling partners compared to other literature methods. In these systems, the distinct nature of alkynes and the 1,10-phenanthroline ligand are also crucial to achieve high selectivity.[41]

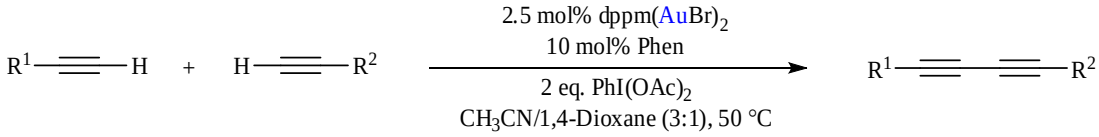

Scheme 4. *Gold-catalyzed oxidative cross-coupling of terminal alkynes*[41]

Zhao and co-workers reported a gold-catalyzed N^1-selective alkenylation reaction of 1-sulfonyl-1,2,3-triazoles with alkynes. The products were synthesized selectively in yields up to 92%. The reaction takes place in a “one-pot two-steps” manner, where the sulfonyl group of 1,2,3-triazole derivatives is transformed to alkenyl groups. This procedure provides a novel approach for the synthesis of vinyltriazoles, which are potentially bioactive building blocks.[42]

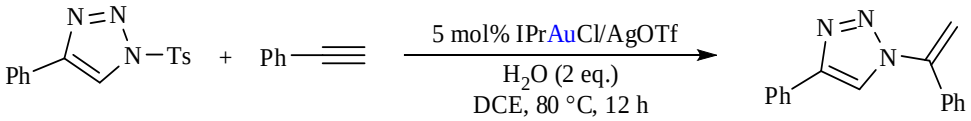

Scheme 5. *N^1-Selective alkenylation of 1-sulfonyl-1,2,3-triazoles with alkynes via gold catalysis*[42]

Cramer and co-workers demonstrated an addition reaction of *N*-hydroxyimides to terminal alkynes catalyzed by gold(I). In the scope of the reaction, they tested a wide variety of aryl-, alkenyl-, and alkyl-alkynes decorated with several functional groups including halogens, phthalimides, esters, and ethers and they also tested a range of *N*-hydroxyimides with good yields.[43]

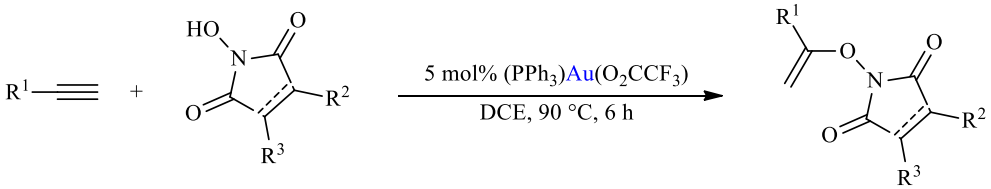

Scheme 6. *Gold-catalyzed addition of N-hydroxyimides to terminal alkynes*[43]

2.2 Silver-catalyzed syntheses

In recent decades, silver has been widely applied in numerous organic reactions. Silver-catalyzed transformations are continuously gaining larger importance not only in academic research but also in industry. This is also evidenced by the growing number of articles and reviews on this topic.[5, 44–46] The use of silver in organic chemistry can be classified into homogeneous and heterogeneous silver-mediated or catalyzed reaction areas.

2.2.1 Homogeneous catalysis

Recently, silver(I)-catalyzed reactions have become significant synthetic methods for numerous organic transformations. Homogeneous silver sources have been playing important role in catalytic transformations. In most cases, complexes or commercially available silver salts are used.

The application of silver salts as catalysts in various reactions is simple and cost-efficient and they can be used extensively in varied organic transformations with good conversion and selectivity.

Lei and co-workers developed a silver-catalyzed co-cyclization of terminal alkynes and isocyanides for the synthesis of pyrroles. In the scope of the reaction arylacetylene reactants with various substitution patterns of the aryl ring (*ortho*, *meta* or *para*) were tested in the synthesis of the corresponding products with good yields. This synthetic strategy represents an

efficient and simple protocol providing an atom-economical way for the preparation of substituted pyrroles with high selectivity and good yields.[47]

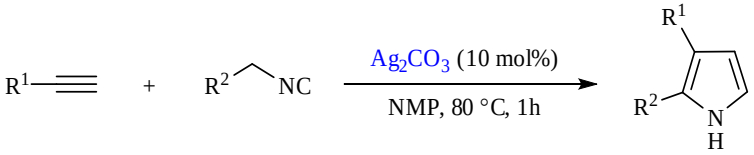

Scheme 7. *Ag_2CO_3-catalyzed cycloaddition of terminal alkynes with isocyanides*[47]

The same authors demonstrated a silver-mediated highly selective oxidative C−H/C−H functionalization of 1,3-dicarbonyl compounds with terminal alkynes for the direct synthesis of polysubstituted furans and pyrroles in a single step. In this reaction, good to excellent yields and perfect selectivity were achieved. This protocol resulted in polysubstituted furans and pyrroles from simple starting materials in an atom-economical and simple way under mild conditions.[48]

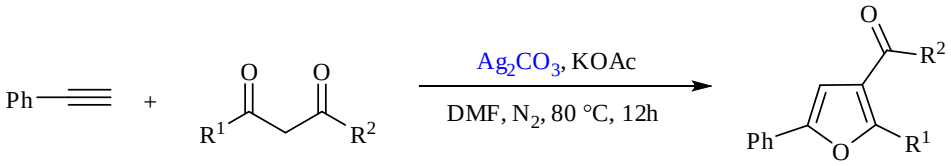

Scheme 8. *Silver-mediated oxidative C−H/C−H functionalization for the direct synthesis of polysubstituted furans*[48]

Xu and co-workers developed a new approach for the synthesis of alkyl aryl sulfides with a silver-catalyzed decarboxylative C−S cross-coupling reaction of aliphatic carboxylic acids, applying diaryl disulfides as the sulfur source and $K_2S_2O_8$ as the oxidant. This reaction was performed under mild conditions and it tolerated many functional groups.[49]

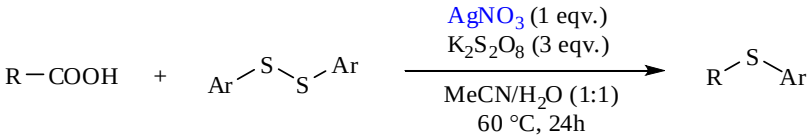

Scheme 9. *Silver-catalyzed decarboxylative C−S cross-coupling of aliphatic carboxylic acids*[49]

Ohkuma and co-workers demonstrated an Ag_2O-catalyzed reaction of TMSCN and benzylic phosphates for the synthesis of less-stable benzylic isonitriles. In the traditional silver(I)-mediated stoichiometric isocyanation reaction of benzylic halides, secondary benzylic isonitriles could not be obtained with high yield. In contrast, it became possible with this procedure. The catalytically active species was $(TMS)[Ag(CN)_2]$ formed *in situ*.[50]

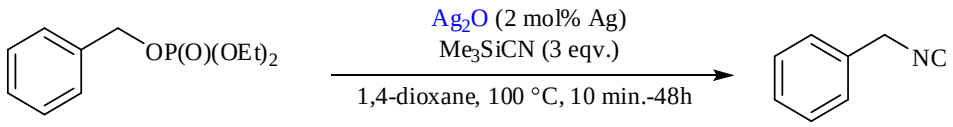

Scheme 10. *Selective formation of less-stable benzylic isonitriles catalyzed by Ag_2O*[50]

Silver-(I) complexes are used in many different catalytic transformations and reactions as catalysts. Silver complexes with P- and N-based ligands (such as phen, Py, bipy, PPh_3, BINAP) in comparison with the simple silver salts (such as AgI, Ag_2CO_3, $AgSbF_6$, AgOTf), were observed to be more active and stable species by decreasing efficiently the energy barrier for the transformations. The most commonly used complexes are *N*-heterocyclic carbene (NHC)–silver(I) preparations, chiral silver phosphates, trispyrazolylborate–silver(I), and silver complexes with P,O-type or pyridine-containing ligands.[51]

Yamamoto and co-workers developed a new catalytic enantioselective allylation reaction of aldehydes with allyltributyltin catalyzed by a BINAP silver(I) complex. They achieved appropriate yields and outstanding *ee* values in the scope of the reaction. Furthermore, catalyst synthesis could be easily performed [stirring an equimolar mixture of silver(I) triflate and (*S*)-BINAP in tetrahydrofuran (THF) solvent for 10 min at room temperature].[52]

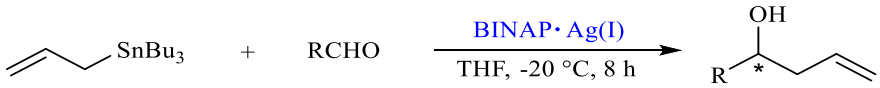

Scheme 11. *Asymmetric allylation of aldehydes induced by a chiral silver(I) complex*[52]

Helquist and co-workers described an intramolecular hydroamination reaction of a variety of primary aminoalkynes catalyzed by silver–phenanthroline complexes. The catalysts were reused for the second time without loss of catalytic activity and they proved to be cost-prohibitive and sensitive.[53]

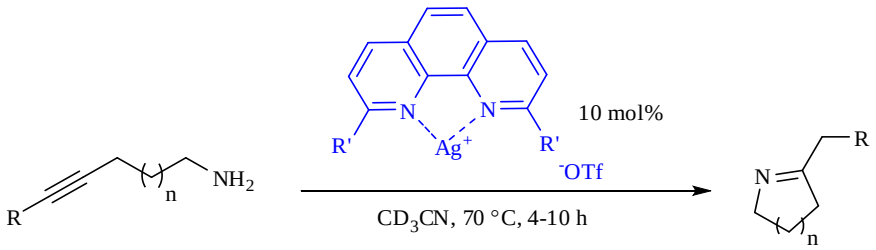

Scheme 12. *Intramolecular hydroamination of aminoalkynes catalyzed by silver-phenanthroline complex*[53]

Li and co-workers developed the first decarboxylative chlorination of aliphatic carboxylic acids with *tert*-butyl hypochlorite catalyzed by a Ag(I) complex [silver

triflate−bis(1,10-phenanthroline) complex] with high yields under mild conditions. This method has excellent functional group compatibility and it can be used generally.[54]

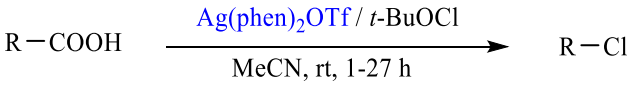

Scheme 13. *Decarboxylative chlorination of aliphatic carboxylic acids catalyzed by Ag(phen)$_2$OTf complex catalyst*[54]

In the work of Cazin and co-workers, a cationic heteroleptic bis-*N*-heterocyclic carbene silver complex was shown to promote alkynylation of ketones. This catalyst was effective in aqueous media and its activity was excellent (1 mol% of catalyst without the need of additives) under mild conditions in water solvent.[55]

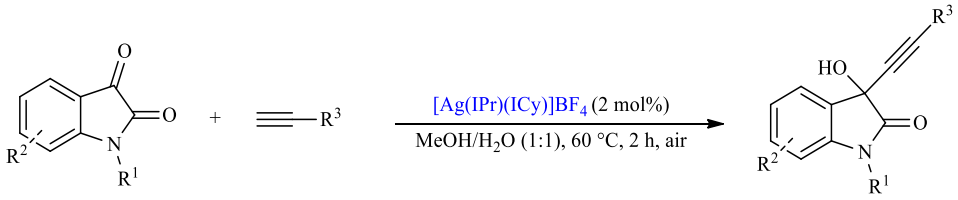

Scheme 14. *Alkynylation of ketones catalyzed by light-stable silver N-heterocyclic carbene*[55]

2.2.2 Heterogeneous catalysis

Heterogeneous catalysts containing silver play a key role in the production of potential chemical intermediates and the catalytic elimination of environmental pollutants.[56] Therefore, the development and the use of silver-containing heterogeneous catalysts are an important and rewarding task from an environmental chemistry point of view.

In recent years, nanocatalysis has become very popular, especially in the production and use of nanoparticles as catalysts.[57–59] Advantages of nanoparticle catalysts include the use of environmentally benign synthetic processes, efficiency, and selectivity as well as the recovery of the catalyst using a combination of a heterogeneous support.[60, 61] A literature survey indicates that the application of supported nanoparticles predominates amongst the heterogeneous silver-mediated synthesis methods.[62] One of the reasons is that silver nanoparticles can be immobilized in numerous ways on various surfaces, for example hydrotalcite materials,[63] silica,[64] activated charcoal,[65] alumina,[66] graphene oxide,[67] graphene[68] or carbon nanotubes.[69] In supported nanoparticles, the catalytic metal is typically attached to the surface via weak van der Waals forces,[70, 71] which is the main limitation of these materials. This method often results in limited robustness and catalytic stability, especially under harsh reaction conditions, for example under high-pressure, high-temperature, and

continuous-flow conditions or in the presence of bases and ligands.[72, 73] In spite of this, nanosilvers play important role in catalysis, which is evidenced by the widely explored fine chemical synthesis with this group of catalysts.[62] In the fields of environmental sciences and organic synthesis, the application of nanosilver-catalyzed reduction of nitroaromatics has received significant attention for decades. Shimizu and co-workers developed a highly chemoselective reduction of the nitro group of substituted nitroaromatics catalyzed by silver clusters supported on θ-Al_2O_3. Conventional heterogeneous catalysts based on platinum-group metals showed lower selectivity than this type of catalysts. In this work, the preferential transfer of the H^+/H^- pair to the polar bonds in the nitro group resulted in the high chemoselectivity. To investigate the scope of the reaction, the hydrogenation of a series of nitroaromatic compounds with alkene, carbonyl, nitrile, and amide substituents was tested in the presence of Ag/Al_2O_3 catalyst (this was the suitable catalyst in this case).[74] On the other hand, the reusability or robustness of the catalyst was not mentioned in the article.

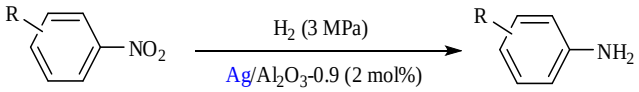

Scheme 15. *Nanosilver-catalyzed hydrogenation of nitroaromatic compounds*[74]

In the synthesis of biologically active molecules or fine chemicals, alkylation has been of great interest for many years. The *N*-alkylation of nitrogen-containing compounds is of particular value in the diverse synthesis methods of substituted amides or amines. The reaction of amines with alkylating agents or alkyl halides is a well-known procedure for the preparation of *N*-alkylamines.[75] Shi and co-workers designed a highly effective Ag/Mo hybrid catalyst material with specific $Ag_6Mo_{10}O_{33}$ stoichiometry and crystal structure for the alkylation of amines, amides, carboxamides, sulfonamides, and aromatic ketones with alcohols. In this work, the mild reaction conditions were similar to those used in conventional homogeneous systems without additional organic ligand. The yields of the reactions were ~90% in almost every case. The catalyst was reused in the second round after recovery with results similar to those obtained in the first round.[76]

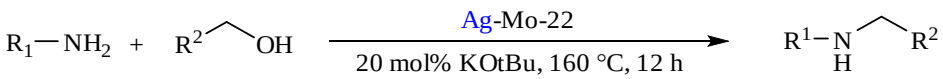

Scheme 16. *Alkylation of amines with alcohols catalyzed by a Ag/Mo hybrid material*[76]

The three-component coupling reaction of alkynes, amines, and aldehydes (A^3-coupling) is significant in organic synthesis, due to the numerous useful chemicals prepared

with this process. In this type of A^3-coupling reactions, nanosilver catalysts have been found to be adequate heterogeneous preparations offering the opportunity for green synthesis of the desired materials. Liu and co-workers developed an AgSBA-15 catalyst for A^3-coupling reactions of aldehydes, amines, and terminal alkynes in glycol acting as an environmentally benign catalyst. The catalyst could be reused four times after easy recovery without any significant change in catalytic activity.[77]

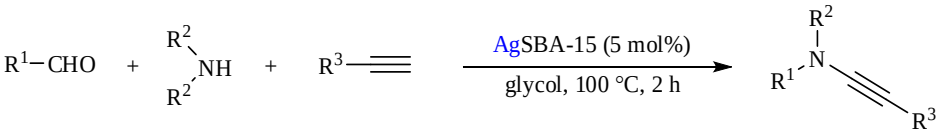

Scheme 17. *Three-component synthesis of propargylamines catalyzed by AgSBA-15*[77]

The preparation of amides by selective hydration of nitriles is a significant reaction in the topic of nanosilver-catalyzed transformations for the synthesis of fine chemicals. Kaneda and co-workers discovered a process to carry out the hydration of various nitriles into amides in water as solvent utilizing hydroxyapatite-supported silver nanoparticles (AgHAP). The scope of the diverse nitrile starting materials was surveyed and the yields were excellent in almost every case. This catalyst was reused four times without significant changes in yields.[78]

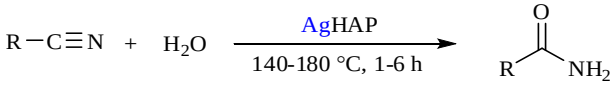

Scheme 18. *Hydroxyapatite-supported silver nanoparticles inducing selective hydration of nitriles to amides*[78]

In asymmetric synthesis, supported silver nanoparticles could be commonly applied as heterogeneous catalysts. In a study, a Rh/Ag bimetallic catalyst has been developed for this reaction. It is a robust and active bimetallic material in asymmetric 1,4-additions of arylboronic acids to enones catalyzed by chiral metal nanoparticles without active metal leaching. In the scope of the reaction, various substrates were tested with high yields and *ee* values. The catalyst was reused 14 times with variable yields and excellent *ee*.[79]

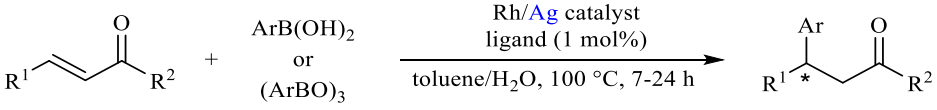

Scheme 19. *Asymmetric 1,4-addition reactions of arylboronic acids to enones catalyzed by Rh/Ag bimetallic catalyst*[79]

Lingaiah and co-workers developed a heterogeneous silver salt catalyst of 12-tungstophosphoric acid ($Ag_3PW_{12}O_{40}$, AgTPA) for the preparation of propargylamines under mild conditions by A^3-coupling reaction without any co-catalyst. In the scope of the reaction

diverse amines and aldehydes were tested for the synthesis of the corresponding propargylamines. Furthermore, the AgTPA catalyst was reused four times without the loss of catalytic activity.[80]

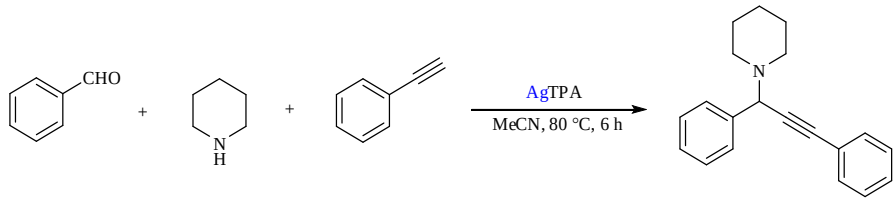

Scheme 20. *Three-component coupling of an aldehyde, an amine, and an alkyne catalyzed by the silver salt of 12-tungstophosphoric acid*[80]

Lingaiah and co-workers also discovered a heterogeneous silver-exchanged silicotungstic acid (STA) catalyst for the solvent-free hydration of alkynes. The catalyst was reused in five consecutive catalyst cycles without loss of activity. In this work, the hydration of non-activated alkynes to the corresponding carbonyl compounds was investigated without addition of any acid co-catalyst.[81]

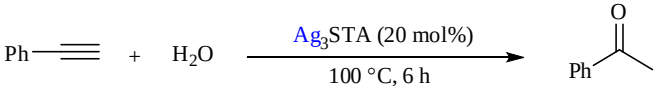

Scheme 21. *Hydration of alkynes over a heterogeneous silver-exchanged silicotungstic acid catalyst*[81]

Yuan and co-workers developed a polystyrene-supported NHC silver complex [PS-NHC-Ag(I)] and demonstrated its successful use in the synthesis of α-alkylidene cyclic carbonates in the reaction of various secondary and tertiary propargylic alcohols with CO_2 under mild conditions. This catalyst proved to be efficient and robust upon reusing 15 times without loss of catalytic activity. Advantages of this method are a simple work-up procedure, low catalyst loading, mild conditions, and high yields.[82]

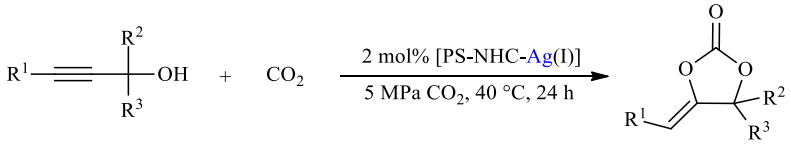

Scheme 22. *Reaction of carbon dioxide and propargylic alcohols catalyzed by polystyrene-supported N-heterocyclic carbene–silver complex*[82]

Kim and co-workers executed the deprotection of diverse substituted alkyl and phenolic TBDMS ethers at room temperature in methanol applying silver-exchanged silicotungstic acid (AgSTA) salt as heterogeneous catalyst. A comparison with other heterogeneous catalysts demonstrated that the AgSTA sample affords high performance in alkyl and phenolic

desilylation reactions in short reactions. In this system, the catalyst worked with high stability (it was reused in six cycles) and the synthesis could be executed easily with high yields and conversions even at room temperature.[83]

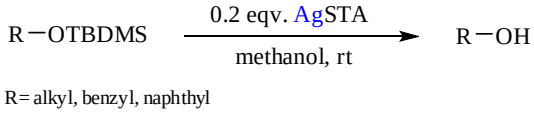

Scheme 23. *Deprotection of tert-butyldimethylsilyl (TBDMS) ethers promoted by silver salt of silicotungstic acid*[83]

Pitchumani and co-workers developed a one-pot A^3-coupling reaction to prepare the corresponding propargylamines catalyzed by Ag(I)-exchanged K10 montmorillonite clay. In the scope of the reaction, they found outstanding yields of the desired products. The catalyst was reused six times with only a slight decrease in activity. This reaction did not require activator or additional co-catalyst and water was the only by-product; consequently, it can be considered as a highly atom-economical methodology. Furthermore, the catalyst could also be applied in the coupling of formaldehyde, aliphatic, and aromatic aldehydes under solvent-free conditions.[84]

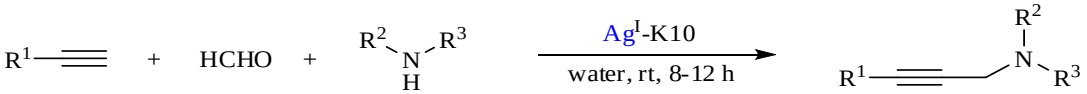

Scheme 24. *The use of Ag(I)-exchanged K10 montmorillonite clay in the one-pot synthesis of propargylamines*[84]

Zhang and co-workers developed a continuous-flow process for a three-component coupling and a cascade intramolecular 1,3-dipolar cycloaddition reaction mediated by PANF-NHC-Ag. After 24 h of operation, the Ag-immobilized catalyst showed no silver leaching and no loss in activity under the applied reaction conditions. The diastereoselective synthesis of fused triazoles was performed in a simple flow reactor under high pressure and temperature with good yields.[85]

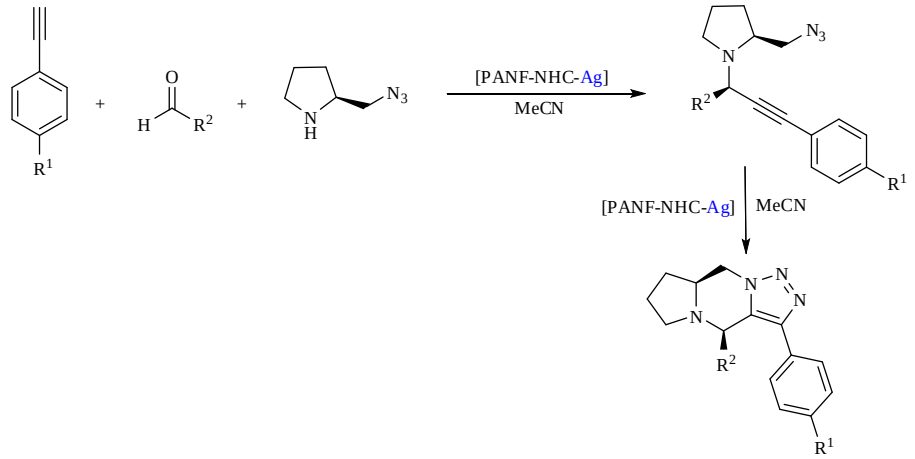

Scheme 25. *Cascade three-component coupling and intramolecular 1,3-dipolar cycloaddition reactions under flow chemistry conditions catalyzed by PANF-NHC-Ag*[85]

2.3 Flow chemistry

Initially, continuous-flow processes were employed in the industrial manufacture of various simple products, for example in oil refining.[86] However, as a promising technology for sustainable production of pharmaceuticals and fine chemicals, continuous-flow techniques have been attracting increasing attention in recent decades.[87, 88] This process offers notable advantages over conventional batch techniques, such as high reproducibility, facile automation, improved safety or process reliability. In flow reactors, large surface-area-to-volume ratios[89] allow accurate reaction control through rapid heat transfer and mixing.[90, 91] The synthesis in flow chemistry can be scaled up by parallel coupling of identical flow reactors (the process is known as numbering up)[92] or by running a single reactor for extended periods of time.[93] Flow reactors include narrow channels which made typically of glass, stainless steel, polymers or silicon.[94] These channels are connected to reservoirs containing solvent and/or reagents in the case of synthetic applications. The reagents are pumped together to the active reactor zones mainly with laminar flow and mixing occurs via radial diffusion.[95] Under controlled conditions, the reagents are reacted for specified reaction times, thus minimizing side reactions.[96] Depending on internal channel dimensions, the different types of reactors such as microreactor chip, coil-type mesoreactor, and reactor columns can be distinguished.[97, 98] Heterogeneous catalysis is usually performed in reactor columns, which has the advantage of more sustainable chemical synthesis including the possibility of facile catalyst regeneration and reusability.[99] Indeed, with the continuous-flow methodology, accurate and constant reaction parameters (temperature, time, amount of reagents and solvents, efficient mixing, etc.) can be easily ensured.[100] This technique has proved to be very auspicious for performing chemistry that is difficult to carry out under batch conditions, such as synthesis via unstable or reactive

intermediates[101–103] and the use of highly reactive reagents like hazardous gases and highly active substances (hydrogen, oxygen, carbon monoxide, azides).[104–106]

Nowadays, continuous-flow synthesis is becoming an important tool in synthetic organic and medicinal chemistry. Numerous active pharmaceutical ingredients (APIs),[87, 107, 108] nanomaterials[109–111] or other complex materials[112–114] were synthesized by this methodology reaching high yields. The application of continuous-flow methodology and heterogeneous catalysis in a reactor column can facilitate a scalable and cleaner flow organic synthesis process. In general, in this type of continuous-flow set-up, the catalyst is placed in a packed-bed reactor and the reaction mixture is flown through the reactor using adequate pumping systems.[99] A very high ratio between the active catalyst and the substrates/reagents are accessible when the reagents are flowing through the packed catalyst bed. In these reactors, heterogeneous catalysts can be handled, reused, and recycled easily. Moreover, the separation of the reaction products is more straightforward in contrast to the traditional segmented processes.[115] Other advantages of heterogeneous catalysis in combination with flow technology are as follows: catalysts are potentially recycled over numerous times, small amounts of catalyst can be employed in many cases, more efficient use of resources and generation of less waste, and improved heat transfer and accurate temperature control.[116–118] The most significant examples of continuous-flow processing in combination with heterogeneous catalysis are transition metal-catalyzed hydrogenation reactions (in modern organic synthesis, these have recently become an almost routine technique).[119] Despite these benefits, there are very few examples for the application of heterogeneous silver catalysts in continuous-flow processes.[120, 121] The simple reason is that robust and stable heterogeneous silver catalyst are rare. Besides, under flow conditions (high temperature, high pressure), increased requisition, compatibility, activity, reusability, and robustness of the catalyst are pivotal requirements.[122–124] Therefore, there is a need to develop heterogeneous catalysts that can be used under these conditions.

3. EXPERIMENTAL SECTION

3.1 General information

Reagents and materials were commercially available and used as received. NMR spectra were recorded on Bruker Avance DRX 400 or 500 spectrometers in $CDCl_3$ or DMSO-d6 as solvent, with tetramethylsilane as internal standard. ^{1}H spectra were recorded at 400.1 or 500.1 MHz, ^{13}C at 100.6 or 125.0 MHz. GC-MS analysis were carried out with a Thermofisher Scientific DSQ II Single Quadrupole GC/MS, on a 30 m×0.25 mm×0.25 μm TG-5SILMS capillary column (Thermo Scientific). The measurement parameters were as follows: column oven temperature: 30 °C (0–2 min), 30 to 250 °C heating with 10 °C/min (2–24 min), and 250 °C (24–26 min); injection temperature: 240 °C; ion source temperature: 200 °C; EI: 70 eV; carrier gas: He, at 1.5 mL min^{-1}; injection volume: 2 μl; split ratio: 1:50; and mass range: 50–500 m/z.

3.2 Synthesis of the silver–bismuth hybrid material

AgBi-HM was prepared by using the urea hydrolysis method.[125] In this process, the pH can be precisely controlled through the temperature of the co-hydrolysis process. In a typical synthesis, appropriate amounts of $AgNO_3$ (3.73 g) and $Bi(NO_3)_3{\cdot}5H_2O$ (5.36 g) each were dissolved in 50 mL 5 wt% nitric acid. After mixing, urea (7.05 g) dissolved in 100 mL of deionized water was added to the solution and stirred for 72 h at 130 °C. As an alternative way of the synthesis, after addition of the urea solution to the mixture of the required salts, the reaction mixture was placed into an oven for 24 h at 105 °C. The obtained material was filtered, washed with aqueous thiosulfate solution, water, and ethanol four times, and dried at 60 °C to obtain the final product.

3.3 General procedure for batch reactions

A typical procedure for the catalytic reactions was as follows. The appropriate solvent, the corresponding starting material (reagent if necessary), and the silver-containing hybrid material as catalyst were combined in an oven-dried Schlenk tube equipped with a magnetic stir bar. The reaction mixture was stirred at a selected temperature and reaction time. Then the mixture was cooled to room temperature and the catalyst was filtered off. The crude samples were analyzed by ^{1}H NMR and GC-MS (in order to determine conversion and product ratio) and then purified by chromatographic techniques to isolate the desired products. Flash column chromatographic purification (performed on Merck silica gel 60, particle size 63–200 mm) and analytical thin-layer chromatography (TLC, performed on Merck silicagel 60 F254 plates) were carried out using mixtures of *n*-hexane/ethyl acetate (EtOAc) as eluent. When using TLC, the

compounds were visualized by means of UV or $KMnO_4$. Work-up and purification were performed in each case as detailed in the attached publications.

3.4 General procedure for continuous-flow reactions

To examine the catalytic reactions under flow conditions, a continuous-flow set-up was assembled (Figure 1). The system consisted of an HPLC pump (JASCO PU-2085), a stainless steel cartridge with internal dimensions of 30 × 2.1 mm, 50 × 2.1 mm or 100 × 4.6 mm and a 10-bar backpressure regulator (BPR; IDEX) to enable the overheating of the solvents. The column was charged with the corresponding amount of AgBi-HM and sealed with compatible frits (0.5 μm pore size). Parts of the system were connected with stainless steel capillary tubing (internal diameter 250 μm). The catalyst bed was immersed into an oil bath for heating purposes. For each reaction, the appropriate starting material was dissolved in the corresponding solvent and the solution was pumped continuously under the selected conditions. Between two experiments, the system was washed by pumping solvent at a flow rate of 0.5 mL min^{-1}. The crude products were analyzed by NMR spectroscopy to determine conversions and selectivities. If necessary, column chromatographic purification of the crude materials was carried out with a mixture of *n*-hexane and EtOAc as eluent. The reaction products were characterized by NMR and MS techniques.

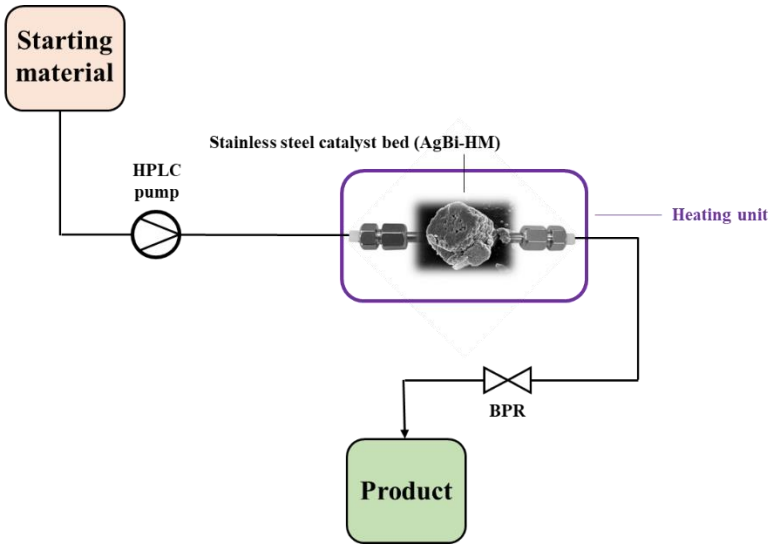

Figure 1. *Experimental setup for the continuous-flow experiments*

4. RESULTS AND DISCUSSION

4.1 Synthesis and characterization of AgBi-HM

Materials based on layered double hydroxide (LDH) served as the basis and inspiration of catalyst synthesis. In our previous work, we applied successfully this type of materials as catalysts.[126] The organized layers in the LDH-like structure allow facile control over catalytic properties. Ag(I) in solid materials prefers octahedral coordination.[127] The typical LDH layers include di- and trivalent metal cations;[128, 129] however, instead of the divalent one, monovalent cationic component is also known.[130] The trivalent cation Bi(III) was selected, because the ionic radii of Bi(III) and Ag(I) are comparable (117 and 129 pm), and an octahedral coordination is preferred in the solid state.[127] However, the synthesis of the planned LDH phase could not be executed successfully, because a beyerite-like solid was prepared. Beyerite [$CaBi_2O_2(CO_3)_2$] has a layered structure, which involve Ca(II) ions fixed among the layers of $BiO(CO)_3$.[131] Therefore, we turned into the immobilization of Ag(I) instead of the Ca(II) cations in the lattice, which could result in considerable and stable catalytic activity.

In the urea method, the pH can be accurately controlled through the temperature of hydrolysis; therefore, it was chosen for the preparation of the catalyst in the co-hydrolysis of the metal salts. The detailed synthesis process of the hybrid material is described in the *Experimental* section.

The as-prepared AgBi-HM material was characterized by numerous methods including X-ray diffractometry (XRD), UV/VIS/NIR DRS spectroscopy, Raman spectroscopy, ICP–AES, thermogravimetry (TG), XPS, AFM, scanning electron microscopy (SEM), transmission electron microscopy (TEM), and BET surface measurement. The detailed results of the structure of the hybrid material are in the article of appendix I.[132]

4.2 Silver-catalyzed direct synthesis of nitriles from terminal alkynes

Alkynyl compounds have emerged as diverse intermediates for the atom-economical synthesis of a wide variety of significant products, because of their great availability and the excellent transformability of C≡C bonds.[133] Alkynes are notable compounds in the field of cyclization and various coupling reactions[134] including the well-established click chemistry.[135] In addition, they play an important role in numerous other catalytic transformations.[136, 137] The activation of C≡C bonds of alkynyl compounds often takes place by silver catalysis (d^{10} electronic configuration).[5] Silver-mediated σ- or π-activation of terminal or internal alkynes are carried out in numerous synthetic methods as a consequence of this pronounced alkynophilicity.[138, 139] Most of these significant reactions employ relatively

large amounts of precious metals and rely on homogeneous silver catalysts; however, there are some examples of heterogeneous applications as well.[140]

Aliphatic and aromatic nitriles are of emerging importance in pharmaceutical, fine chemical, and natural product syntheses, because of their excellent versatility. Organic nitriles are particularly important intermediates for the production of numerous heterocycles,[141] and they are essential precursors for amines, aldehydes, amides, and diverse carboxylic acid derivatives.[142] Moreover, the cyano group represents a vital motif in varied medicinally or biologically relevant structures, including several FDA-approved drugs such as rilpivirine and letrozole.[6, 143] Numerous traditional strategies are known in nitrile synthesis. These include cyanations mediated by metal cyanides or metalloid cyanides,[7] Sandmeyer reactions,[144] Schmidt reaction of aldehydes with azides,[145] ammoxidation of aromatic hydrocarbons,[146] and dehydration of amides and oximes.[147] However, these methods have several drawbacks, including serious environmental concerns such as toxic metal waste and cyanide salts, harsh reaction conditions, the use of expensive catalysts, limited scope or selectivity issues. To circumvent these limitations, Jiao and co-workers implemented a silver-catalyzed direct synthesis of organic nitriles from terminal alkynes by C≡C bond cleavage reaction, under reasonably mild conditions in the presence of a suitable nitrogen source.[8]

Since silver-containing catalytic systems with efficient reusability feature are scarce, in general, soluble salts are employed as catalyst sources in silver-mediated nitrogenation of alkynes. Therefore, the novel silver–bismuth hybrid material (AgBi-HM) was applied as heterogeneous catalyst in direct synthesis of different nitriles from terminal alkynes.[132]

4.2.1 Optimization

For the model reaction of direct nitrogenation, *p*-methoxyphenylacetylene with $TMSN_3$ as nitrogen source was chosen. In Scheme 26 the possible reaction product (4-methoxybenzonitrile **2**), the side-product [(1-azidovinyl)-4-methoxybenzene **1**], and another side product [5-(4-methoxyphenyl)-1*H*-1,2,3-triazole **3**] are shown. Side product **2** was probably formed via a thermal azide–alkyne cycloaddition as a side reaction.[148] Jiao and co-workers proposed a reaction mechanism (Scheme 27), where nitrile formation occurs via a vinyl azide intermediate.[8]

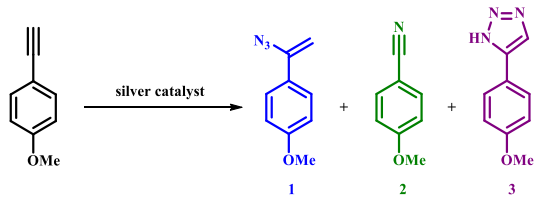

Scheme 26. *Model reaction: nitrogenation of p-methoxyphenylacetylene with $TMSN_3$ as nitrogen source*

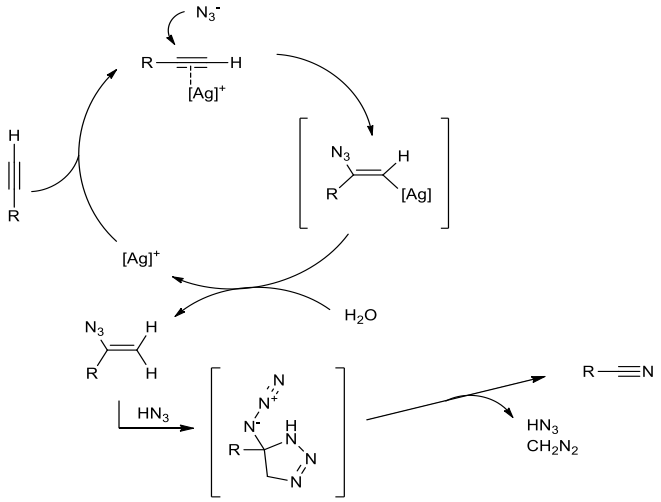

Scheme 27. *Proposed reaction mechanism of silver-catalyzed direct synthesis of nitriles from terminal alkynes*

The catalytic activity of AgBi-HM was directly compared with commercially available Ag(I) salts (Table 1). $AgBF_4$ and Ag_2CO_3 showed comparable results to the hybrid material: the nitrile/triazole ratio was 88 : 12 and 87 : 13, respectively, and the conversion was 100% in both cases. Other Ag(I) salts resulted in lower product selectivities or/and incomplete conversions. AgOAc and AgOTf proved to be less effective among the commercial catalysts [only traces of (1-azidovinyl)-4-methoxybenzene (**1**) could be detected in the crude product]. A test reaction was carried out with 10 mol% of $Bi(NO_3)_3 \cdot 5H_2O$ as catalyst to confirm that the Bi(III) component of the hybrid material is inactive as concerns nitrile formation (Table 1, entry 11). Furthermore, a significant decrease in conversion was observed, when the AgBi-HM-catalyzed nitrogenation of *p*-methoxyphenylacetylene was tested under argon atmosphere (Table 1, entry 12).

Table 1. *Investigation of various catalysts in the direct nitrogenation of p-methoxyphenylacetylene with $TMSN_3$ as nitrogen source. Reaction conditions: 1 equiv. (0.25 M) alkyne, 2 equiv. $TMSN_3$, 10 mol% catalyst, DMSO as solvent, 80 °C, 24 h reaction time*

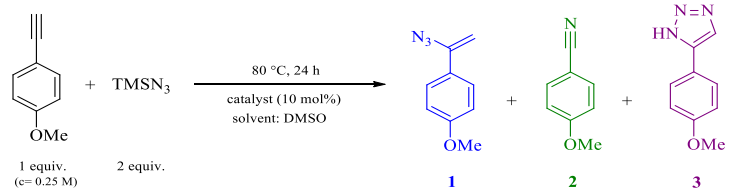

Entry	Catalyst	Conv. (%)[a]	Product selectivity (%)[a]		
			1	**2**	**3**
1	AgBi-HM	100	0	91	9
2	Ag_2CO_3	100	0	88	12
3	AgOAc	88	2	81	17
4	AgOTf	83	2	71	27
5	Ag_2SO_4	89	0	78	22
6	$AgBF_4$	100	0	87	13
7	$AgPF_4$	100	0	67	33
8	Ag_2O	100	0	81	19
9	$AgNO_3$	100	0	80	20
10	$Bi(NO_3)_3$	0	0	0	0
11	no catalyst	7	0	0	100
12[b]	AgBi-HM	73	0	85	15

[a] *Determined by ^{1}H-NMR analysis of the crude product.* [b] *Under argon atmosphere*

In the next step, we set out to investigate the effects of all significant reaction parameters in order to determine the optimum conditions for a sustainable methodology. The role of the reaction medium was first examined and strong dependence was observed on the quality of the solvent applied. Only dipolar aprotic solvents bearing an amide moiety and dimethyl sulfoxide (DMSO) proved to be acceptable: DMSO and *N*,*N*-dimethylacetamide (DMA) worked similarly well (the conversion was 100% and 90%, the nitrile/triazole ratio was 91 : 9 and 87 : 13, Table 2, entries 1 and 2). The application of *N*,*N*-dimethylformamide (DMF) and *N*-methylpyrrolidone (NMP) resulted in lower conversions (72% and 41%) but still good selectivities towards the formation of nitrile (84% and 76%, Table 2, entries 3 and 4). This notable dependence is possibly related to the stability of the *trans* alkenyl silver complex key intermediate and the nucleophilicity of the azide anion (strongly depending on the solubilizing

properties of the solvent applied).[149] In other polar and non-polar solvents, only very low conversions were observed even extending the reaction time to 72 h.

Table 2. *Investigation of various solvents in the AgBi-HM-catalyzed nitrogenation of p-methoxyphenylacetylene with $TMSN_3$ as nitrogen source*

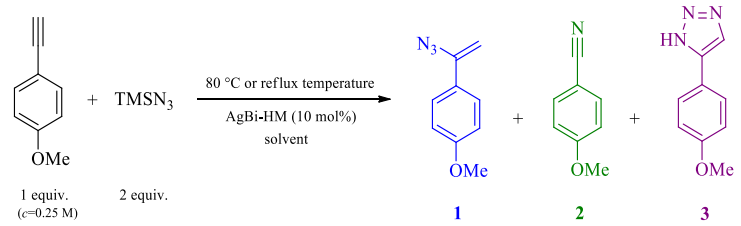

#	Solvent	Reaction time	Conv. (%)[a]	Product selectivity (%)[a]		
				1	**2**	**3**
1	DMSO	24 h	100	0	91	9
2	DMA	24 h	82	0	87	13
3	DMF	24 h	72	0	84	16
4	NMP	24 h	41	2	76	22

[a] Determined by ^{1}H-NMR analysis of the crude product

In further attempts to improve the selectivity and the rate of the reaction, the role of the temperature was explored carefully (Figure 2). A substantial increase in the reaction rate was observed with the elevation of the temperature (the conversion of *p*-methoxyphenylacetylene was 91% after 1 h at 130 °C). On the other hand, higher temperatures promoted the formation of the triazole side product via thermal azide–alkyne cycloaddition. In the investigation of the role of reaction time, the total conversion was observed to increase gradually with the reaction time (Figure 2). A substantial amount of vinyl azide was detected in the initial stages of the reaction. The amount of the nitrile product, in turn, grew continuously, while the intermediate was consumed. After 1 h of stirring at 80 °C, the triazole by-product was detected and its ratio in the reaction mixture became steady around 10% after 6 h.

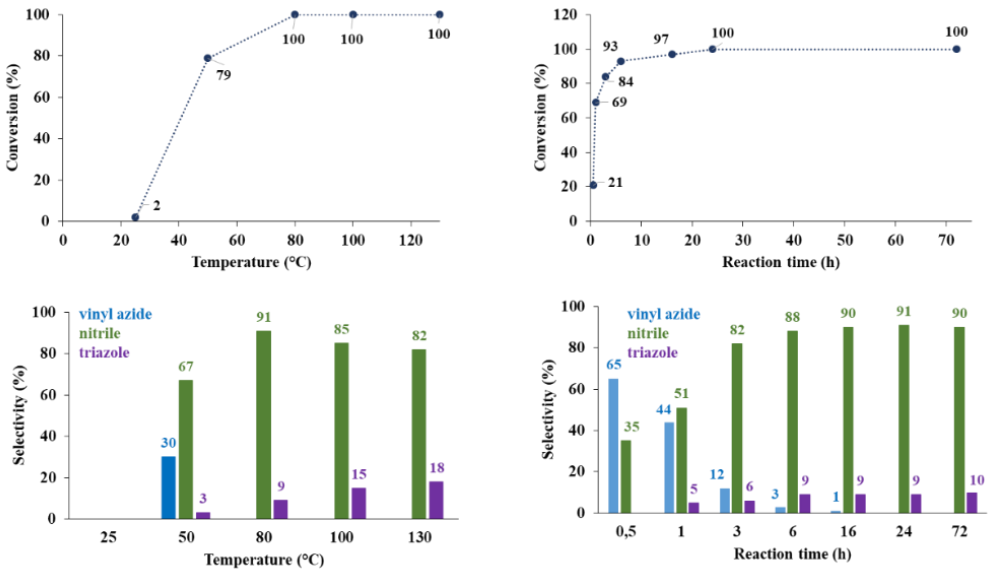

Figure 2. *Investigation of the effects of the temperature and the reaction time on the AgBi-HM-catalyzed nitrogenation of p-methoxyphenylacetylene with $TMSN_3$ as nitrogen source. Reaction conditions: 1 equiv. (0.25 M) alkyne, 2 equiv. $TMSN_3$, 10 mol% catalyst, DMSO as solvent*

Diphenylphosphoryl azide (DPPA) and sodium azide (NaN_3) were also studied as nitrogen sources, besides $TMSN_3$. No conversion was observed with the use of DPPA, while NaN_3 did not work well either resulting in a conversion of merely 8% with triazole as the main product. We reduced the excess of $TMSN_3$, but 2 equiv. were necessary for the reaction to complete (lower amounts caused a sharp decrease in conversion). Without detectable change in conversion or selectivity, we were able to decrease the catalyst loading to 5 mol%, under the previously set conditions (80 °C, 24 h, DMSO as solvent, 2 equiv. of $TMSN_3$ as nitrogen source). A table collecting these experimental results is in attached article I.[132]

Trace amounts of H_2O are required for successful nitrile formation, according to the suggested reaction mechanism of direct alkyne nitrogenation.[8] Thus, we expected that the presence of excess H_2O (2 equiv.) might have a beneficial effect on the reaction rate. However, this had no significant impact on the reaction progress. Note, that as a consequence of competitive silver-catalyzed alkyne hydration, a small amount of *p*-methoxyacetophenone appeared among the reaction products.[150]

4.2.2 Investigation of the scope and applicability of the reaction

Based on the findings of parameter optimization, the reaction was operated most efficiently at 80 °C reaction temperature and in a reaction time of 24 h with a substrate concentration of 0.25 M, 2 equiv. $TMSN_3$, 5 mol% AgBi-HM catalyst in DMSO solvent. With

these conditions in hand, we finally carried out a study to investigate the substrate scope and applicability of the method (Table 3). In the reactions of phenylacetylene and its substituted derivatives containing methoxy, methyl, *tert*-butyl or bromo moieties, quantitative conversions and selectivities around 90% were observed (Table 3, entries 1–5). Multisubstituted phenylacetylene derivatives are known to be less reactive in silver-mediated nitrogenation.[8] However, they gave excellent results under these conditions, even with 3-ethynylthiophene (Table 3, entries 6–8). In addition, enhanced triazole formation led to slightly lower selectivities in the case of benzoic acid propargyl ester, phenyl propargyl ether, and *p*-nitrobenzoic acid propargyl ester (in the range of 73–81%) displaying outstanding reactivities (conversions were in the range 95–100%) (Table 3, entries 9–11). The transformation of aliphatic alkynes (open-chain alkynes with varying chain length) and a cyclic alkyne took place satisfactorily providing the corresponding nitriles with outstanding conversions (in the range of 96–100%) and selectivities around 90% (Table 3, entries 12–15). Nitrogenation of internal alkynes (for example, oct-4-yne or ethyl phenylpropiolate) was also attempted, but no nitrile formation was observed.

Table 3. *Substrate scope of the AgBi-HM-catalyzed direct alkyne nitrogenation*

Entry	Alkyne	Conv. (%)[a]	Product select. (%)[a]			Entry	Alkyne	Total conv. (%)a	Product select. (%)a		
			1	**2**	**3**				**1**	**2**	**3**
1	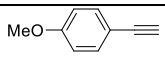	100	0	90	10						
2	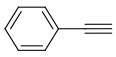	100	0	91	9	**9**	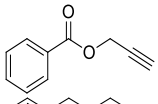	100	0	74	26
3	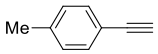	100	0	92	8	**10**	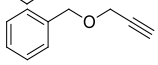	100	0	81	19
4	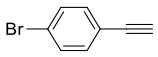	100	0	90	10	**11**	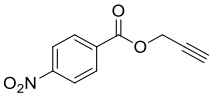	95	0	73	27
5	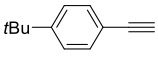	100	0	93	7	**12**	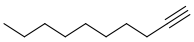	100	0	89	11
6	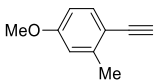	100	0	94	6	**13**	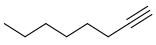	100	0	90	10
7	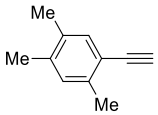	100	0	94	6	**14**	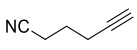	96	0	93	7
8	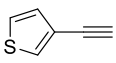	100	0	90	10	**15**	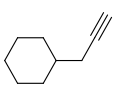	98	0	87	13

[a] Determined by ^{1}H-NMR analysis of the crude product

4.2.3 Investigation of the catalyst reusability and the heterogeneous nature of the reaction

In principle, the possibility of reusing and recycling the catalytic material is one of the primary benefits of heterogeneous catalysis. However, several drawbacks could significantly limit the sustainable application of these materials in practice (for example the erosion of the catalyst structure, leaching of the active components or irreversible substrate deposition).[151] The same portion of AgBi-HM catalyst was applied in the reaction of *p*-methoxyphenylacetylene with $TMSN_3$ carried out repeatedly at 80 °C in the presence of 2 equiv. of $TMSN_3$ and 5 mol% catalyst in DMSO solvent. The catalyst was removed by centrifugation and reused after washing and drying between each cycle. Decrease in selectivity or activity was not observed even after 10 consecutive catalytic cycles (Figure 3). The conversion of *p*-methoxyphenylacetylene was almost complete in every case (97–100%), and the selectivity of the nitrile product was found to be around 90% in all reactions. Vinyl azide intermediate was not detected, in contrast to small amounts of triazole, which was detected in all crude product mixtures.

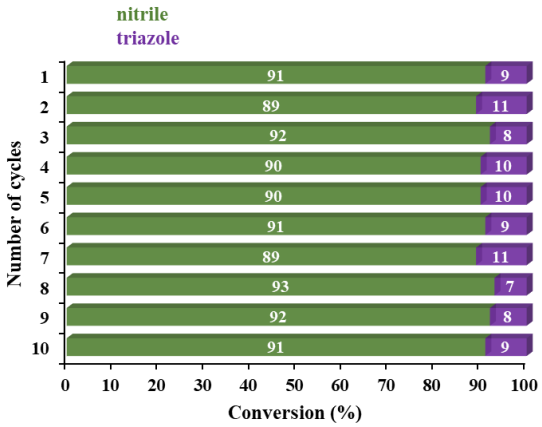

Figure 3. *Testing the reusability of the AgBi-HM catalyst in the direct nitrogenation of p-methoxyphenylacetylene with $TMSN_3$ as nitrogen source. Reaction conditions: 0.25 M alkyne, 2 equiv. $TMSN_3$, 5 mol% catalyst, DMSO as solvent, 80 °C, 24 h reaction time*

A hot filtration test was carried out in order to verify the heterogeneous nature of the reaction. The nitrogenation of *p*-methoxyphenylacetylene with $TMSN_3$ as nitrogen source was performed under the optimized reaction conditions (80 °C, DMSO as solvent, 2 equiv. of $TMSN_3$, 5 mol% catalyst) (Figure 4). The AgBi-HM catalyst was filtered off after 1 h and the filtrate was stirred for an additional 23 h at 80 °C. As seen in Figure 3, the conversion of *p*-methoxyphenylacetylene after 1 h was 65%, and it remained the same after 1 + 23 h with a product distribution of 47% vinyl azide, 49% nitrile, and 4% triazole. After 1 + 23 h, all vinyl azide intermediate was consumed as evidenced by the NMR measurements showing the

disappearance of the alkenyl CH_2 signals at 4.9 and 5.3 ppm. Thermal triazole formation proceeded somewhat further. Jiao and co-workers proposed that only the initial hydroazidation step was silver-catalyzed and the final vinyl azide to nitrile transformation requires no silver catalyst (these observations are in good accordance with our results).[8]

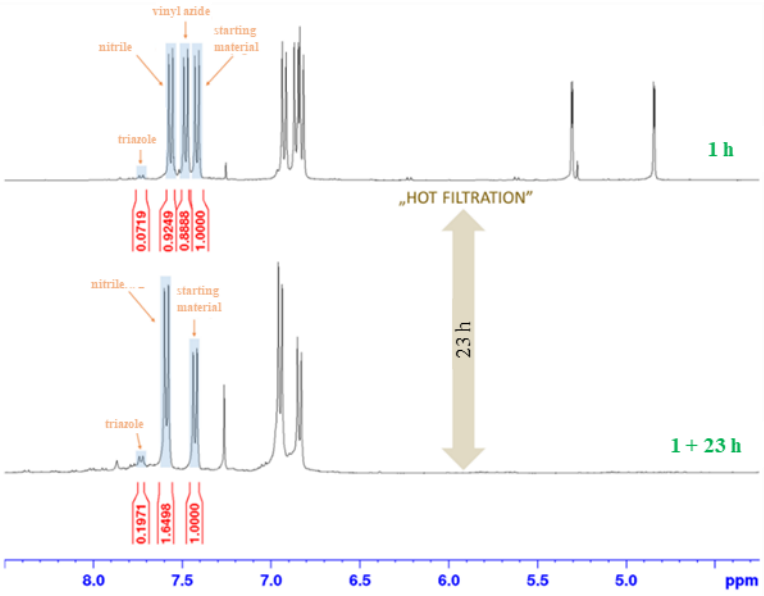

Figure 4. *^{1}H NMR spectroscopic analysis (400.1 MHz, $CDCl_3$) of the AgBi-HM-catalyzed reaction of p-methoxyphenylacetylene with $TMSN_3$ as nitrogen source. Reaction conditions: 1 equiv. (0.25 M) alkyne, 2 equiv. $TMSN_3$, 5 mol% catalyst, DMSO as solvent, 80 °C. Ar–H signals are marked with blue rectangles*

4.2.4 Examination of the used catalyst

Many of the methods applied for the freshly-made material were utilized for the structural characterization of the used catalyst (Figure 5). The post-reaction X-ray pattern looks the same as the freshly made material. As demonstrated by the Raman spectra of the freshly-made and the used samples, the structure did not change. Both the carbonate ion (the anionic component) and the silver ion attachment to the carbonate oxygen remained the same. As proved by the ICP–AES measurement, the solids survived the recycling test without losing any of its components (the used catalyst gave a formula very similar to that of the freshly-made one: $Ag_{0.17}Bi_{0.91}O_2CO_3$). According to XPS measurements, no change was detectable in the oxidation states of any of the cationic components. The layered structure is preserved in the used catalyst sample as well, as indicated by the high resolution TEM image. We can declare that, as confirmed by all material characterization data of the used sample, AgBi-HM is a highly robust heterogeneous catalyst preserving its structure even after an extended use.

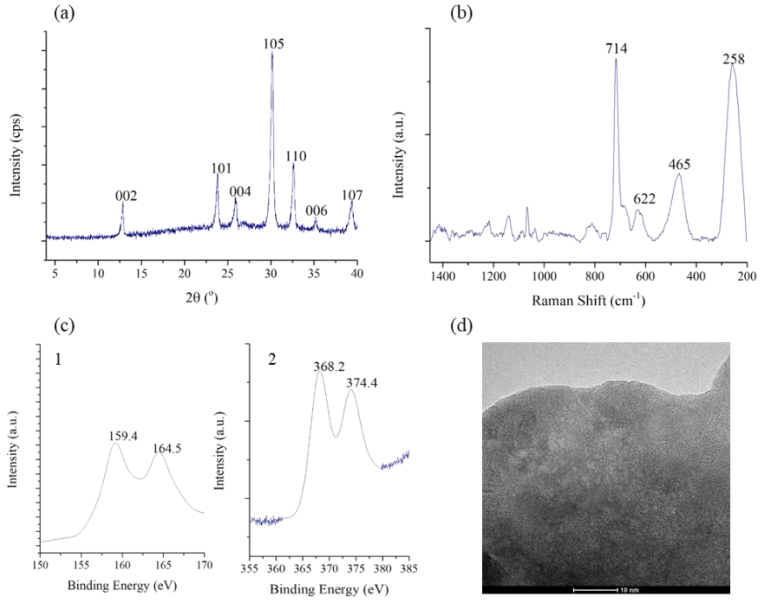

Figure 5. *Characterization of the used catalyst: a) X-ray pattern, b) Raman spectra, c) XPS measurement (Ag3d (1) and Bi4f (2) XPS spectra), d) high-resolution TEM image*

4.3 Investigating the stability and solvent-compatibility of the AgBi-HM catalyst under continuous-flow conditions

The effects of diverse solvents and reaction conditions on the structure of the material were explored to collect valuable data on the applicability of AgBi-HM for organic synthesis in continuous-flow mode. For these experiments, a simple flow reactor set-up was applied as detailed in the *Experimental* section. An extensive list of solvents was compiled for the stability tests, which included Dichloromethane (CH_2Cl_2), Chloroform ($CHCl_3$), EtOAc, acetone, diethyl ether, methanol (MeOH), ethanol, propan-2-ol, H_2O, MeCN, THF, NMP, *n*-hexane, toluene, DMF, DMSO, DMA. The tests were performed at 25, 50, 100, 150, and 200 °C, typically used in catalytic flow reactions. In each test, the solvent was pumped for 90 min at 0.05 mL min^{-1} flow rate through a catalyst bed containing a sample of AgBi-HM. The treated hybrid material sample was examined by XRD and IR spectroscopy in every case to explore the effect of diverse solvents on the AgBi-HM sample under flow conditions. The results of the stability tests are summarized in the article of appendix II,[152] and the complete collection of diffractograms is found in the related SI file.

4.4 Silver-catalyzed benzyl alcohol dehydrogenations under continuous-flow conditions

In synthetic organic chemistry as well as in pharmaceutical and fine chemical industries, the dehydrogenation/catalytic oxidation of alcohols have essential significance, as a result of the ubiquity of carbonyl compounds.[10, 153, 154] In contrast, catalytic oxidations, the oxidant-free

dehydrogenation methods are generally more selective, due to the lack of over-oxidation, better atom efficiency, and cleaner performance.[63, 155] Nevertheless, these reactions have a significant synthetic challenge, because of commonly required harsh conditions. In fact, the liquid-phase catalytic methodologies often suffer from important drawbacks including limited substrate scope, low activity or the necessity to use various additives,[156–158] in contrast to the well-established industrial methods for gas-phase alcohol dehydrogenations.[9, 159]

Inspired by these features, we explored the synthetic capability of the AgBi-HM catalyst under demanding flow conditions in selected catalytic dehydrogenation of benzylic alcohols.[152]

4.4.1 Optimization

The catalytic dehydrogenation of 4-methylbenzyl alcohol was selected as a model reaction and the effects of the most important reaction conditions were investigated. First, a test reaction was carried out with AgBi-HM catalyst under batch conditions and, in parallel, another reaction was performed applying $AgNO_3$ as catalyst under the same conditions (Scheme 28). After stirring the starting material for 24 h in toluene at 110 °C, 62% conversion was observed with the hybrid catalyst material. In contrast, $AgNO_3$ gave only a conversion of 15% (selectivity was 100% in both reactions). No conversion was observed without catalyst.

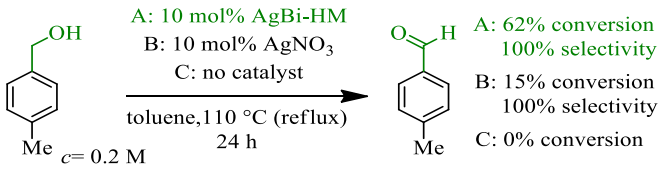

Scheme 28. *Catalytic dehydrogenation of 4-methylbenzyl alcohol under batch conditions*

Considering that AgBi-HM proved to be compatible with various solvents even at high temperatures (demonstrated in our previous article[152]), a comprehensive solvent screening was performed at 180 °C (Table 4). In CH_2Cl_2, acetone, EtOAc, and acetonitrile (MeCN), conversions of 20–46% were observed but the selectivity was very low (Table 4, entries 1–4). In DMSO, MeOH, THF or toluene, selective aldehyde product formation was detected (Table 4, entries 5–8). The best result was registered in toluene (92%, Table 4, entry 8). Therefore, toluene was selected as solvent for additional parameter optimization.

Table 4. *Investigating the effects of various solvents on the dehydrogenation reaction of 4-methylbenzyl alcohol under continuous-flow conditions*

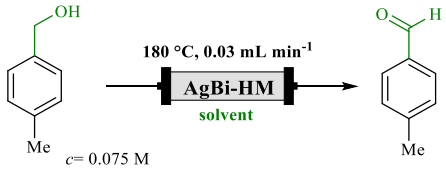

Entry	Solvent	Conversion[a] (%)	Selectivity[a] (%)
1	acetone	20	traces
2	CH_2Cl_2	36	traces
3	EtOAc	46	25
4	MeCN	27	40
5	DMSO	8	100
6	MeOH	4	100
7	THF	22	100
8	toluene	92	100

[a] *Determined by ^{1}H NMR analysis of the crude product*

The reaction temperature was found to have notable role both on conversion and selectivity (Figure 6a). The conversion improved remarkably upon gradual increase of the temperature: 92% conversion and 100% selectivity were measured at 180 °C. At 200 °C the benzylation reaction of toluene with the substrate appeared as a competing side reaction (the conversion increased, but the selectivity was only 62%). This type of benzylations is known in the literature requiring, however, higher temperatures and the presence of various metal catalysts.[160, 161] Thus, 180 °C was selected as the optimal temperature.

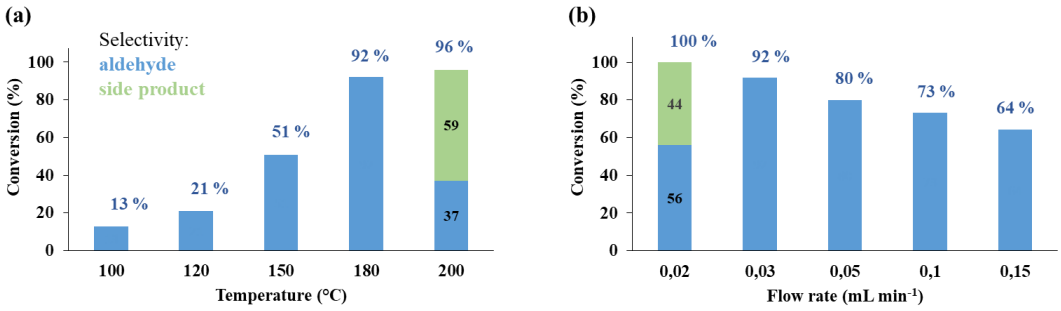

Figure 6. *Investigating the effects of temperature (a) and flow rate (b) on the AgBi-HM-catalyzed dehydrogenation of 4-methylbenzyl alcohol. Reaction conditions: c = 0.075 M, toluene as solvent, 0.03 mL min^{-1} flow rate for the temperature study, and 180 °C temperature for the flow-rate study)*

The residence time also had significant impacts on the reaction outcome (Figure 6b). At 0.02 mL min^{-1} flow rate (residence time of approximately 75 min), the conversion reached 100%; however, increasing gradually the flow rate to 0.15 mL min^{-1}, the conversion gradually

decreased from 100% to 64%. At the same time, at 0.02 mL/min^{-1} flow rate, the competing benzylation was also observed, which reduced the selectivity to 56%. Therefore, a flow rate of 0.03 mL min^{-1} (50 min residence time) was selected as optimum parameter affording a conversion of 92% and full selectivity.

The effects of substrate concentration were also explored with 0.075 M concentration showing the best results. Note, that the higher concentrations (0.1 and 0.15 M) led to side-product formation and lower selectivity.

4.4.2 Investigation of the scope and applicability of the reaction

Based on the findings of extended optimizations, reactions were carried out most effectively at 0.03 mL min^{-1} flow rate and 180 °C reaction temperature with a substrate concentration of 0.075 M. We started to explore the substrate scope of the method with these optimized conditions in hand (Table 5).

Table 5. *AgBi-HM-catalyzed dehydrogenation of diversely substituted benzyl alcohols under continuous-flow conditions*

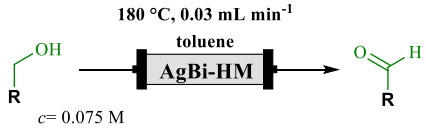

Entry	Substrate	Conversion[a] (%)	Selectivity[a] (%)	Entry	Substrate	Conversion[a] (%)	Selectivity[a] (%)
1	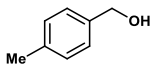	92	100	6	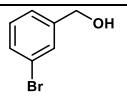	59	100
2	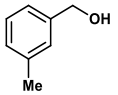	82	100	7	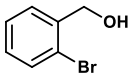	18	100
3	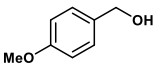	95	100	8	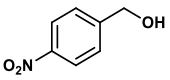	73	100
4	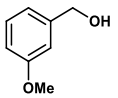	36	100	9	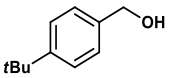	43	100
5	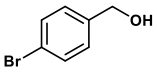	70	100	10	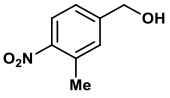	40	100

[a] Determined by ^{1}H NMR analysis of the crude product

In the case of *para*-substituted benzyl alcohol derivatives containing methyl, methoxy, bromo, and nitro groups, outstanding conversions were found. The transformation also worked well with *meta*-substituted benzyl alcohols (conversions were in the range of 36–82%). 3-

Methyl-4-nitrobenzyl alcohol, a bisubstituted derivative, gave an appropriate conversion of 40%. Dehydrogenation reaction of 2-bromobenzyl alcohol was also carried out; however, due to the notable steric hindrance generated by the *ortho*-bromo moiety, the conversion was merely 18%. In all reactions, aldehyde formation with full selectivity was detected without any side products.

4.5 Silver-catalyzed decarboxylation of carboxylic acids and silver-catalyzed decarboxylative deuteration under batch and flow conditions

Carboxylic acids are easily accessible, inexpensive materials and they have diverse structures. Therefore, these are ideal starting materials for several transformations.[11] Decarboxylation of carboxylic acids is significant in noble metal catalysis, where it plays an important role in the formation of many C–X, C–H, and C–C bonds.[13, 162] Cu, Ag, Pd, Au, and Rh are the most widely used catalysts in this type of reactions. In most cases, copper complex catalysts in the presence of bases or ligands are often applied for the protodecarboxylation of carboxylic acids (these are used mostly for *ortho*-substituted benzoic acid transformations). Whereas a few examples of heterogeneous catalysts can be found, homogeneous catalysts are predominated in copper-catalyzed examples.[163–165] Protodecarboxylation promoted by Pd complexes has also been explored, but the reactions require the use of large or stoichiometric amount of catalyst and the scope of the reaction is also limited.[166–168] Only a few studies have been performed in the field of Au-catalyzed protodecarboxylation due to its high cost. Nevertheless, in first insight, this reaction type revealed some reactivity trend similar to that of silver catalysts.[169–171] But silver-catalyzed protodecarboxylation reactions can be implemented under milder conditions, and they are inexpensive, and some carboxylic acids can be activated more effectively. Note, that with a few exceptions, heterogeneous examples cannot be found in the literature.[66, 172–174]

In decarboxylative cross-coupling reactions, the noble-metal-catalyzed decarboxylation of the carboxylic acid is the key step.[12] In the field of medical, analytical or pharmaceutical chemistry, many synthetic methods are able to incorporate deuterium (D) into various organic materials.[175] In contrast to high demand, synthetic processes for the selective incorporation of a single deuterium into an aromatic ring are limited.[12, 176, 177] These methods involve halogen/D exchange in most cases, which are commonly mediated by strong bases; therefore, there are limitations in functional group scope. Furthermore, H/D exchange reactions can be also performed with the application of noble metal catalysts[178] or strong bases[179] and acids.[180]

To the best of our knowledge, decarboxylation of carboxylic acids and decarboxylative deuteration of carboxylic acids was not reported using the combination of heterogeneous silver catalyst and continuous-flow technology so far. Therefore, we explored this reaction type under batch and flow conditions in the presence of our AgBi-HM catalyst.[181]

4.5.1 Optimization in batch system

For the catalytic model reaction, the decarboxylation of 2-nitrobenzoic acid was chosen to demonstrate the catalytic performance of our AgBi-HM preparation (Scheme 29).

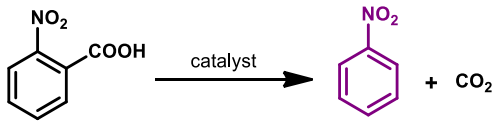

Scheme 29. *Model reaction: decarboxylation of 2-nitrobenzoic acid*

In this reaction type, the most frequently applied noble metal catalysts are silver- and copper-containing salts or complexes; hence, the hybrid material was compared with these commercially available catalysts (Figure 7). Based on literature data, DMF was the initial choice as solvent, 1 equiv. of substituted benzoic acid (0.15 M) and 15 mol% KOH were applied and the reaction mixture was stirred at 110 °C for 24 h. AgOAc, Ag_2O, Ag_2CO_3, and $AgNO_3$ revealed similar results compared to the hybrid material: the conversion was 96%, 97%, 95%, and 96% (almost quantitative) and the selectivity was 100% in every case. In the case of copper salts, the conversion was acceptable [CuOAc: 68%, $Cu(NO_3)_2$: 70%]. The exception is $CuBr_2$, which was less effective in this reaction with a conversion of 39%. However, we were delighted to find full conversion and selectivity in the presence of 5 mol% AgBi-HM. In addition, potassium 2-nitrobenzoate (which is the part of the proposed reaction mechanism by Toy and co-workers) appeared in these examples.[66] Besides, this model reaction was also carried out in the presence of 5 mol% of $Bi(NO_3)_3 \times 5H_2O$ as catalyst [Bi(III) is a structural element of the hybrid material], but it was inactive in the decarboxylation of 2-nitrobenzoic acid.

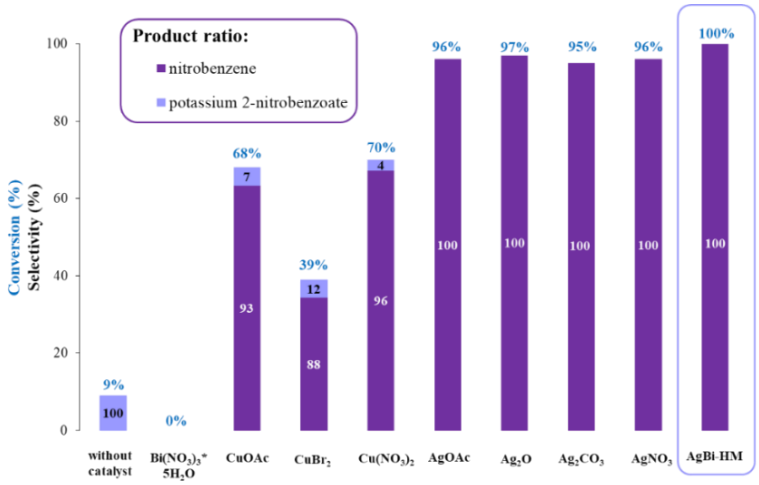

Figure 7. *Investigation of various catalysts in the decarboxylation of 2-nitrobenzoic acid. Reaction conditions: 1 equiv. (0.15 M) substrate, 5 mol% catalyst, 15 mol% KOH, DMF as solvent, 110 °C, 24 h reaction time*

After these promising preliminary results, we started to investigate the effects of the major reaction parameters in order to define the optimum conditions for the reaction process.

Table 6. *Investigation of various solvents in the AgBi-HM-catalyzed decarboxylation of 2-nitrobenzoic acid*

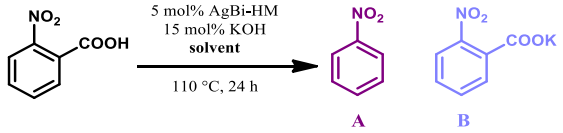

Entry	Solvent	Conversion (%)[a]	Product Selectivity (%)[a]	
			A	B
1	**DMF**	**100**	**100**	**0**
2	*MeCN*	*85*	*100*	*0*
3	*DMA*	*62*	*85*	*15*
4	EtOAc	11	100	0
5	toluene	3	100	0
6	NMP	7	0	100
7	DMSO	8	0	100

[a] Determined by ^{1}H NMR analysis of the crude product

Besides DMF, MeCN and DMA as dipolar aprotic solvents proved to be suitable reaction medium (Table 6). In MeCN the conversion was 85% with a selectivity of 100% (Table 6, entry 2) and in DMA the corresponding values are 62% and 85%, respectively (Table 6, entry 3). However, DMSO and NMP are also dipolar aprotic solvents. Nevertheless, formation of nitrobenzene was not promoted in these solvents (Table 6, entry 6, 7). In addition, we tested the

reaction in toluene and EtOAc (Table 6, entry 4, 5), but these resulted in very low conversions (3% and 11%).

Figure 8 demonstrates the effect of reaction time and temperature. The conversion increases gradually with the reaction time reaching completion after 24 h, but after 1 h the conversion already was 31%. These data led us to conclude that the reaction time should be 24 h to achieve optimum results. On the other hand, the reaction does not take place at lower temperature (based on literature data). Therefore, as expected, nitrobenzene product was not detected at 25 and 50 °C. However, at higher temperatures, nitrobenzene could be detected (a conversion of 45% at 80 °C) and the conversion was complete at 110 °C. Therefore, 110 °C was selected as the reaction temperature with quantitative conversion and full selectivity in 24 h.

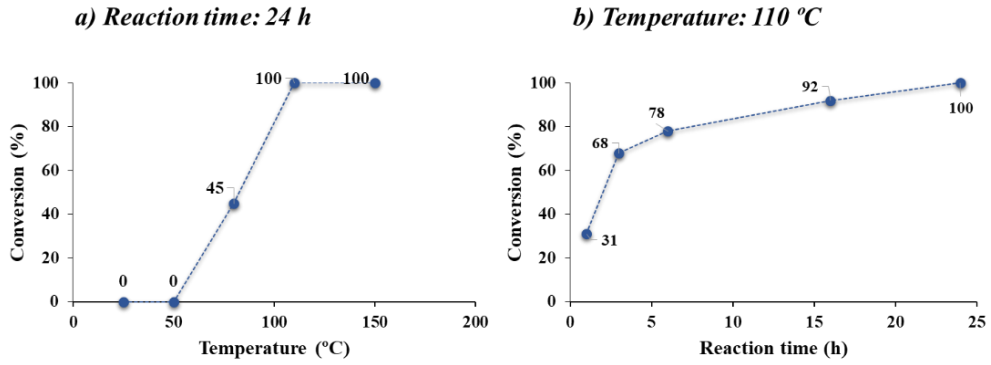

Figure 8. *Investigation of different temperatures (a) and reaction times (b) in the decarboxylation of 2-nitrobenzoic acid. Reaction conditions: 1 equiv. (0.15 M) substrate, 5 mol% AgBi-HM catalyst, 15 mol% KOH, DMF as solvent*

Finally, we examined the effect of concentration, catalyst loading and the quantity of KOH base (Table 7). The hybrid catalyst material was effective in the range of 0.1 and 0.25 M concentration (conversions between 100% and 63%) with full selectivity in every case. Based on these results, the optimal concentration was 0.15 M (Table 7, entries 1–4). With the use of 1 mol% hybrid material, the conversion was 25%, but the transformation was complete in the presence of 5 mol% catalyst (Table 7, entries 5–9). The presence of a potassium base proved to be necessary to obtain high conversion.[66] Nevertheless, we reduced its quantity and the optimal amount of the base corresponded to 15 mol%. Note, that without base, the conversion remained below 10% (Table 7, entries 10–14). In our study, we applied KOH as base, because no precipitation was involved and it ensured a pumpable clear solution when being combined with the substrate. This is a significant issue, when considering the upcoming continuous-flow experiments.

Table 7. *Investigation of concentration, catalyst loading and the quantity of KOH in the AgBi-HM-catalyzed decarboxylation of 2-nitrobenzoic acid*

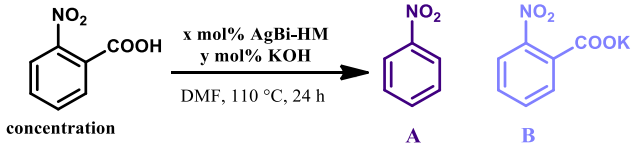

Entry	Concentration (mol/dm^3)	Catalyst loading (mol%)	KOH (mol%)	Conversion (%)[a]	Product Selectivity (%)[a]	
					A	B
1	**0.25**	5	15	63	100	0
2	**0.2**	5	15	86	100	0
3	**0.15**	5	15	100	100	0
4	**0.1**	5	15	100	100	0
5	0.15	**-**	15	9	0	100
6	0.15	**1**	15	25	100	0
7	0.15	**3**	15	69	93	7
8	0.15	**5**	15	100	100	0
9	0.15	**10**	15	100	100	0
10	0.15	5	**-**	8	100	0
11	0.15	5	**5**	80	100	0
12	0.15	5	**10**	85	100	0
13	0.15	5	**15**	100	100	0
14	0.15	5	**20**	100	100	0

[a] *Determined by ^{1}H NMR analysis of the crude product*

4.5.2 Investigation of the scope and applicability of the reaction in batch system

We set out to examine the applicability and scope of the synthesis method (Table 8), after establishing an optimal set of conditions for the decarboxylation of 2-nitrobenzoic acid (DMF as solvent, 0.15 M concentration, 110 ºC temperature, 24 h reaction time). The scope of the reaction was explored using various substituted aromatic carboxylic acids. Under the applicability of the process, the presence of an *ortho* substituent was necessary for decarboxylation to proceed in high yields over the heterogeneous AgBi-HM catalyst. In the first step of the applicability of the reaction, the conversion of 100% was observed with 2-nitrobenzoic acid (Table 8, entry 1). In the case of 5-methoxy-2-nitrobenzoic acid, both the conversion and selectivity were 100% (Table 8, entry 2). The same results were found with two nitro groups present at the *meta* positions (Table 8, entry 3). Nevertheless, replacing the strongly electron-withdrawing nitro group with a bromo substituent led to a lower conversion of 80%

(Table 8, entry 4). Carboxylic acids with activating substituents, such as 2-methoxybenzoic acid (Table 8, entry 5) and 2,6-dimethoxybenzoic acid (Table 8, entry 6), gave good reactivity. When there is one chloro group at the *ortho* position, the chlorobenzene product is not formed in the presence of AgBi-HM catalyst (Table 8, entry 7). In turn, 2,4-dichlorobenzoic acid with two chloro groups present at the *ortho* and *para* positions gave a conversion of 92% (Table 8, entry 9).

Table 8. *Exploring the decarboxylation of various carboxylic acids under batch conditions*

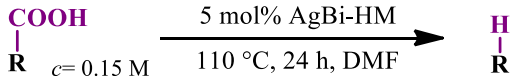

Entry	Substrate	Conversion[a] (%)	Selectivity[a] (%)	Entry	Substrate	Conversion[a] (%)	Selectivity[a] (%)
1	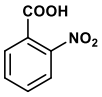	100	100	9	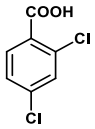	92	100
2	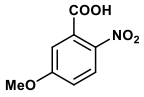	100	100	10	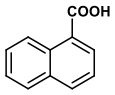	49	100
3	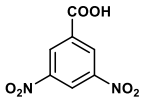	100	100	11	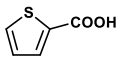	100	100
4	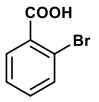	80	100	12	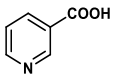	86	100
5		74	100	13	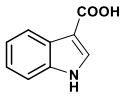	100	100
6	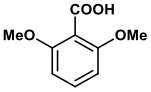	65	100	14	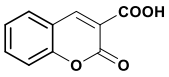	100	100
7		traces	-	15	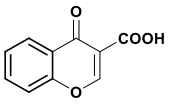	97	100
8		traces	-				

[a] Determined by ^{1}H NMR analysis of the crude product

On the other hand, *ortho*-hydroxybenzoic acid (Table 8, entry 8) was practically inert for decarboxylation over AgBi-HM catalyst. Acceptable results were obtained with 1-naphthoic acid starting material (Table 8, entry 10), and the decarboxylation of heteroaromatic carboxylic acids also underwent with high conversions (Table 8, entries 11 and 12). Excellent conversions (97–100%) and selectivities were also achieved in decarboxylations of fused heteroaromatic substrates; for instance, in the case of indole-3-carboxylic acid, coumarin-3-carboxylic acid,

and chromone-3-carboxylic (Table 8, entries 13–15). These results indicated that the AgBi-HM catalyst could tolerate a range of substituents such as nitro, methoxy or bromo groups as well as heteroaromatic, fused heteroaromatic, disubstituted carboxylic acids, or 1-naphthoic acid species.

4.5.3 Investigation of catalyst reusability

Sustainable application of heterogeneous catalysts is limited when irreversible substrate erosion or deposition takes place, or even the leaching of active components occurs.[182] We investigated the reusability and robustness of our catalyst in the AgBi-HM-catalyzed decarboxylation reaction. The reaction of 2-nitrobenzoic acid was explored repeatedly (conditions were as follows: 110 °C, DMF as solvent, 15 mol% KOH, 24 h, 5 mol% catalyst loading) applying the same portion of AgBi-HM. The catalyst was reused after washing and drying steps and it was removed between each cycle by centrifugation. Decrease in the activity or selectivity was not registered after 10 consecutive catalytic cycles (Figure 9). The selectivity was 100% in all reactions and the conversion of nitrobenzene was steady in the range of 82–100%. In any of the crude product mixtures analyzed, side product was not detected.

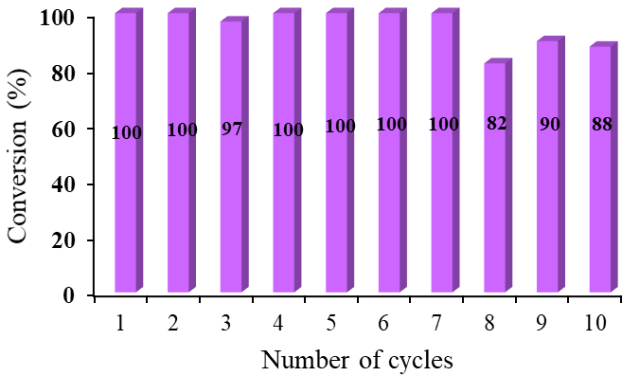

Figure 9. *Testing the reusability of the AgBi-HM catalyst in decarboxylation of 2-nitrobenzoic acid. Reaction conditions: 1 equiv. (0.15 M) substrate, 5 mol% catalyst, 15 mol% KOH, DMF as solvent, 110 °C, 24 h reaction time. The selectivity was 100% in every case*

4.5.4 Optimization in flow system

After establishing convincing batch results, we started to study the effects of the major reaction parameters in order to determine the optimum conditions for a sustainable flow process of the decarboxylation of carboxylic acids. As a model reaction, the decarboxylation of 2-nitrobenzoic acid was used again (Scheme 29) and we explored the effect of the quality of the solvents, flow rate, temperature, and concentration. We tested dipolar aprotic solvents under flow conditions, because these showed the best performances in batch reactions. Fine results

were observed in DMF, MeCN, and DMA; however, the 100% conversion and selectivity were only achieved in MeCN (Table 9, entries 1–3). The results showed that the concentrations had milder influence on the reaction, but the conversion and the selectivity were only complete at a concentration of 0.1 M (Table 9, entry 3–5).

Table 9. *Investigation of various solvents and concentrations in the AgBi-HM-catalyzed decarboxylation of 2-nitrobenzoic acid in flow reactor*

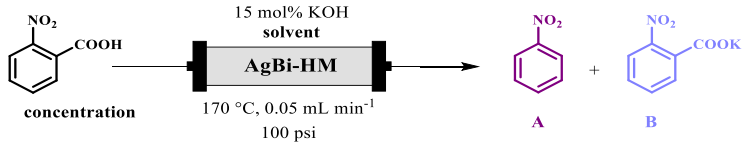

Entry	Solvent	Concentration (mol/dm^3)	Conversion (%)[a]	Product Selectivity (%)[a]	
				A	B
1	**DMA**	0.1	81	100	0
2	**DMF**	0.1	90	89	11
3	**MeCN**	**0.1**	100	100	0
4	MeCN	**0.15**	96	100	0
5	MeCN	**0.2**	85	100	0

[a] *Determined by ^{1}H NMR analysis of the crude product*

In the next step, the effect of the temperature was explored, where the results showed again that no decarboxylation occurs at low temperatures (even at 100 ºC the conversion was only 13%). For complete transformation and selectivity, 170 ºC was required (Figure 10a). The reduction of the flow rate from 0.15 mL min^{-1} eventuated an increase in the reaction rate with conversions of 89%, 100%, and 100% at 100, 50, and 0.03 mL min^{-1}, respectively (Figure 10b). At the optimal flow rate (0.05 mL min^{-1}) the residence time was 10.5 min.

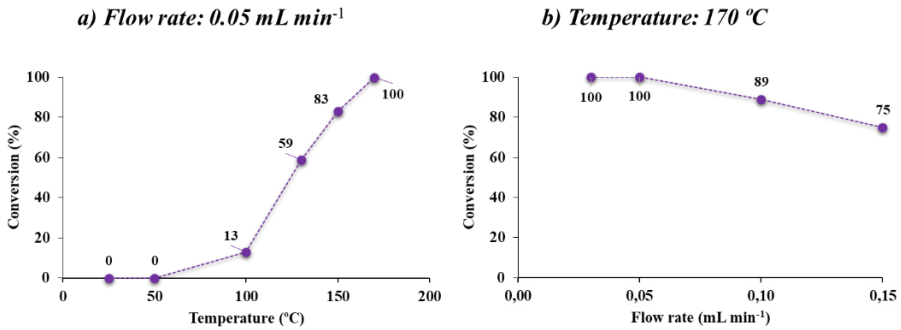

Figure 10. *Investigation of different temperature (a) and flow rate (b) in the decarboxylation of 2-nitrobenzoic acid in flow reactor. Reaction conditions: 1 equiv. (0.1 M) substrate, 15 mol% KOH, MeCN as solvent, 100 psi pressure*

4.5.5 Investigation of the scope and applicability of the reaction in flow system

Table 10. *Exploring the decarboxylation of various carboxylic acids in flow reactor*

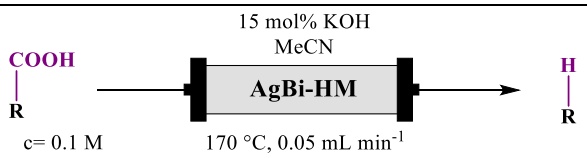

Entry	Substrate	Conversion[a] (%)	Selectivity[a] (%)	Entry	Substrate	Conversion[a] (%)	Selectivity[a] (%)
1	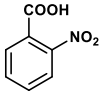	100	100	8		23	100
2	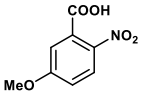	100	100	9[b]	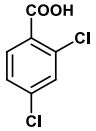	87	100
3	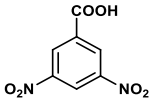	100	100	10	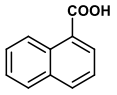	48	100
4	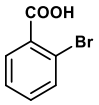	100	100	11[b]	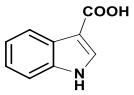	100	100
5[b]		100	100	12[b]	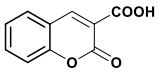	100	100
6	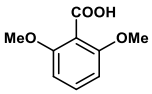	100	100	13[b]	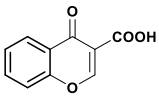	100	100
7		100	100				

[a] Determined by ^{1}H NMR analysis of the crude product

We set out to explore the scope and applicability of the flow methodology, after having established an optimal set of conditions for the decarboxylation of 2-nitrobenzoic acid (Table 10). The optimal conditions were as follows: MeCN as solvent, 0.1 M concentration, 15 mol% KOH, 100 psi pressure, 170 ºC temperature, and 10.5 min residence time (0.05 mL min^{-1} flow rate). Outstanding results were achieved for various *ortho*-substituted or disubstituted benzoic acids, and in the case of 1-naphthoic acid (Table 10, entry 1–7, 9, 10). Furthermore, acceptable results were also achieved for carboxylic acids containing hydroxyl group (activating substituents). However, in most of the cases, these materials did not react well in harmony with literature observations (Table 10, entry 8). 2-Methylbenzoic acid also remained inert in this

system. No product could be detected at the end of the reactions in the decarboxylation of heteroaromatic carboxylic acids, that is, these reactions were unsuccessful. The fused heteroaromatic substrates (Table 10, entries 11–13) gave complete conversion and selectivity under flow conditions. In entry 5, 9, and 11–13, the starting substrate was immiscible with the MeCN solvent used so far. Therefore, these reactions were carried out in DMF, because a homogeneous reaction mixture is fundamental for carrying out the flow reactions. No side-product formation was observed and the selectivity was 100% for all substrates used.

4.5.6 Investigation of the large-scale synthetic capability of AgBi-HM in flow system

The transformation of 2-nitrobenzoic acid was repeated in the gram scale to explore the preparative capabilities of the silver-mediated decarboxylation of carboxylic acids (Figure 11). In this investigation, a 20-h reaction window was monitored with a reduced 5-min residence time corresponding to a flow rate of 0.1 mL min^{-1}, applying 15 mol% KOH at a temperature of 170 ºC and a pressure of 100 psi. In addition, in order to avoid any product precipitation and possible clogging in the reactor channels, the concentration of the starting material was set to 0.1 M during the long experiment. To our delight, no side-product formation was found and the conversion remained steady around 80%. After then, only a slight loss in catalytic activity was observed, and a satisfying conversion of 71% could still be detected at the end of the experiment. Finally, 1.207 g of nitrobenzene was isolated after purification corresponding to an overall yield of 82%.

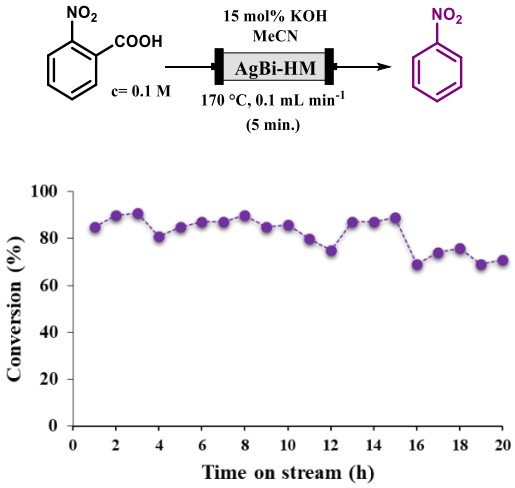

Figure 11. *Investigation of the large-scale synthetic capability of the AgBi-HM sample in the decarboxylation of 2-nitrobenzoic acid*

4.5.7 Characterization of the used AgBi-HM catalysts

To confirm that the hybrid material did not suffer structural damage or change under the reusability and the scale-up experiments, the used catalysts were explored extensively by TG,

SEM-EDX, and XRD methods (Figure 12). Thermal analysis demonstrated that weight losses occurred in three endothermic steps and the original structure was kept up to 380 °C as observed in both used samples. Nevertheless, in the case of the recovered AgBi-HM used in the batch process, some change could be detected (greater weight loss, lower temperatures), which can be caused by trace amounts of organic contaminants on the surface (Figure 12 a, b). The X-ray diffraction patterns of the used catalyst did not show any structural deformations and amorphizations (Figure 12 c). The SEM image displays a lamellar (plate-like) morphology in the used material similar to that observed in the freshly-made catalyst (Figure 12 d). SEM images also confirmed that organic contaminants remained on the surface, which resulted in difficulties to analyze the original morphology, because larger aggregates up to 10 µm were formed. To sum up, it could be confirmed that the AgBi-HM sample is a highly robust heterogeneous catalyst, which proved to be highly stable from a structural point of view after extended use and tests under extreme conditions and application in batch and flow reactions.

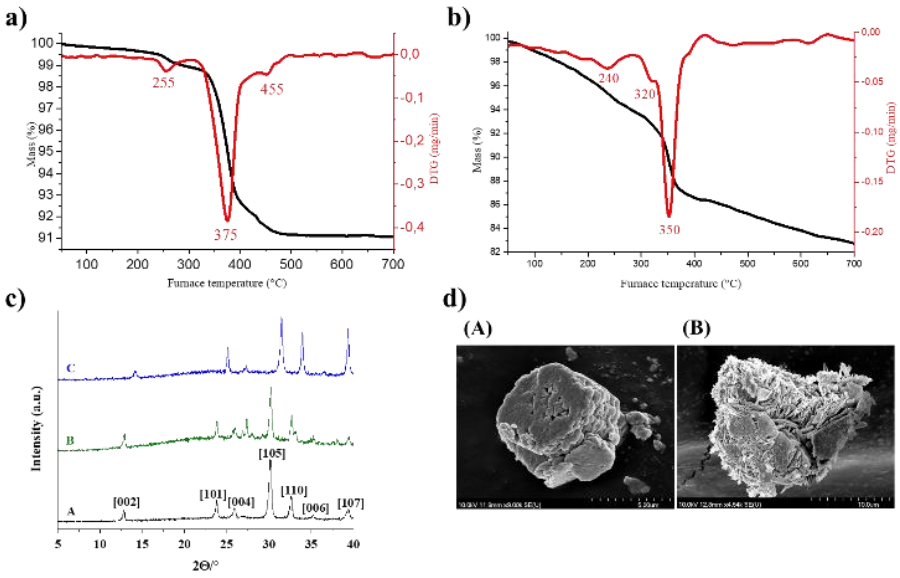

Figure 12. *a) Thermal behavior of the AgBi-HM catalyst used in flow reactor, b) Thermal behavior of the AgBi-HM catalyst used in batch reactor c) X-ray pattern of the untreated sample (A), the used catalyst in batch reactor (B), the catalyst used in flow reactor (C), d) SEM image of the untreated sample (A), SEM image of the catalyst used in flow reactor (A)*

4.5.8 Decarboxylative deuteration of carboxylic acids in batch and flow reactor

We tested the AgBi-HM catalyst in a model reaction in the batch system, where the conditions were the same as those applied in simple decarboxylation of 2-nitrobenzoic acid by adding 10 equiv. D_2O to the system and stirring for 24 h at 110 ºC (Scheme 32). The result was convincing: the conversion was 100% and the deuterium incorporation was 98%. After the successful batch results, we tested the hybrid catalyst material in decarboxylative deuteration

of 2-nitrobenzoic acid in a flow reactor (Scheme 30). In the model reaction, we used 10 equiv. D_2O, but deuterated nitrobenzene was only formed with 31% conversion. In the next step, we increased the quantity of D_2O to 20 equiv., which resulted in complete deuterium incorporation and 100% conversion in 10.5 min residence time.

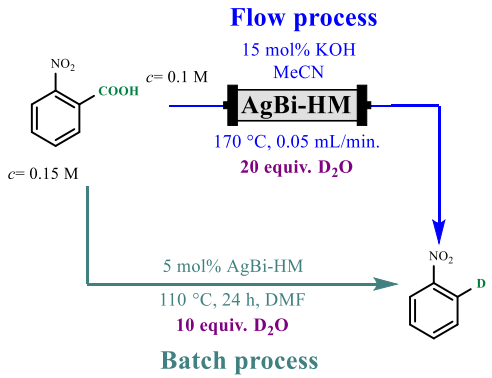

Scheme 30. *Model reaction for silver-catalyzed decarboxylative deuteration under batch and flow conditions*

With these optimized protocols in hand, we investigated the applicability of the reaction with other substituted benzoic acids in both systems (Table 11). The optimized conditions consistently afforded excellent conversions (79–100%) with high deuterium incorporations (76–100%). Thus, these results could demonstrate that AgBi-HM was perfectly suitable for decarboxylative deuteration of carboxylic acids not only in batch reactions, but also in flow chemistry reactions with excellent conversions and high deuterium incorporations.

Table 11. *Exploring the decarboxylative deuteration of various carboxylic acids under batch and flow conditions*

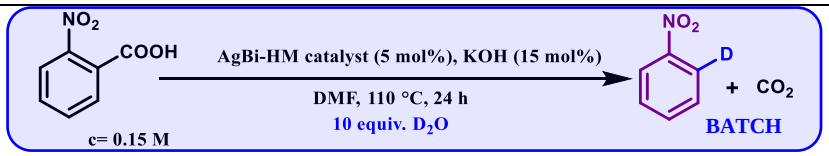

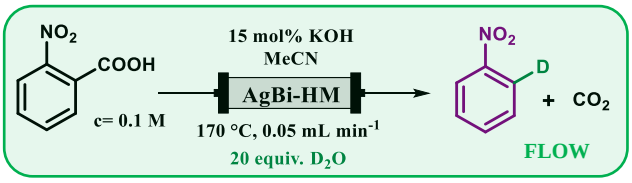

	Product	Conversion[a] (%) (batch)	D%[a] (%) (batch)	Conversion[a] (%) (flow)	D%[a] (%) (flow)
1	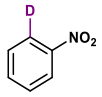	100	98	100	100
2		88	100	100	100
3	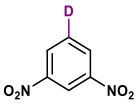	100	100	100	100
4	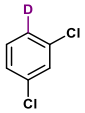	100	100	-	-
5	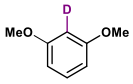	79	76	100	100
6	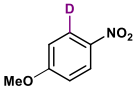	100	86	100	71

[a] *Determined by ^{1}H NMR analysis of the crude product. Selectivity was 100% in every case under batch and continuous-flow conditions.*

5. SUMMARY

In our work, we synthesized and characterized a novel silver–bismuth hybrid catalyst material for application in diverse silver-catalyzed synthesis methods. We utilized the advantages of this novel heterogeneous silver–bismuth hybrid material combined with precisely controlled flow reactor environment or batch process to investigate inexpensive, selective, and sustainable silver-catalyzed synthesis methods. Three different silver-catalyzed reactions were examined in our study. It was confirmed in all three tests, that the CF and/or batch processes employed can further improve the previously known synthetic reaction processes.

AgBi-HM in the direct synthesis of organic nitriles from terminal alkynes proved to be a robust, efficiently recyclable, highly active catalyst. The appropriate reaction parameters were explored for excellent product selectivity and conversion, where waste generation and side-product formation were minimal. A wide variety of aliphatic as well as aromatic alkynes were transformed into the corresponding nitriles with small amounts of triazole as the only unwanted product. The hot filtration test demonstrated the heterogeneous nature of the reaction. The hybrid material could be reused and recycled 10 times without detectable structural degradation or loss of activity. To the best of our knowledge, this reaction is the first example of a heterogeneous noble-metal-catalyzed nitrile synthesis via alkyne activation.

The stability of AgBi-HM was investigated in numerous organic solvents under continuous-flow conditions to aid potential synthetic applications. After the hybrid material was applied successfully in a batch process, a novel continuous-flow protocol was demonstrated for catalytic dehydrogenation of benzylic alcohols. The CF technology combined with heterogeneous silver catalyst was unexplored in the literature. The effects of reaction temperature, residence time, substrate concentration, and various solvents were examined to achieve high conversions and selective aldehyde formation without the need for any additives. The scope and applicability of the flow protocol was also demonstrated, where 10 different aldehyde products were synthesized with excellent or appropriate conversion and complete selectivity.

In the decarboxylation of carboxylic acids, our AgBi-HM preparation proved to be a robust, highly active, and efficiently recyclable catalyst as well. The reaction rate and the product selectivity were accurately optimized in order to achieve high-yielding nitrobenzene formation in batch and flow reactor without any by-product formation. Diverse aromatic benzoic acids were successfully transformed into the corresponding substituted arenes in both reaction pathways. The catalyst could be reused and recycled 10 times under batch conditions

without either the loss of activity or detectable structural degradation. Moreover, gram-scale experiments were also successful under flow conditions: 20 h of use of a single portion of catalyst resulted in 1.207 g nitrobenzene product with high conversion and selectivity. In both processes, the used catalyst was examined by different structural analysis methods to demonstrate that the catalyst did not undergo any structural damage or change.

On the other hand, this silver-containing material was not only applied in decarboxylation of carboxylic acids, but it was an effective catalyst in decarboxylative deuteration of carboxylic acids. These results provided strong inspiration to us to continue this project in the future to develop other sustainable decarboxylative coupling reactions with our robust and reusable AgBi-HM catalyst.

Acknowledgements

This PhD work was carried out in the Institute of Pharmaceutical Chemistry, University of Szeged, during the years 2016–2020.

I would like to express my deep gratitude to my supervisors, *Prof. Dr. Ferenc Fülöp*, *Dr. Sándor B. Ötvös*, and *Prof. Dr. István Pálinkó* for their scientific guidance, useful advice and constructive criticism.

I am grateful to all colleagues at the Institute of Pharmaceutical Chemistry, especially to *Zsanett Lukács-Szécsényi* and *Ádám Georgiádes* for their help, friendship, and the unforgettable memories.

I am grateful to all members of the Material and Solution Structure Research Group, especially to *Gábor Varga* for his help during my PhD studies.

I owe my thanks to *Prof. Árpád Molnár* for revising the English language of my thesis.

Finally, I would like to express my warmest thanks to my family and my friends, especially to *Márton Szabados* for their support during my PhD studies.

References

[1] M. Harmata, *Silver in organic chemistry*, Wiley, Hoboken, 2010.
[2] D. Yu, M. X. Tan, Y. Zhang, *Adv. Synth. Catal.*, **2012**, *354*, 969-974.
[3] J. An, G. Sun, H. Xia, *ACS Sustain. Chem. Eng.*, **2019**, *7*, 6696-6706.
[4] W.-J. Chen, B.-H. Cheng, Q.-T. Sun, H. Jiang, *ChemCatChem*, **2018**, *10*, 3659-3665.
[5] G. Fang, X. Bi, *Chem. Soc. Rev.*, **2015**, *44*, 8124-8173.
[6] F. F. Fleming, *Nat. Prod. Rep.*, **1999**, *16*, 597-606.
[7] J. Kim, H. J. Kim, S. Chang, *Angew. Chem. Int. Ed.*, **2012**, *51*, 11948-11959.
[8] T. Shen, T. Wang, C. Qin, N. Jiao, *Angew. Chem. Int. Ed.*, **2013**, *52*, 6677-6680.
[9] F. Cardona, C. Parmeggiani, C. Royal Society of, *Transition metal catalysis in aerobic alcohol oxidation*, 2015.
[10] R. Ciriminna, V. Pandarus, F. Béland, Y.-J. Xu, M. Pagliaro, *Org. Process Res. Dev.*, **2015**, *19*, 1554-1558.
[11] L. J. Gooßen, N. Rodríguez, K. Gooßen, *Angew. Chem. Int. Ed.*, **2008**, *47*, 3100-3120.
[12] M. A. Idris, S. Lee, *Synthesis*, **2020**, *52*, 2277-2298.
[13] C. Shen, P. Zhang, Q. Sun, S. Bai, T. S. A. Hor, X. Liu, *Chem. Soc. Rev.*, **2015**, *44*, 291-314.
[14] D. M. D'Souza, T. J. J. Müller, *Chem. Soc. Rev.*, **2007**, *36*, 1095-1108.
[15] M. L. Crawley, B. M. Trost, I. ebrary, *Applications of transition metal catalysis in drug discovery and development an industrial perspective*, John Wiley & Sons, Hoboken, N.J., 2012.
[16] Z. Du, Z. Shao, *Chem. Soc. Rev.*, **2013**, *42*, 1337-1378.
[17] S. H. A. M. Leenders, R. Gramage-Doria, B. de Bruin, J. N. H. Reek, *Chem. Soc. Rev.*, **2015**, *44*, 433-448.
[18] M. M. Díaz-Requejo, P. J. Pérez, *Chem. Rev.*, **2008**, *108*, 3379-3394.
[19] N. T. Patil, Y. Yamamoto, *Chem. Rev.*, **2008**, *108*, 3395-3442.
[20] N. Krause, Ö. Aksin-Artok, V. Breker, C. Deutsch, B. Gockel, M. Poonoth, Y. Sawama, Y. Sawama, T. Sun, C. Winter, *Pure Appl. Chem.*, **2010**, *82*, 1529-1536.
[21] K. Hirano, M. Miura, *Chem. Lett.*, **2015**, *44*, 868-873.
[22] Z. Chen, T. J. Meyer, *Angew. Chem. Int. Ed.*, **2013**, *52*, 700-703.
[23] L. Liang, D. Astruc, *Coordin. Chem. Rev.*, **2011**, *255*, 2933-2945.
[24] D. Liu, C. Liu, H. Li, A. Lei, *Chem. Commun.*, **2014**, *50*, 3623-3626.
[25] S. P. Teong, D. Yu, Y. N. Sum, Y. Zhang, *Green Chem.*, **2016**, *18*, 3499-3502.
[26] X.-Y. Dong, Y.-F. Zhang, C.-L. Ma, Q.-S. Gu, F.-L. Wang, Z.-L. Li, S.-P. Jiang, X.-Y. Liu, *Nat. Chem.*, **2019**, *11*, 1158-1166.
[27] B. M. Sutton, E. McGusty, D. T. Walz, M. J. DiMartino, *J. Med. Chem.*, **1972**, *15*, 1095-1098.
[28] P. Schwerdtfeger, *J. Am. Chem. Soc.*, **1989**, *111*, 7261-7262.
[29] F. Calderazzo, *J. Organomet. Chem.*, **1990**, *400*, 303-320.
[30] G. C. Bond, *Gold Bull.*, **1972**, *5*, 11-13.
[31] A. Stephen, K. Hashmi, *Gold Bull.*, **2004**, *37*, 51-65.
[32] G. C. Bond, P. A. Sermon, G. Webb, D. A. Buchanan, P. B. Wells, *J. Chem. Soc., Chem. Commun.*, **1973**, DOI: 10.1039/C3973000444B, 444b-445.
[33] H. Masatake, K. Tetsuhiko, S. Hiroshi, Y. Nobumasa, *Chem. Lett.*, **1987**, *16*, 405-408.
[34] G. J. Hutchings, *J. Catal.*, **1985**, *96*, 292-295.
[35] A. S. K. Hashmi, G. J. Hutchings, *Angew. Chem. Int. Ed.*, **2006**, *45*, 7896-7936.
[36] A. S. K. Hashmi, M. Rudolph, *Chem. Soc. Rev.*, **2008**, *37*, 1766-1775.
[37] Y. Zhang, X. Cui, F. Shi, Y. Deng, *Chem. Rev.*, **2012**, *112*, 2467-2505.
[38] W. Zi, F. Dean Toste, *Chem. Soc. Rev.*, **2016**, *45*, 4567-4589.
[39] G. J. Hutchings, *ACS Cent. Sci.*, **2018**, *4*, 1095-1101.

[40] R. Ciriminna, E. Falletta, C. Della Pina, J. H. Teles, M. Pagliaro, *Angew. Chem. Int. Ed.*, **2016**, *55*, 14210-14217.
[41] H. Peng, Y. Xi, N. Ronaghi, B. Dong, N. G. Akhmedov, X. Shi, *J. Am. Chem. Soc.*, **2014**, *136*, 13174-13177.
[42] C. Sun, X. Yuan, Y. Li, X. Li, Z. Zhao, *Org. Biomol. Chem.*, **2017**, *15*, 2721-2724.
[43] C. Duchemin, N. Cramer, *Org. Chem. Front.*, **2019**, *6*, 209-212.
[44] S. Medici, M. Peana, G. Crisponi, V. M. Nurchi, J. I. Lachowicz, M. Remelli, M. A. Zoroddu, *Coordin. Chem. Rev.*, **2016**, *327-328*, 349-359.
[45] H. Pellissier, *Chem. Rev.*, **2016**, *116*, 14868-14917.
[46] R. Sreedevi, S. Saranya, G. Anilkumar, *Adv. Synth. Catal.*, **2019**, *361*, 4625-4644.
[47] M. Gao, C. He, H. Chen, R. Bai, B. Cheng, A. Lei, *Angew. Chem. Int. Ed.*, **2013**, *52*, 6958-6961.
[48] C. He, S. Guo, J. Ke, J. Hao, H. Xu, H. Chen, A. Lei, *J. Am. Chem. Soc.*, **2012**, *134*, 5766-5769.
[49] P.-F. Wang, X.-Q. Wang, J.-J. Dai, Y.-S. Feng, H.-J. Xu, *Org. Lett.*, **2014**, *16*, 4586-4589.
[50] T. Yurino, Y. Tange, R. Tani, T. Ohkuma, *Org. Chem. Front.*, **2020**, *7*, 1308-1313.
[51] G. Fang, X. Bi, in *Silver Catalysis in Organic Synthesis*, 2019, DOI: https://doi.org/10.1002/9783527342822.ch11, pp. 661-722.
[52] A. Yanagisawa, H. Nakashima, A. Ishiba, H. Yamamoto, *J. Am. Chem. Soc.*, **1996**, *118*, 4723-4724.
[53] J. M. Carney, P. J. Donoghue, W. M. Wuest, O. Wiest, P. Helquist, *Org. Lett.*, **2008**, *10*, 3903-3906.
[54] Z. Wang, L. Zhu, F. Yin, Z. Su, Z. Li, C. Li, *J. Am. Chem. Soc.*, **2012**, *134*, 4258-4263.
[55] F. Lazreg, M. Lesieur, A. J. Samson, C. S. J. Cazin, *ChemCatChem*, **2016**, *8*, 209-213.
[56] C. Wen, A. Yin, W.-L. Dai, *Appl. Catal. B* **2014**, *160-161*, 730-741.
[57] U. Landman, U. Heiz, *Nanocatalysis*, Springer, Berlin, 2006.
[58] S. B. Kalidindi, B. R. Jagirdar, *ChemSusChem*, **2012**, *5*, 65-75.
[59] V. Polshettiwar, T. Asefa, *Nanocatalysis Synthesis and Applications Polshettiwar/Nanocatalysis*, John Wiley & Sons, Inc., Hoboken, NJ, USA, 2013.
[60] D. L. Feldheim, Metal nanoparticles : synthesis, characterization, and applications, http://www.materialsnetbase.com/ejournals/books/book_km.asp?id=7297).
[61] N. Yan, C. Xiao, Y. Kou, *Coordin. Chem. Rev.*, **2010**, *254*, 1179-1218.
[62] X.-Y. Dong, Z.-W. Gao, K.-F. Yang, W.-Q. Zhang, L.-W. Xu, *Catal. Sci. Technol.*, **2015**, *5*, 2554-2574.
[63] T. Mitsudome, Y. Mikami, H. Funai, T. Mizugaki, K. Jitsukawa, K. Kaneda, *Angew. Chem. Int. Ed.*, **2008**, *47*, 138-141.
[64] A. K. Clarke, M. J. James, P. O'Brien, R. J. K. Taylor, W. P. Unsworth, *Angew. Chem. Int. Ed.*, **2016**, *55*, 13798-13802.
[65] S. Cai, H. Rong, X. Yu, X. Liu, D. Wang, W. He, Y. Li, *ACS Catal.*, **2013**, *3*, 478-486.
[66] X. Y. Toy, I. I. B. Roslan, G. K. Chuah, S. Jaenicke, *Catal. Sci. Technol.*, **2014**, *4*, 516-523.
[67] J. D. Kim, T. Palani, M. R. Kumar, S. Lee, H. C. Choi, *J. Mater. Chem.*, **2012**, *22*, 20665-20670.
[68] N. Salam, A. Sinha, A. S. Roy, P. Mondal, N. R. Jana, S. M. Islam, *RSC Adv.*, **2014**, *4*, 10001-10012.
[69] J. Safari, S. Gandomi-Ravandi, *RSC Adv.*, **2014**, *4*, 11654-11660.
[70] G. Prieto, J. Zečević, H. Friedrich, K. P. de Jong, P. E. de Jongh, *Nat. Mater.*, **2013**, *12*, 34-39.
[71] C. T. Campbell, *Accounts Chem. Res.*, **2013**, *46*, 1712-1719.
[72] L. D. Pachón, G. Rothenberg, *Appl. Organomet. Chem.*, **2008**, *22*, 288-299.
[73] R. Ricciardi, J. Huskens, W. Verboom, *ChemSusChem*, **2015**, *8*, 2586-2605.
[74] K.-i. Shimizu, Y. Miyamoto, A. Satsuma, *J. Catal.*, **2010**, *270*, 86-94.
[75] J. F. Hartwig, *Synlett*, **2006**, *2006*, 1283-1294.

[76] X. Cui, Y. Zhang, F. Shi, Y. Deng, *Chem. Eur. J.*, **2011**, *17*, 1021-1028.
[77] G.-P. Yong, D. Tian, H.-W. Tong, S.-M. Liu, *J. Mol. Catal. A Chem.*, **2010**, *323*, 40-44.
[78] T. Mitsudome, Y. Mikami, H. Mori, S. Arita, T. Mizugaki, K. Jitsukawa, K. Kaneda, *Chem. Commun.*, **2009**, DOI: 10.1039/B902469G, 3258-3260.
[79] T. Yasukawa, H. Miyamura, S. Kobayashi, *J. Am. Chem. Soc.*, **2012**, *134*, 16963-16966.
[80] K. Mohan Reddy, N. Seshu Babu, I. Suryanarayana, P. S. Sai Prasad, N. Lingaiah, *Tetrahedron Lett.*, **2006**, *47*, 7563-7566.
[81] K. T. Venkateswara Rao, P. S. Sai Prasad, N. Lingaiah, *Green Chem.*, **2012**, *14*, 1507-1514.
[82] X. Tang, C. Qi, H. He, H. Jiang, Y. Ren, G. Yuan, *Adv. Synth. Catal.*, **2013**, *355*, 2019-2028.
[83] A. H. Jadhav, A. Chinnappan, R. H. Patil, W.-J. Chung, H. Kim, *Chem. Eng. J.*, **2014**, *236*, 300-305.
[84] M. Jeganathan, A. Dhakshinamoorthy, K. Pitchumani, *ACS Sustain. Chem. Eng.*, **2014**, *2*, 781-787.
[85] J. Cao, G. Xu, P. Li, M. Tao, W. Zhang, *ACS Sustain. Chem. Eng.*, **2017**, *5*, 3438-3447.
[86] M. P. Dudukovic, F. Larachi, P. L. Mills, *Chem. Eng. Sci.*, **1999**, *54*, 1975-1995.
[87] M. Baumann, I. R. Baxendale, *Beilstein J. Org. Chem.*, **2015**, *11*, 1194-1219.
[88] B. Gutmann, D. Cantillo, C. O. Kappe, *Angew. Chem. Int. Ed.*, **2015**, *54*, 6688-6728.
[89] V. Hessel, H. Löwe, *Chem. Eng. Technol.*, **2005**, *28*, 267-284.
[90] A. Nagaki, N. Takabayashi, Y. Tomida, J.-i. Yoshida, *Org. Lett.*, **2008**, *10*, 3937-3940.
[91] J. J. M. van der Linden, P. W. Hilberink, C. M. P. Kronenburg, G. J. Kemperman, *Org. Process Res. Dev.*, **2008**, *12*, 911-920.
[92] W. Ehrfeld, V. Hessel, H. Löwe, *Microreactors : New technology for modern chemistry*, Wiley-VCH, Weinheim, 2000.
[93] A. R. Bogdan, N. W. Sach, *Adv. Synth. Catal.*, **2009**, *351*, 849-854.
[94] K. Geyer, T. Gustafsson, P. H. Seeberger, *Synlett.*, **2009**, *20*, 2382.
[95] C. Wiles, P. Watts, *Eur. J. Org. Chem.*, **2008**, *2008*, 1655-1671.
[96] P. Watts, S. J. Haswell, *Chem. Soc. Rev.*, **2005**, *34*, 235-246.
[97] R. L. Hartman, J. P. McMullen, K. F. Jensen, *Angew. Chem. Int. Ed.*, **2011**, *50*, 7502-7519.
[98] J. Wegner, S. Ceylan, A. Kirschning, *Chem. Commun.*, **2011**, *47*, 4583-4592.
[99] C. G. Frost, L. Mutton, *Green Chem.*, **2010**, *12*, 1687-1703.
[100] T. Razzaq, C. O. Kappe, *Chem. Asian J.*, **2010**, *5*, 1274-1289.
[101] A. Nagaki, S. Yamada, M. Doi, Y. Tomida, N. Takabayashi, J.-i. Yoshida, *Green Chem.*, **2011**, *13*, 1110-1113.
[102] J.-i. Yoshida, Y. Takahashi, A. Nagaki, *Chem. Commun.*, **2013**, *49*, 9896-9904.
[103] I. R. Baxendale, L. Brocken, C. J. Mallia, *Green Process. Synth.*, **2013**, *2*, 211-230.
[104] S. T. R. Müller, T. Wirth, *ChemSusChem*, **2015**, *8*, 245-250.
[105] B. Gutmann, U. Weigl, D. P. Cox, C. O. Kappe, *Chem. Eur. J.*, **2016**, *22*, 10393-10398.
[106] C. J. Mallia, I. R. Baxendale, *Org. Process Res. Dev.*, **2016**, *20*, 327-360.
[107] M. D. Hopkin, I. R. Baxendale, S. V. Ley, *Chem. Commun.*, **2010**, *46*, 2450-2452.
[108] R. Porta, M. Benaglia, A. Puglisi, *Org. Process Res. Dev.*, **2016**, *20*, 2-25.
[109] J. J. Pagano, T. Bánsági Jr., O. Steinbock, *Angew. Chem. Int. Ed.*, **2008**, *47*, 9900-9903.
[110] M. P. Tsang, G. Philippot, C. Aymonier, G. Sonnemann, *ACS Sustain. Chem. Eng.*, **2018**, *6*, 5142-5151.
[111] F. J. Martin-Martinez, K. Jin, D. López Barreiro, M. J. Buehler, *ACS Nano*, **2018**, *12*, 7425-7433.
[112] I. R. Baxendale, J. Deeley, C. M. Griffiths-Jones, S. V. Ley, S. Saaby, G. K. Tranmer, *Chem. Commun.*, **2006**, DOI: 10.1039/B600382F, 2566-2568.
[113] M. Baumann, I. R. Baxendale, S. V. Ley, *Mol. Divers.*, **2011**, *15*, 613-630.
[114] S. Katayama, T. Koge, S. Katsuragi, S. Akai, T. Oishi, *Chem. Lett.*, **2018**, *47*, 1116-1118.
[115] K. Masuda, T. Ichitsuka, N. Koumura, K. Sato, S. Kobayashi, *Tetrahedron*, **2018**, *74*, 1705-1730.

[116] D. Cantillo, C. O. Kappe, *ChemCatChem*, **2014**, *6*, 3286-3305.
[117] R. Munirathinam, J. Huskens, W. Verboom, *Adv. Synth. Catal.*, **2015**, *357*, 1093-1123.
[118] A. Tanimu, S. Jaenicke, K. Alhooshani, *Chem. Eng. J.*, **2017**, *327*, 792-821.
[119] M. Irfan, T. N. Glasnov, C. O. Kappe, *ChemSusChem*, **2011**, *4*, 300-316.
[120] L. Zhang, Z. Liu, Y. Wang, R. Xie, X.-J. Ju, W. Wang, L.-G. Lin, L.-Y. Chu, *Chemical Engineering Journal*, **2017**, *309*, 691-699.
[121] R. L. Papurello, J. L. Fernández, E. E. Miró, J. M. Zamaro, *Chemical Engineering Journal*, **2017**, *313*, 1468-1476.
[122] W. R. Reynolds, P. Plucinski, C. G. Frost, *Catal. Sci. Technol.*, **2014**, *4*, 948-954.
[123] F. Ferlin, L. Luciani, S. Santoro, A. Marrocchi, D. Lanari, A. Bechtoldt, L. Ackermann, L. Vaccaro, *Green Chem.*, **2018**, *20*, 2888-2893.
[124] F. Ferlin, T. Giannoni, A. Zuliani, O. Piermatti, R. Luque, L. Vaccaro, *ChemSusChem*, **2019**, *12*, 3178-3184.
[125] A. Inayat, M. Klumpp, W. Schwieger, *Appl. Clay Sci.*, **2011**, *51*, 452-459.
[126] S. B. Ötvös, Á. Georgiádes, R. Mészáros, K. Kis, I. Pálinkó, F. Fülöp, *J. Catal.*, **2017**, *348*, 90-99.
[127] F. A. Cotton, G. Wilkinson, *Advanced inorganic chemistry : a comprehensive text*, Wiley, New York, N.Y., 1988.
[128] G. Fan, F. Li, D. G. Evans, X. Duan, *Chem. Soc. Rev.*, **2014**, *43*, 7040-7066.
[129] J. Feng, Y. He, Y. Liu, Y. Du, D. Li, *Chem. Soc. Rev.*, **2015**, *44*, 5291-5319.
[130] A. V. Besserguenev, A. M. Fogg, R. J. Francis, S. J. Price, D. O'Hare, V. P. Isupov, B. P. Tolochko, *Chem. Mater.*, **1997**, *9*, 241-247.
[131] V. Malik, M. Pokhriyal, S. Uma, *RSC Adv.*, **2016**, *6*, 38252-38262.
[132] S. B. Ötvös, R. Mészáros, G. Varga, M. Kocsis, Z. Kónya, Á. Kukovecz, P. Pusztai, P. Sipos, I. Pálinkó, F. Fülöp, *Green Chem.*, **2018**, *20*, 1007-1019.
[133] B. M. Trost, C.-J. Li, *Modern alkyne chemistry : catalytic and atom-economic transformations*, 2015.
[134] F. Chen, T. Wang, N. Jiao, *Chem. Rev.*, **2014**, *114*, 8613-8661.
[135] M. Meldal, C. W. Tornøe, *Chem. Rev.*, **2008**, *108*, 2952-3015.
[136] R. Chinchilla, C. Nájera, *Chem. Rev.*, **2014**, *114*, 1783-1826.
[137] P. Gao, X.-R. Song, X.-Y. Liu, Y.-M. Liang, *Chem. Eur. J.*, **2015**, *21*, 7648-7661.
[138] Q.-Z. Zheng, N. Jiao, *Chem. Soc. Rev.*, **2016**, *45*, 4590-4627.
[139] R. K. Kumar, X. Bi, *Chem. Commun.*, **2016**, *52*, 853-868.
[140] Z. Zhou, C. He, L. Yang, Y. Wang, T. Liu, C. Duan, *ACS Catal.*, **2017**, *7*, 2248-2256.
[141] L.-G. Xie, S. Niyomchon, A. J. Mota, L. González, N. Maulide, *Nat. Commun.*, **2016**, *7*, 10914.
[142] Z. Rappoport, *The chemistry of the cyano group*, 1970.
[143] F. F. Fleming, L. Yao, P. C. Ravikumar, L. Funk, B. C. Shook, *J. Med. Chem.*, **2010**, *53*, 7902-7917.
[144] H. H. Hodgson, *Chem. Rev.*, **1947**, *40*, 251-277.
[145] B. V. Rokade, K. R. Prabhu, *J. Org. Chem.*, **2012**, *77*, 5364-5370.
[146] A. Martin, B. Lücke, *Catal. Today*, **2000**, *57*, 61-70.
[147] M. K. Singh, M. K. Lakshman, *J. Org. Chem.*, **2009**, *74*, 3079-3084.
[148] R. Huisgen, *Angew. Chem. Int. Ed.*, **1963**, *2*, 565-598.
[149] T. B. Phan, H. Mayr, *J. Phys. Org. Chem.*, **2006**, *19*, 706-713.
[150] M. B. T. Thuong, A. Mann, A. Wagner, *Chem. Commun.*, **2012**, *48*, 434-436.
[151] G. Ertl, *Handbook of heterogeneous catalysis*, Wiley-VCH, Weinheim; Weinheim, 2008.
[152] R. Mészáros, S. B. Ötvös, G. Varga, É. Böszörményi, M. Kocsis, K. Karádi, Z. Kónya, Á. Kukovecz, I. Pálinkó, F. Fülöp, *Mol. Catal.*, **2020**, *498*, 111263.
[153] C. Parmeggiani, C. Matassini, F. Cardona, *Green Chem.*, **2017**, *19*, 2030-2050.
[154] V. V. Torbina, A. A. Vodyankin, S. Ten, G. V. Mamontov, M. A. Salaev, V. I. Sobolev, O. V. Vodyankina, *Catalysts*, **2018**, *8*, 447.

[155] J. Zheng, J. Qu, H. Lin, Q. Zhang, X. Yuan, Y. Yang, Y. Yuan, *ACS Catal.*, **2016**, *6*, 6662-6669.
[156] K.-i. Shimizu, K. Sugino, K. Sawabe, A. Satsuma, *Chem. Eur. J.*, **2009**, *15*, 2341-2351.
[157] V. L. Sushkevich, I. I. Ivanova, E. Taarning, *ChemCatChem*, **2013**, *5*, 2367-2373.
[158] D. K. Kurhe, T. A. Fernandes, T. S. Deore, R. V. Jayaram, *RSC Adv.*, **2015**, *5*, 46443-46447.
[159] F. Liu, H. Wang, A. Sapi, H. Tatsumi, D. Zherebetskyy, H.-L. Han, L. M. Carl, G. A. Somorjai, *Catalysts*, **2018**, *8*, 226.
[160] J. Choudhury, S. Podder, S. Roy, *J. Am. Chem. Soc.*, **2005**, *127*, 6162-6163.
[161] A. K. Maity, P. N. Chatterjee, S. Roy, *Tetrahedron*, **2013**, *69*, 942-956.
[162] T. Patra, D. Maiti, *Chem. Eur. J.*, **2017**, *23*.
[163] L. J. Gooßen, W. R. Thiel, N. Rodríguez, C. Linder, B. Melzer, *Adv. Synth. Catal.*, **2007**, *349*, 2241-2246.
[164] M. T. Keßler, C. Gedig, S. Sahler, P. Wand, S. Robke, M. H. G. Prechtl, *Catal. Sci. Technol.*, **2013**, *3*, 992-1001.
[165] Z. Li, Z. Fu, H. Zhang, J. Long, Y. Song, H. Cai, *New J. Chem.*, **2016**, *40*, 3014-3018.
[166] S. Pan, B. Zhou, Y. Zhang, C. Shao, G. Shi, *Synlett*, **2016**, *27*, 277-281.
[167] M. H. Al-Huniti, M. A. Perez, M. K. Garr, M. P. Croatt, *Org. Lett.*, **2018**, *20*, 7375-7379.
[168] R. A. Daley, J. J. Topczewski, *Synthesis*, **2020**, *52*, 365-377.
[169] S. Dupuy, S. P. Nolan, *Chem. Eur. J.*, **2013**, *19*, 14034-14038.
[170] S. Dupuy, L. Crawford, M. Bühl, S. P. Nolan, *Chem. Eur. J.*, **2015**, *21*, 3399-3408.
[171] H. Hikawa, F. Kotaki, S. Kikkawa, I. Azumaya, *J. Org. Chem.*, **2019**, *84*, 1972-1979.
[172] J. Cornella, C. Sanchez, D. Banawa, I. Larrosa, *Chem. Commun.*, **2009**, DOI: 10.1039/B916646G, 7176-7178.
[173] S. Seo, J. B. Taylor, M. F. Greaney, *Chem. Commun.*, **2012**, *48*, 8270-8272.
[174] K. Zhan, Y. Li, *Catalysts*, **2017**, *7*, 314.
[175] J. Atzrodt, V. Derdau, W. J. Kerr, M. Reid, *Angew. Chem. Int. Ed.*, **2018**, *57*, 1758-1784.
[176] M. Rudzki, A. Alcalde-Aragonés, W. I. Dzik, N. Rodríguez, L. J. Gooßen, *Synthesis*, **2012**, *44*, 184-193.
[177] R. Grainger, A. Nikmal, J. Cornella, I. Larrosa, *Org. Biomol. Chem.*, **2012**, *10*, 3172-3174.
[178] G. Erdogan, D. B. Grotjahn, *J. Am. Chem. Soc.*, **2009**, *131*, 10354-10355.
[179] G. S. Coumbarides, M. Dingjan, J. Eames, A. Flinn, J. Northen, *J. Labelled Comp. Radiopharm.* , **2006**, *49*, 903-914.
[180] P. S. Kiuru, K. Wähälä, *Steroids*, **2006**, *71*, 54-60.
[181] R. Mészáros, A. Márton, M. Szabados, G. Varga, Z. Kónya, Á. Kukovecz, F. Fülöp, I. Pálinkó, S. B. Ötvös, *Green Chem.*, **2021**, 23, 4685-4696.
[182] J. M. Thomas, W. J. Thomas, *Principles and practice of heterogeneous catalysis*, VCH, Weinheim, 1997.

Appendix

I

An article presented by Dr. Sándor B. Ötvös, Profs. István Pálinkó and Ferenc Fülöp *et al.* of the University of Szeged, Hungary.

A mineralogically-inspired silver–bismuth hybrid material: an efficient heterogeneous catalyst for the direct synthesis of nitriles from terminal alkynes

A solid material with structurally-bound silver catalytic centers was designed. It showed remarkable activity in silver-catalyzed C≡C bond activation to yield organic nitriles directly from terminal alkynes with less environmental concerns than the classical methods. The heterogeneous nature of the reaction was demonstrated and the solid catalyst could be recycled numerous times without loss of activity and degradation of structure.

As featured in:

See Sándor B. Ötvös, István Pálinkó, Ferenc Fülöp *et al.*, *Green Chem.*, 2018, **20**, 1007.

ROYAL SOCIETY OF CHEMISTRY

rsc.li/greenchem

Registered charity number: 207890

Green Chemistry

PAPER

View Article Online
View Journal | View Issue

Cite this: *Green Chem.*, 2018, **20**, 1007

A mineralogically-inspired silver–bismuth hybrid material: an efficient heterogeneous catalyst for the direct synthesis of nitriles from terminal alkynes†

Sándor B. Ötvös, *[a,b] Rebeka Mészáros,[a] Gábor Varga,[c,d] Marianna Kocsis,[a,c,d] Zoltán Kónya,[e,f] Ákos Kukovecz,[f] Péter Pusztai,[f] Pál Sipos,[d,g] István Pálinkó *[c,d] and Ferenc Fülöp *[a,b]

The synthesis and characterization of a silver-containing hybrid material is reported as a novel heterogeneous noble metal catalyst. In order to eliminate the need for traditional immobilization techniques, and to create a solid material with structurally-bound silver catalytic centers, the layered structure of a naturally occurring mineral served as the basis of the initial catalyst design. The novel material was prepared by means of the urea-mediated homogeneous precipitation of the corresponding metal nitrates, and was fully characterized by means of diverse instrumental techniques (X-ray diffractometry, Raman, IR, UV-Vis, EPR, X-ray photoelectron spectroscopies, thermal methods as well as atomic force, scanning and transmission electron microscopies). The as-prepared material exhibited outstanding activity in silver-catalyzed C≡C bond activation to yield organic nitriles directly from terminal alkynes with less environmental concerns as compared to the classical synthesis methods. The effects of the reaction time, the temperature, as well as the role of various solvents, nitrogen sources and additives were carefully scrutinized in order to achieve high-yielding and selective nitrile formation. The heterogeneous nature of the reaction was verified and the solid catalyst was recycled and reused numerous times without loss of its activity or degradation of its structure, thereby offering a sustainable synthetic methodology.

Received 14th August 2017,
Accepted 7th January 2018

DOI: 10.1039/c7gc02487h

rsc.li/greenchem

Introduction

Silver-mediated transformations have attained much importance in organic syntheses, which is exemplified by the large number of related review articles published in the last couple of years.[1] Silver-based heterogeneous catalysts play historical roles in industrial oxidation processes, and they are also important in environmental applications (*e.g.*, in catalytic elimination of pollutants).[2] Fine-chemical syntheses (either in industry or in academic research) typically rely on Ag(I) salts or (*in situ* generated) complexes as homogeneous sources for the catalytically active metal.[1,3]

Because of environmental and economic reasons, there is increasing need for heterogeneous noble metal catalysts. A literature survey indicates that amongst heterogeneous silver-mediated processes, the application of supported nanoparticles predominates.[4] This can be explained by the fact that silver nanoparticles can readily be immobilized on various surfaces, such as activated charcoal,[5] silica,[6] alumina,[7] carbon nanotubes,[8] hydrotalcite materials,[9] graphene[10] or graphene oxide.[11] The main limitation of supported nanoparticles is that the catalytic metal is typically attached to the surface *via* weak forces,[12] which often results in limited catalyst stability and robustness, especially under demanding reaction conditions, such as high-temperature, high-pressure and continuous-flow conditions or in the presence of coordinating ligands

[a]*Institute of Pharmaceutical Chemistry, University of Szeged, Eötvös u. 6, H-6720 Szeged, Hungary. E-mail: otvossandor@pharm.u-szeged.hu*
[b]*MTA-SZTE Stereochemistry Research Group, Hungarian Academy of Sciences, Eötvös u. 6, H-6720 Szeged, Hungary. E-mail: fulop@pharm.u-szeged.hu*
[c]*Department of Organic Chemistry, University of Szeged, Dóm tér 8, H-6720 Szeged, Hungary. E-mail: palinko@chem.u-szeged.hu*
[d]*Material and Solution Structure Research Group, Institute of Chemistry, University of Szeged, Aradi Vértanúk tere 1, H-6720 Szeged, Hungary*
[e]*MTA-SZTE Reaction Kinetics and Surface Chemistry Research Group, Hungarian Academy of Sciences, Rerrich B. tér 1, H-6720 Szeged, Hungary*
[f]*Department of Applied and Environmental Chemistry, University of Szeged, Rerrich B. tér 1, H-6720 Szeged, Hungary*
[g]*Department of Inorganic and Analytical Chemistry, University of Szeged, Dóm tér 7, H-6720 Szeged, Hungary*

†Electronic supplementary information (ESI) available: UV-vis, IR, EPR, XPS, ICP-AES spectra and spectral data, AFM, TEM and SAED images on the fresh AgBi HM sample; Raman, XPS and ICP-AES data on the used catalyst sample; additional reaction optimization data; NMR and MS data of the reaction products. See DOI: 10.1039/c7gc02487h

and bases.[13] Alternatively, there are only a few examples for heterogenized silver complexes and silver-exchanged materials (*e.g.*, heteropoly acids) as reusable silver catalysts.[14]

Due to the excellent transformability of C≡C bonds and because of their excellent availability, alkynyl compounds have emerged as versatile intermediates for the atom-economic synthesis of a wide array of valuable products.[15] Alkynes are important components in numerous catalytic transformations, such as diverse coupling and cyclization reactions[16] including the well-established click chemistry.[17] Because of these beneficial features, alkyne-based catalytic reactions are generating continuously increasing interest.[15] Due to its d^{10} electronic configuration, silver plays a marked role in the activation of C≡C bonds of alkynyl compounds.[1g] As a consequence of this pronounced alkynophilicity, a large number of practical synthesis methods have been devised *via* silver-mediated σ- or π-activation of terminal or internal alkynes.[1a,1b,1g,18] Most of these important reactions rely on homogeneous silver catalysts and employ relatively large amounts of the precious metal. Very recently, Duan and co-workers reported a pioneering methodology for the heterogeneous catalytic activation of internal alkynes by introducing a porous silver coordination polymer for the cyclization of propargylic alcohols with CO_2.[19]

Because of their incredible versatility, aromatic and aliphatic nitriles are of outstanding importance in fine chemical, pharmaceutical and natural product syntheses. Organic nitriles are essential precursors for amines, amides, aldehydes and various carboxylic acid derivatives,[20] and they are particularly important as intermediates for the production of valuable heterocycles.[21] In addition, the cyano group represents a vital motif in various biologically and medicinally relevant structures, including numerous FDA-approved drugs like letrozole and rilpivirine.[22] Traditional strategies in nitrile synthesis involve Sandmeyer[23] and metal cyanide (or metalloid cyanide)-mediated cyanation reactions,[24] dehydration of amides and oximes,[25] ammoxidation of aromatic hydrocarbons[26] and the Schmidt reaction of aldehydes with azides.[27] However, these methods suffer from multiple limitations, including serious environmental concerns (*e.g.*, cyanide salts and toxic metal waste), the use of expensive catalysts or harsh reaction conditions, selectivity issues and limited scope. To circumvent these drawbacks, Jiao and co-workers recently demonstrated a silver-catalyzed C≡C bond cleavage reaction to yield organic nitriles directly from terminal alkynes in the presence of a suitable nitrogen source and under reasonably mild conditions.[28]

In chemical industry, the concept of catalytic materials from naturally occurring minerals has notable historical roots,[29] with the family of synthetic zeolites as the best-known examples.[30] Due to economic and environmental reasons, the application of synthetic minerals and mineral-derived materials as designer catalysts has drawn significant attention in organic syntheses. For example, layered double hydroxides (LDHs) have emerged in diverse catalytic applications as catalyst supports or catalyst precursors or as the actual catalysts.[31] Unlike silicate-based cationic clays, only relatively few anionic clays occur naturally;[32] however, most of them can easily be synthesized.[33] These layered materials can be comfortably modified, and they frequently offer peculiar catalytic properties due to the intrinsic characteristics of the layers (surface acid–base character), the interlayer modifier (*e.g.*, redox-active intercalated complexes) and the sterically constrained environment, which may give rise to various selectivity effects.[34] Thus, LDHs may be tailored to specific needs with relative ease.[35] Traditional immobilization of metal catalysts on various prefabricated supports is often accompanied by negative effects such as poor accessibility, random anchoring or disturbed geometry of the active sites, which may result in reduced activity and/or selectivity; and in the case of unsatisfactory catalyst-support interactions, the possible leaching of the metal component may lead to serious environmental concerns.[36] In contrast, catalytic materials with structurally bound active centers (*e.g.* LDHs with layers of active metals) exhibit increased thermodynamic stability and robustness as compared with the classically immobilized ones.[37]

In recent years, we have been active in this field concentrating on the synthesis, modification, structural characterization and catalytic applications of LDHs.[38] During this work, we were able to prepare a thus far unknown Ba(II)Fe(III)-LDH,[39] which refuted the generally accepted wisdom that for the formation of an LDH material, the ionic radii of the cationic components must be similar in size. As concerns catalytic applications, we not only exploited synthetic LDHs as catalyst carriers (intercalated catalysts),[40] but we also showed that a copper-containing primary LDH can act as a highly active and robust solid catalyst even under demanding reaction conditions (high-temperature/high-pressure continuous-flow conditions).[41]

Although silver-containing minerals are scarce in nature, we speculated that a mineralogically-inspired catalyst design may aid the development of a robust heterogeneous silver catalyst. Our aim was to eliminate the need for classical immobilization techniques, and to prepare a solid catalyst containing Ag(I) as a constituent. As a proof of the concept, we were intrigued to explore the direct nitrogenation of alkynes to organic nitriles. To the best of our knowledge, this transformation has not yet been achieved by using a heterogeneous noble metal catalyst. Thus, we wish to present our results on the synthesis and characterization of a novel silver-containing hybrid material as a recyclable and highly selective heterogeneous catalyst for the sustainable synthesis of organic nitriles from terminal alkynes.

Experimental

Synthesis of the silver–bismuth hybrid material

All chemicals used were analytical grade Sigma-Aldrich products, and were applied without further purification.

In a typical synthesis using the urea hydrolysis method,[42] appropriate amounts of $Bi(NO_3)_3{\cdot}5H_2O$ (5.36 g) and $AgNO_3$ (3.73 g) were dissolved in 50–50 mL 5 wt% nitric acid. After mixing, urea (7.05 g) dissolved in 100 mL of deionized water was added to the solution and stirred for 72 h at 130 °C. The

obtained colored product was filtered, washed with aqueous thiosulfate solution, water and ethanol four times, and dried at 60 °C to obtain the final product (material C). The syntheses of all byproducts (materials A and B) were carried out the same way except leaving out either the silver or the bismuth salt.

For control purposes, the catalyst synthesis was also carried out using high purity (99.999%) metal salts (Sigma-Aldrich).

Characterization of the silver–bismuth hybrid material

The X-ray diffraction (XRD) patterns were recorded on a Rigaku XRD-MiniFlex II instrument applying $Cu_{K\alpha}$ radiation (λ = 0.15418 nm), 40 kV accelerating voltage at 30 mA.

The structure-building inorganic components were identified by Raman microscopy and IR spectroscopy. Raman spectra were recorded with a Thermo Scientific™ DXR™ Raman microscope at an excitation wavelength of 635 nm applying 10 mW laser power and averaging 20 spectra with an exposure time of 6 seconds. The instruments for recording the IR spectra were a BIO-RAD Digilab Division FTS-65A/896 (mid-range spectra) and a BIO-RAD Digilab Division FTS-40 vacuum FT-IR spectrophotometer (far-range spectra) with 4 cm^{-1} resolution. The 4000–600 and 600–100 cm^{-1} wavenumber ranges were recorded, but only the most relevant parts are displayed and discussed. 256 scans were collected for each spectrum. The mid IR spectra were recorded in diffuse reflectance mode, while for the far IR spectra the Nujol mull technique was used between two polyethylene windows (the suspension of 10 mg sample and a drop of Nujol mull).

UV–vis spectra were registered on an Ocean Optics USB4000 spectrometer with a DH-2000-BAL UV–vis-NIR light source measuring diffuse reflectance and using $BaSO_4$ as reference. The spectra were analyzed with the SpectraSuite package.

Electron paramagnetic resonance (EPR) spectra were recorded with a BRUKER EleXsys E500 spectrometer (microwave frequency 9.51 GHz, microwave power 12 mW, modulation amplitude 5 G, modulation frequency 100 kHz) in quartz EPR tubes at room temperature. Approximately 10 mg of samples were used for each measurement, and the spectra were recorded without any additional sample preparation. All recorded EPR spectra were simulated with a home-made computer program.[43]

X-ray photoelectron spectra (XPS) were recorded using a SPECS instrument equipped with a PHOIBOS 150 MCD 9 hemispherical electron energy analyzer using $Al_{K\alpha}$ radiation ($h\nu$ = 1486.6 eV). The X-ray gun was operated at 210 W (14 kV, 15 mA). The analyzer was operated in the FAT mode, with the pass energy set to 20 eV. The step size was 25 meV, and the collection time in one channel was 250 ms. Typically, 5–10 scans were added up to acquire a single spectrum. Energy referencing was not applied. In all cases the powder-like samples were evenly laid out on one side of a double-sided adhesive tape, the other side being attached to the sample holder of the XPS instrument. The samples were evacuated at room temperature, and then inserted into the analysis chamber of the XPS instrument.

The topology of the as-prepared sample was studied by atomic force microscopy (AFM) on an NT-MDT SOLVER scanning probe microscope. Measurement was performed in the tapping mode at room temperature and atmospheric pressure in air. The non-contact silicon cantilevers had typical force constant of 42 N m^{-1} and resonance frequency of 278.8 kHz. For imaging, an SSS-NCH-10 tip (nominal radius of curvature: 2 nm, length: 15 μm) manufactured by NANOSENSORS was used with 0.43 kHz scanning rate and 700 × 700 pixel resolution.

The morphology of the as-prepared sample was studied by scanning electron microscopy (SEM). The SEM image was registered on an S-4700 scanning electron microscope (SEM, Hitachi, Japan) with accelerating voltage of 10–18 kV.

More detailed images, both of the as-prepared and the used samples, were captured by transmission electron microscopy (TEM), and information on the crystal structures was gathered by selected area diffraction (SAED). For these measurements, an FEI Tecnai™ G^2 20 X-Twin type instrument was used, operating at an acceleration voltage of 200 kV.

The thermal behavior of the hybrid sample was investigated by thermogravimetry (TG) and differential thermogravimetry (DTG). The silver-containing sample was studied with a Setaram Labsys derivatograph operating in air at 5 °C min^{-1} heating rate. For the measurements, 20–30 mg of the samples were applied.

The specific surface areas were measured by the Brunauer–Emmett–Teller (BET) method (adsorption of N_2 at 77 K).[44] For these measurements, a NOVA3000 instrument was applied (Quantachrome, USA). The samples were flushed with N_2 at 100 °C for 5 h to clean the surface of any adsorbents.

The amount of metal ions was measured by ICP–AES on a Thermo Jarell Ash ICAP 61E instrument. Before measurements, a few milligrams of the samples measured with analytical accuracy were digested in 1 cm^3 cc. nitric acid; then, they were diluted with distilled water to 50 cm^3 and filtered.

General procedure for the catalytic reactions

All the materials and reagents were of analytical grade and were used as received without purification.

A typical procedure for the catalytic alkyne-nitrile transformation is as follows. Dimethyl sulfoxide (DMSO, 2 mL), the corresponding alkyne (0.5 mmol, 1 equiv.), trimethylsilyl azide ($TMSN_3$, 1 mmol, 2 equiv.) and the silver-containing hybrid material as catalyst (44.2 mg, corresponding to 5 mol% Ag loading) were combined in an oven-dried Schlenk tube equipped with a magnetic stir bar. The reaction mixture was stirred for 24 h at 80 °C. Then, the mixture was cooled to room temperature, and the catalyst was filtered off. Brine (10 mL) was next added, and the resultant liquid was extracted with CH_2Cl_2 (3 × 10 mL). The combined organic layers were dried over Na_2SO_4, and concentrated under reduced pressure. The crude samples were checked by ^1H NMR and GC-MS (in order to determine conversion and product ratio) and were purified by chromatographic techniques to isolate the desired products. Flash column chromatographic purification (performed on Merck silica gel 60, particle size 63–200 mm) and analytical thin-layer chromatography (TLC, performed on Merck silica

gel 60 F254 plates) were carried out using mixtures of *n*-hexane/EtOAc as eluent. When using TLC, the compounds were visualized by means of UV or $KMnO_4$.

Investigation of the catalyst reusability

For investigation of the catalyst reusability, the reaction of *p*-methoxy phenylacetylene with $TMSN_3$ was carried out multiple times utilizing a single portion of catalyst. DMSO (5 mL), *p*-methoxy phenylacetylene (1.25 mmol, 1 equiv.), $TMSN_3$ (2.5 mmol, 2 equiv.) and the heterogeneous silver catalyst (110.5 mg, corresponding to 5 mol% Ag loading) were combined in an oven-dried Schlenk tube equipped with a magnetic stir bar. The reaction mixture was stirred for 24 h at 80 °C. The mixture was next cooled to room temperature, and the solid material was removed by centrifugation. The liquid phase was extracted, dried and evaporated as detailed above. The removed catalyst was washed with DMSO (four times), and was dried in nitrogen flow before the next cycle. The conversion and selectivity were determined after each cycle by using ^{1}H NMR.

Characterization of the reaction products

The nitrile products were characterized by NMR spectroscopy and mass spectrometry. ^{1}H NMR and ^{13}C NMR spectra were recorded on a Bruker Avance DRX 400 spectrometer, in $CDCl_3$ as solvent, with trimethylsilane as internal standard at 400.1 and 100.6 MHz, respectively. GC-MS analyses were performed on a Thermo Scientific Trace 1310 Gas Chromatograph coupled with a Thermo Scientific ISQ QD Single Quadrupole Mass Spectrometer using a Thermo Scientific TG-SQC column (15 m × 0.25 mm ID × 0.25 μm film). Measurement parameters were as follows. Column oven temperature: from 50 to 300 °C at 15 °C min^{-1}; injection temperature: 240 °C; ion source temperature: 200 °C; electrospray ionization: 70 eV; carrier gas: He at 1.5 mL min^{-1}; injection volume: 2 μL; split ratio: 1 : 33.3; and mass range: 25–500 *m*/*z*. The analytical data can be found in the ESI.†

Results and discussion

The proof of the concept – catalytic application of the silver–bismuth hybrid material in direct alkyne-nitrile transformations and comparison to other silver-based catalysts

In order to show that it is worthwhile to spend time and energy on the characterization of the newly developed silver–bismuth hybrid material (AgBi HM), let us demonstrate its performance in a catalytic model reaction (Scheme 1) in comparison with other silver-based catalysts (Fig. 1).

The direct nitrogenation of *p*-methoxyphenylacetylene with $TMSN_3$ as nitrogen source was chosen as a model reaction (Scheme 1).

DMSO was the initial choice of solvent, and the reaction mixture, containing 1 equiv. of alkyne (0.25 M) and 2 equiv. of $TMSN_3$, was stirred at 80 °C for 24 h.

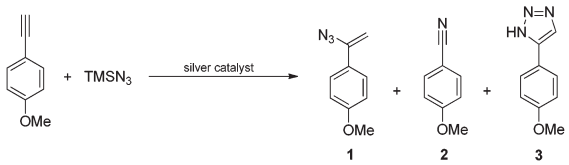

Scheme 1 Model reaction: Nitrogenation of *p*-methoxyphenylacetylene with $TMSN_3$ as nitrogen source.

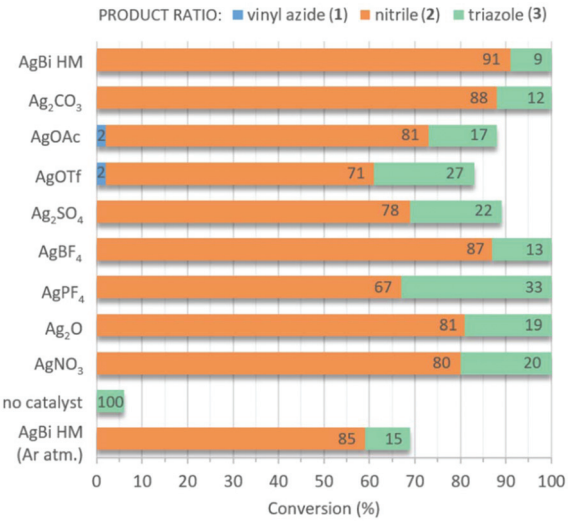

Fig. 1 Investigation of various catalysts in the direct nitrogenation of *p*-methoxyphenylacetylene with $TMSN_3$ as nitrogen source (see Scheme 1). Reaction conditions: 1 equiv. (0.25 M) alkyne, 2 equiv. $TMSN_3$, 10 mol% catalyst, solvent: DMSO, 80 °C, 24 h reaction time.

We were delighted to find complete conversion in the presence of 10 mol% AgBi HM. ^{1}H NMR analysis of the crude material indicated an excellent selectivity of 91% towards the formation of 4-methoxybenzonitrile (**2**). The side product obtained at an extent of 9% was found to be 5-(4-methoxyphenyl)-1*H*-1,2,3-triazole (**3**), which was presumably formed *via* a thermal azide–alkyne cycloaddition as a side reaction.[45] This was corroborated by the finding that without the silver catalyst under otherwise identical conditions, a conversion of merely 6% occurred and triazole **3** was formed exclusively.

The catalytic performance of the AgBi HM was directly compared with commercially available Ag(I) salts (Fig. 1). Ag_2CO_3 and $AgBF_4$ gave comparable results to the hybrid material: the conversion was quantitative in both cases and the nitrile/triazole ratio was 88 : 12 and 87 : 13, respectively. Further Ag(I) salts furnished incomplete conversions and/or lower product selectivities. Among the commercial catalysts tested, AgOAc and AgOTf proved less effective. In these instances, traces of 1-(1-azidovinyl)-4-methoxybenzene (**1**) could also be detected in the crude product mixture. On the basis of the reaction mechanism proposed by Jiao and co-workers (Scheme 2),[28a] following a silver-mediated alkyne activation and the attack of the azide anion, nitrile formation occurs *via* a vinyl azide intermediate.[46] The presence of the corresponding vinyl azide byproduct in

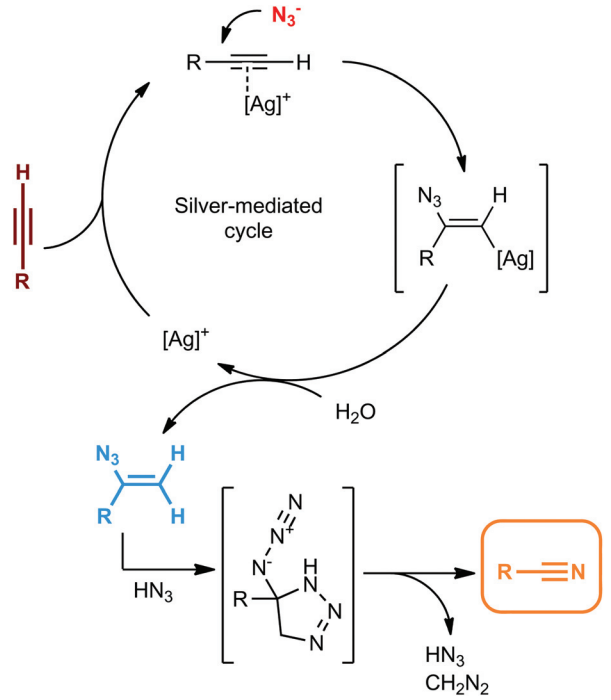

Scheme 2 Possible mechanism of the silver-mediated formation of nitriles from terminal alkynes.[28a]

the reaction mixture therefore indicates the incompleteness of the reaction.

As corroborated by a test reaction carried out with 10 mol% of $Bi(NO_3)_3{\cdot}5H_2O$ as catalyst, the Bi(III) component of the hybrid material is inactive as concerns nitrile formation. When the AgBi HM-catalyzed nitrogenation of *p*-methoxyphenylacetylene was repeated under argon atmosphere, a significant conversion decrease occurred verifying the oxidative nature of the reaction.

Synthesis and characterization of the silver–bismuth hybrid material

Our previous experiences with LDH-based materials served as the basis of the catalyst synthesis. An LDH-like structure was desired, because organized layers allow easier control over the catalytic properties, and Ag(I) prefers octahedral coordination in solid materials.[47] Although LDH layers typically consist of di- and trivalent metal cations,[31] our initial concept was supported by the fact that an LDH with a monovalent cationic component (instead of the divalent one) is already known.[48] Bi(III) was chosen as a possible trivalent cation, since it also prefers octahedral coordination in solids,[49] and the ionic radii of Ag(I) and Bi(III) are comparable: 129 and 117 pm, respectively.[50] (As was referred to above, we were able to prepare LDHs with much larger differences in ionic radii.) Moreover, we identified a mineral called beyerite ($CaBi_2O_2(CO_3)_2$), which has a layered structure, and contains Ca(II) ions fixed among the layers of $BiO(CO)_3$.[51] It was reckoned that if we could incorporate Ag(I) ions instead of Ca(II), we may well form a basis for success, since we would have a structure having Ag(I) ions immobilized in a lattice which is less ordered than that of beyerite, which thus may have considerable catalytic activity. All these factors gave enough inspiration to start with the synthesis.

The urea method was chosen for the co-hydrolysis of the metal salts, since in this way the pH can precisely be controlled through the temperature of hydrolysis.[42] Appropriate amounts of $Bi(NO_3)_3{\cdot}5H_2O$ and $AgNO_3$ were thus dissolved in nitric acid and urea was added to the solution. After stirring for 72 h, the precipitate was filtered, washed, dried and then carefully characterized.

The X-ray diffractograms indicated that the most suitable temperature for the co-hydrolysis was 130 °C. At this temperature, a novel material (assigned as AgBi HM) was formed (Fig. 2, trace C). The diffractogram obtained was very different from those of the components (Fig. 2, traces A and B), and it is not their sum either. It was also found that using a temperature of 100 °C for the co-hydrolysis yielded a material having similar features to Ag_2O–Ag_2CO_3–$AgNO_3$ after hydrolysis (Fig. 2, trace D), *i.e.*, it was probably an Ag_2O–Ag_2CO_3 mixture supported over material A. For catalytic purposes, especially in the liquid phase, this substance would be inappropriate, as the silver component would surely be leached out, since it is not a constituent of the crystal lattice of the support.

Material A was indexed as $Bi_2O_2CO_3$,[52] material B is a mixture of Ag_2O and Ag_2CO_3,[53] and material D is Ag_2O–Ag_2CO_3 supported over BiO_2CO_3. Carbonation is due mainly to urea as well as the airborne CO_2. In LDH chemistry, carbonation is disadvantageous in most cases, since the carbonate ion is firmly attached to the positively charged layers, preventing its modification *via* anion exchange. In this instance, however, it is not a problem, since our goal is fixing Ag(I), while keeping its catalytic activity on one hand, and keeping it in a position which is non-leachable on the other. As has been mentioned already, the X-ray pattern of material C differs from those of the con-

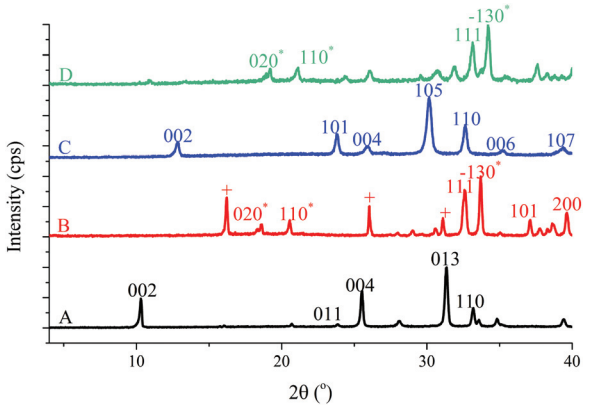

Fig. 2 The X-ray patterns of the hydrolyzed $Bi(NO_3)_3{\cdot}5H_2O$ (A),[50] the hydrolyzed mixture of Ag_2O–Ag_2CO_3–$AgNO_3$ (B, where + denotes Ag_2O, indices denote Ag_2CO_3),[53] the $Bi(NO_3)_3{\cdot}5H_2O$–$AgNO_3$ mixture co-hydrolyzed at 130 °C (C)[51] and the $Bi(NO_3)_3{\cdot}5H_2O$–$AgNO_3$ mixture co-hydrolyzed at 100 °C (D, where + denotes Ag_2O, indices denote Ag_2CO_3).

stituents, and is not their sum either. It resembles the X-ray pattern of beyerite (a mineral with various polymorphs but an approximate formula of $CaBi_2O_2(CO_3)_2$), but it is definitely not the same.

UV–vis–near IR DRS spectra as well as the EPR spectra also revealed that material C is a novel substance, and is not a physical mixture of materials A and B (Fig. S1 and S2†). Regarding this work, this is important information, and these spectra are only used as further support for the decisive X-ray diffractograms.

Raman spectroscopy is the method of choice to identify the anionic component(s) (Fig. 3). The observed shifts were assigned as given in Table 1. It is seen that the anion is carbonate in the hybrid material, and there is no nitrate present. One can arrive at the same conclusion from studying the FT-IR spectra (Fig. S3 and Table S1†). The IR spectrum of material C reveals that there is no surface OH.

In order to learn more about the novel AgBi HM, elemental analysis was performed by the ICP–AES method and a formula of $Ag_{0.17}Bi_{0.88}O_2CO_3$ was obtained; for the data, see Table S2.†

Since the intended use of the hybrid substance is a heterogeneous catalyst, its thermal stability is an important feature. Thermal analysis revealed that the original structure was kept up to 380 °C, then, weight losses occurred in three endothermic steps, and no more weight losses could be observed from 510 °C until 700 °C, the maximum temperature applied (Fig. 4). The three steps altogether resulted in 7.5 wt% weight loss (4 wt% + 2 wt% + 1.5 wt%). Since there is no surface OH, all the weight loss should be due to the evolution of CO_2. On a molar basis, it can be calculated that 22 g CO_2, *i.e.*, half of the carbon content, remained in the heat-treated sample. Consequently, the residue should contain a mixture of oxides, as well as carbonates. Nevertheless, the most important message is that the temperature in the hybrid material-catalyzed reactions must be kept under 380 °C. The three-step weight loss may give some structural information as well.

As far as the cationic components of material C are concerned, the XPS spectra attest that the silver and the bismuth components of the hybrid material are in the +1 and +3 oxidation states, respectively (Fig. S4†).[60] The shift of ~0.2 eV in the hybrid catalyst material indicates some electron transfer towards Ag^+; this seemed to be advantageous in our probe reaction of oxidative nature, which might be the reason for outstanding catalytic activity.

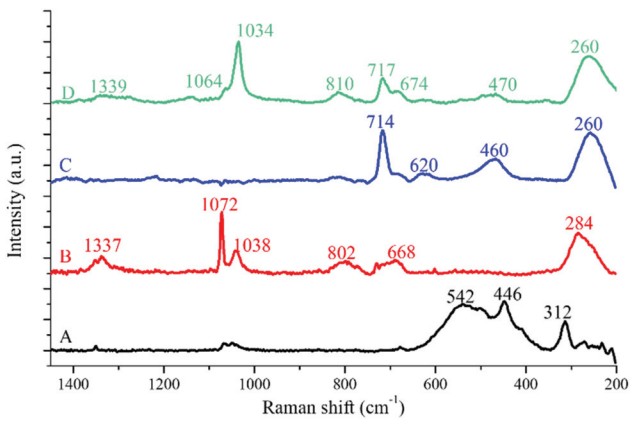

Fig. 3 The Raman spectra of the hydrolyzed $Bi(NO_3)_3{\cdot}5H_2O$ (A), the hydrolyzed mixture of Ag_2O–Ag_2CO_3–$AgNO_3$ (B), the $Bi(NO_3)_3{\cdot}5H_2O$–$AgNO_3$ mixture co-hydrolyzed at 130 °C (C) and the $Bi(NO_3)_3{\cdot}5H_2O$–$AgNO_3$ mixture co-hydrolyzed at 100 °C (D).

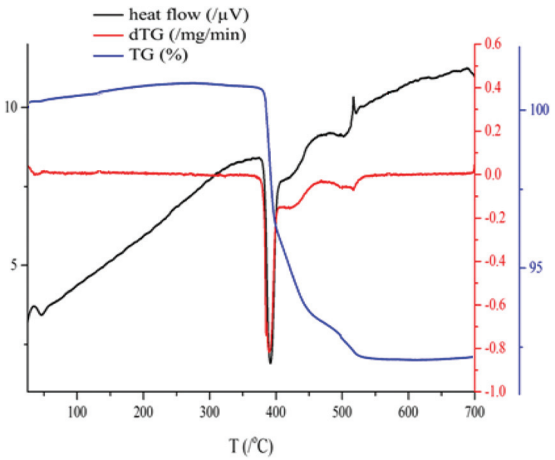

Fig. 4 Thermal analytical curve obtained during the heat treatment of the AgBi HM.

Table 1 Observed Raman shifts and their assignations. A: The hydrolyzed $Bi(NO_3)_3{\cdot}5H_2O$, B: the hydrolyzed mixture of Ag_2O–Ag_2CO_3–$AgNO_3$, C: the $Bi(NO_3)_3{\cdot}5H_2O$–$AgNO_3$ mixture co-hydrolyzed at 130 °C, and D: the $Bi(NO_3)_3{\cdot}5H_2O$–$AgNO_3$ mixture co-hydrolyzed at 100 °C

	Raman shift (cm^{-1})										
Samples	a	b	c	d	e	f	g	h	i	j	k
A	—	312	446	542	—	—	—	—	—	—	—
B	284	—	—	—	—	668	—	802	1038	1072	1337
C	260	—	460	—	620	—	714	—	—	—	—
D	260	—	470	—	—	674	717	810	1034	1064	1339

a: Ag–O(carbonate) bending,[54] b: Bi–O–Bi stretching,[55] c: bridging Bi–O–Bi bonds in $[BiO_6]$,[56] d: Bi=O stretching,[57] e: Bi–O stretching,[58] f: ν_4 in-plane deformation of the nitrate anion,[59] g: ν_4 in-plane deformation of the carbonate anion,[57] h: ν_2 out-of-plane bending mode of the nitrate anion,[59] i: ν_1 symmetric mode of the nitrate anion,[59] j: Ag–O stretching/bending modes,[60] k: ν_3 antisymmetric mode of the nitrate anion.[60]

The AFM measurement indicates a smooth outer surface (Fig. S5†), and the SEM image displays a lamellar morphology (Fig. 5a), which is verified by the high-resolution TEM measurement (Fig. 5b). On the enlarged version of the TEM image (Fig. S6a†), it was possible to measure the basal spacing (0.645 nm, the thickness of one layer plus the interlayer space), which is the d_{002} value attested by the SAED image (Fig. S6b†). This value was determined because it can be directly compared to the one calculated from X-ray diffraction using the reflection at the lowest angle (Table 2). The table also contains the BET surface areas as well as the particle size. It is seen that the calculated basal spacing compares well to the one measured on the TEM image.

The basal spacing is small (note that it also includes the thickness of one layer) and the low BET surface indicates that the interlayer space (*i.e.* the inner surface) is not accessible even for the nitrogen molecules. In our model reaction, the sizeable organic molecules (Scheme 1 and the compounds in Table 5) can only use the outer surface of the AgBi HM, and as the activities observed attest, they can use it efficiently.

Let us sum up what we have learnt from these measurements. In our hands, we have a hybrid material containing Ag(I) and Bi(III) cationic and carbonate anionic components, the latter in three possible positions. The silver ion is the minor cationic component, probably a guest in the bismuth-carbonate lattice. (Indeed, the X-ray diffractogram resembles that of beyerite $[CaBi_2O_2(CO_3)_2]$.) This is a material with a layered structure, keeping this structure up to 380 °C. The Bi(III) ions are constituents of the layers and they are connected *via* one of the oxygen atoms of the carbonate ions. The silver ions are attached to the carboxylate end of the carbonate ions, thus forming a separate layer residing among the Bi(III) containing layers.

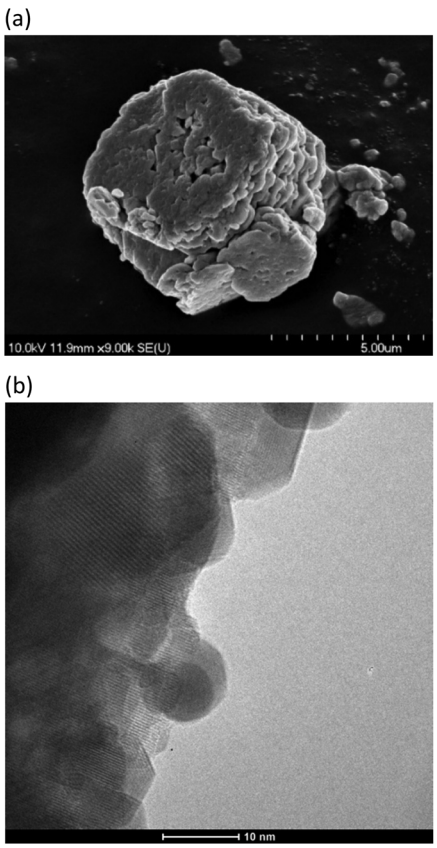

Fig. 5 The SEM (a) and the high-resolution TEM (b) images of the AgBi HM. (SEM – scanning electron microscopy, TEM – transmission electron microscopy.)

Table 2 The basal spacing (d from the Bragg equation), the particle thickness (from the Scherrer equation) and the BET surface area of the AgBi HM

Sample	*d* (nm)	Particle thickness (nm)	BET surface area ($m^2\ g^{-1}$)
AgBi HM	0.680	29.61	3.0

Optimization and extension of the probe reaction

Encouraged by the promising preliminary results, we set out to investigate the effects of all the important reaction parameters in order to determine the optimum conditions for a sustainable methodology. As the next step, the role of the reaction medium was explored. Strong dependence was registered on the nature of the solvent applied. Besides DMSO, only dipolar aprotic solvents exhibiting an amide moiety proved acceptable: *N*,*N*-dimethylacetamide (DMA) worked similarly well as DMSO (the conversion was 90% and the nitrile/triazole ratio was 87 : 13, Table 3, entries 1 and 3), whereas the application of *N*,*N*-dimethylformamide (DMF) and *N*-methylpyrrolidone

Table 3 Investigation of various solvents in the AgBi HM-catalyzed nitrogenation of *p*-methoxyphenylacetylene with $TMSN_3$ as nitrogen source

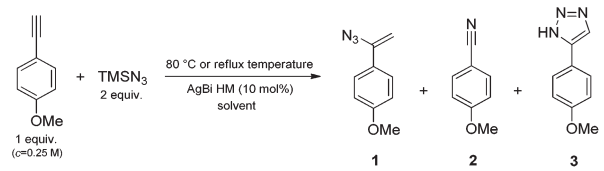

#	Solvent	Time (h)	Conv.[a] (%)	Product selectivity[a] (%) 1	2	3
1	DMSO	24	100	0	91	9
2	DMF	24	72	0	84	16
3	DMA	24	90	0	87	13
4	NMP	24	41	2	76	22
5	EtOAc	72	7	n.d.[b]		
6	THF[c]	72	5	n.d.[b]		
7	MeCN	72	Traces	n.d.[b]		
8	Toluene	72	Traces	n.d.[b]		
9	CH_2Cl_2	72	Traces	n.d.[b]		
10	Acetone	72	Traces	n.d.[b]		
11	*n*-Hexane	72	0	—		

[a] Determined by ^1H NMR analysis of the crude product. [b] Not determined. [c] THF = tetrahydrofuran.

(NMP) resulted in lower conversions (72% and 41%, respectively) but still good selectivities towards the formation of nitrile **2** (84% and 76%, respectively, Table 3, entries 2 and 4). In other solvents investigated, including polar and non-polar ones, only very low conversions were detected even upon prolonging the reaction time to 72 h (Table 3, entries 5–11). This remarkable dependence is possibly related to the nucleophilicity of the azide anion and the stability of the *trans* alkenyl silver complex key intermediate, which are strongly dependent on the solubilizing properties of the solvent applied.[61] The choice of DMSO as preferable reaction medium was further corroborated by the fact that, according to Pfizer's solvent selection guide for medicinal chemistry, it is a usable solvent, whereas most amide solvents are designated as undesirable.[62]

Fig. 6 displays the effects of the reaction time on the progress of the model reaction at 80 °C. As was expected, the total conversion increases gradually with the reaction time reaching completion after slightly longer than 16 h. In the initial stages of the reaction, a substantial amount of vinyl azide **1** can be detected. It is clearly visible that as intermediate **1** is consumed, the amount of the nitrile product grows continuously. After 6 h, only traces of vinyl azide remain, and the ratio of nitrile **2** becomes constant at around 90%. It was also found that triazole **3** appeared as a side product after 1 h of stirring at 80 °C, and its ratio in the reaction mixture became steady around 10% after 6 h. These results led us to conclude that the reaction time should be in the range of 16–24 h to achieve optimum results.

In attempts to improve the rate and the selectivity of the reaction, the role of the temperature was examined carefully (see Fig. S7† for the detailed representation of the experimental data). Elevation of the temperature resulted in a substantial increase in the reaction rate (the conversion of *p*-methoxyphenylacetylene was 91% after 1 h at 130 °C); however, at the expense of the product selectivity: higher temperatures promoted the formation of the triazole side product *via* thermal azide–alkyne cycloaddition. For example, at 130 °C, a nitrile/triazole ratio of 80 : 20 occurred after 24 h of stirring, whereas at 50 °C, triazole **3** was barely formed (to an extent of merely 3%, although conversion was only 79%). 80 °C was selected as the reaction temperature of choice with an excellent nitrile/triazole ratio of 91 : 9 and quantitative conversion in 24 h.

According to the suggested reaction mechanism of the direct alkyne nitrogenation (Scheme 2), trace amounts of H_2O are required for the successful nitrile formation.[28a] First of all, after the attack of the azide anion, the resulting *trans* alkenyl silver intermediate should be hydrolyzed to give the corresponding vinyl azide, and a small portion of H_2O may also be crucial to generate some HN_3 necessary for the final vinyl azide-nitrile transformation. We thus speculated that H_2O added to the reaction mixture might have a beneficial effect on the reaction rate. In contrast to our assumption, the presence of excess H_2O (2 equiv.) had no significant effects on the reaction progress. In a 0.5–72 h reaction time window, similar conversions were measured as earlier without H_2O (see Fig. S8† *vs.* Fig. 6); however, a small amount of *p*-methoxyacetophenone appeared among the reaction products as a consequence of competitive silver-catalyzed alkyne hydration.[63] These results suggest that none of the reaction steps involving the presence of H_2O is rate determining.

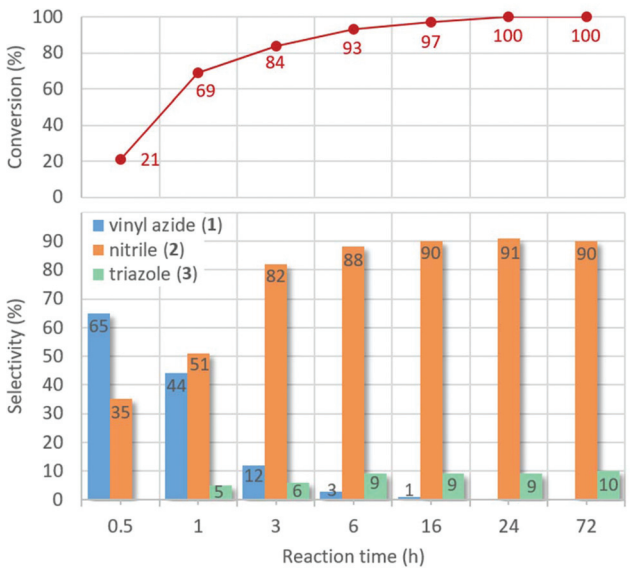

Fig. 6 Investigation of the effects of the reaction time on the AgBi HM-catalyzed nitrogenation of *p*-methoxyphenylacetylene with $TMSN_3$ as nitrogen source (see Scheme 1). Reaction conditions: 1 equiv. (0.25 M) alkyne, 2 equiv. $TMSN_3$, 10 mol% catalyst, solvent: DMSO, 80 °C.

Table 4 Investigation of the effects of various nitrogen sources and fine-tuning of the catalyst loading and the nitrogen source amount in the AgBi HM-catalyzed nitrogenation of *p*-methoxyphenylacetylene

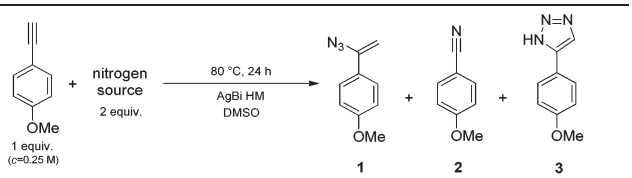

#	N. source	N. source amount (ekv)	Catalyst loading (mol%)	Conv.[a] (%)	Prod. selectivity[a] (%)		
					1	**2**	**3**
1	$TMSN_3$	2	10	100	0	91	9
2	NaN_3	2	10	8	0	18	82
3	DPPA	2	10	0	n.d.[b]		
4	$TMSN_3$	1.5	10	91	0	87	13
5	$TMSN_3$	1.1	10	80	0	89	11
6	$TMSN_3$	2	5	100	0	90	10
7	$TMSN_3$	2	1	76	2	89	9
8[c]	$TMSN_3$	2	5	100	0	90	10

[a] Determined by ^{1}H NMR analysis of the crude product. [b] Not determined. [c] Ultra-high purity AgBi HM was used as catalyst (synthesized from 99.999% pure metal salts).

Besides $TMSN_3$, NaN_3 and diphenylphosphoryl azide (DPPA) were also investigated as nitrogen sources. However, no conversion was detected in the case of DPPA, and NaN_3 did not work well either resulting in a conversion of merely 8% with triazole **3** as the main product (Table 4, entries 2 and 3). We tried to reduce the excess of $TMSN_3$ applied, but it was found that 2 equiv. were necessary for the reaction to complete: lower amounts resulted in a sharp decrease in conversion (Table 4, entries 4 and 5). Gratifyingly, under the previously set conditions (80 °C, 24 h, DMSO as solvent, 2 equiv. of $TMSN_3$ as nitrogen source), we were able to lower the catalyst loading to 5 mol% without detectable change in conversion or selectivity (Table 4, entry 6).

It is well-known that Cu(I) compounds are excellent catalysts for the 1,3-dipolar cycloaddition of organic azides and alkynes to yield 1,2,3-triazoles.[17] In order to exclude the possibility of copper contaminations in the catalytic material contributing consistently to triazole side product formation, the synthesis of the AgBi HM was repeated using ultra-high purity (99.999%) silver and bismuth salts. The model reaction was then carried out with the high purity catalyst under optimized reaction conditions. The amount of triazole present as a side product was exactly the same as with the ordinary AgBi HM as catalyst (Table 4, entries 6 *vs.* 8). This finding, in combination with the fact that Ag(I) itself is not active as catalyst in azide–alkyne cycloadditons,[64] suggests that the observed triazole formation (the ratio of triazole **3** was 10% under optimized conditions) can indeed be explained by thermal cycloaddition as a competing reaction pathway.

A range of alkynes exhibiting diverse substitution patterns were next submitted to the optimized reaction conditions. We were delighted to find quantitative conversions and selectivities around 90% in reactions of phenylacetylene and its substituted derivatives containing methyl, *tert*-butyl or bromo moieties (Table 5, entries 1–5). Even multisubstituted phenylacetylene derivatives and 3-ethynylthiophene gave outstanding results (Table 5, entries 6–8), although they are known to be less reactive in the silver-mediated nitrogenation.[28a] Phenyl propargyl ether, benzoic acid propargyl ester and *p*-nitrobenzoic acid propargyl ester displayed excellent reactivities (conversions were in the range 95–100%); however, enhanced triazole formation led to slightly lower selectivities (in the range of 73–81%, Table 5, entries 9–11). The nitrogenation of aliphatic alkynes went smoothly to open chain alkynes with varying chain length and a cyclic alkyne were transformed into the corresponding nitriles with excellent conversions (in

Table 5 Substrate scope of the AgBi HM-catalyzed direct alkyne nitrogenation

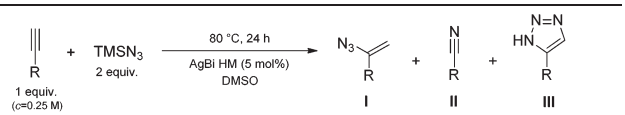

#	Alkyne	Conv.[a] (%)	Prod. selectivity[a] (%)		
			I	II	III
1	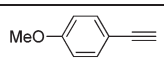	100	0	90	10
2	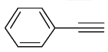	100	0	91	9
3	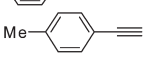	100	0	92	8
4	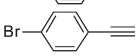	100	0	90	10
5	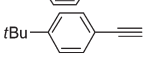	100	0	93	7
6	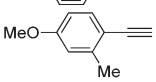	100	0	94	6
7	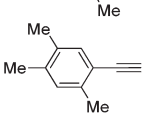	100	0	94	6
8	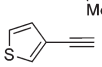	100	0	90	10
9	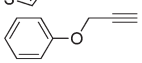	100	0	81	19
10	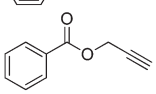	100	0	74	26
11	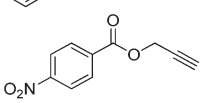	95	0	73	27
12	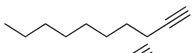	100	0	89	11
13	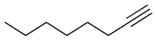	100	0	90	10
14	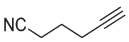	96	0	93	7
15	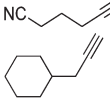	98	0	87	13

[a] Determined by ^1H NMR or GC-MS analysis of the crude product.

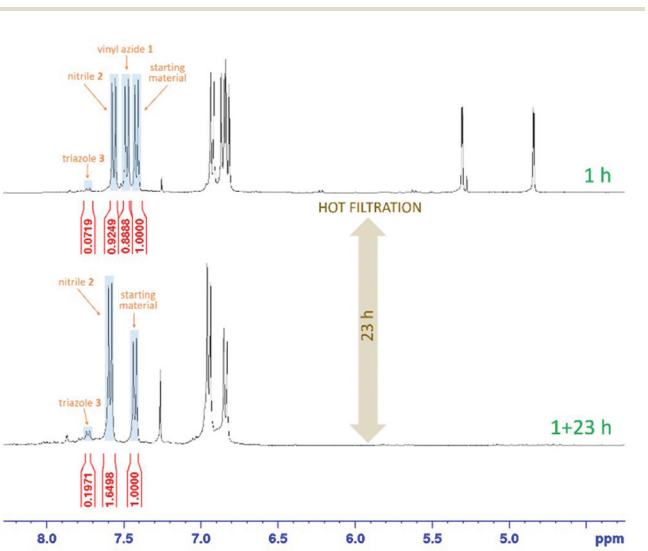

Fig. 7 ^1H NMR spectroscopic analysis (400.1 MHz, $CDCl_3$) of the AgBi HM-catalyzed reaction of *p*-methoxyphenylacetylene with $TMSN_3$ as nitrogen source (see Scheme 1). Reaction conditions: 1 equiv. (0.25 M) alkyne, 2 equiv. $TMSN_3$, 5 mol% catalyst, solvent: DMSO, 80 °C. After 1 h, the catalyst was removed, and the filtrate was stirred for another 23 h (hot filtration). Ar–H signals are marked with blue rectangles.

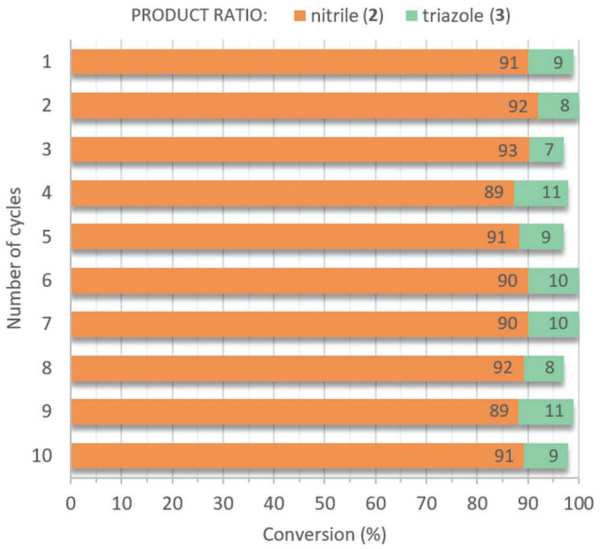

Fig. 8 Testing the reusability of the AgBi HM catalyst in the direct nitrogenation of *p*-methoxyphenylacetylene with $TMSN_3$ as nitrogen source (see Scheme 1). Reaction conditions: 1 equiv. (0.25 M) alkyne, 2 equiv. $TMSN_3$, 5 mol% catalyst, solvent: DMSO, 80 °C, 24 h reaction time.

the range of 96–100%) and selectivities around 90% (Table 5, entries 12–15). Reactions of internal alkynes (such as ethyl phenylpropiolate or oct-4-yne) were also attempted; however, in these cases no nitrile formation occurred.

In order to verify the heterogeneous nature of the reaction, the hot filtration test was attempted. The nitrogenation of *p*-methoxy phenylacetylene with $TMSN_3$ as nitrogen source was carried out under the optimized reaction conditions (80 °C, DMSO as solvent, 2 equiv. of $TMSN_3$, 5 mol% catalyst loading). After 1 h, the AgBi HM catalyst was filtered off, and the filtrate was stirred at 80 °C for another 23 h. As can be seen in Fig. 7, the conversion of *p*-methoxy phenylacetylene was 65% after 1 h, and remained the same after 1 + 23 h. It is worth mentioning that after 1 h, the product distribution of the reaction was as follows: 47% vinyl azide **1**, 49% nitrile **2** and 4% triazole **3**. According to our NMR measurements, after 1 + 23 h, all vinyl azide intermediate was consumed (as nicely demonstrated by the disappearance of the alkenyl CH_2 signals at 4.9 and 5.3 ppm in Fig. 7) and thermal triazole formation proceeded somewhat further to yield a final nitrile/triazole ratio of 89 : 11. These results are in good accordance with the mechanistic observations of Jiao and co-workers that it is only the initial hydroazidation step which is silver-mediated, while the final vinyl azide-nitrile transformation requires no silver catalyst.[28a]

Theoretically, one of the primary benefits of heterogeneous catalysis is the possibility of recycling and reusing the catalytic material, but, in practice, negative effects such as leaching of the active components, erosion of the catalyst structure and irreversible substrate deposition may significantly limit the sustainable application of these materials.[29] Although the hot filtration test verified the predominantly heterogeneous nature of the AgBi HM-catalyzed nitrogenation reaction, we were intrigued to explore the robustness and reusability of our catalyst. The reaction of *p*-methoxyphenylacetylene with $TMSN_3$ was carried out repeatedly (conditions were as follows: 80 °C, DMSO as solvent, 2 equiv. of $TMSN_3$, 5 mol% catalyst loading) utilizing the same portion of AgBi HM as catalyst. Between each cycle, the catalyst was removed by centrifugation and reused after washing and drying. We were delighted to find that no decrease in activity or selectivity occurred even after 10 consecutive catalytic cycles (Fig. 8). The conversion of *p*-methoxyphenylacetylene was steady in the range of 97–100%, and the selectivity towards the anticipated nitrile product was found to be around 90% in all reactions. Besides small amounts of triazole **3**, no vinyl azide byproduct was detected in any of the crude product mixtures analyzed.

The catalyst sample used in repeated runs was structurally characterized by many of the methods applied for the freshly-made material. The results of the most important methods, which are decisive in determining whether our material is a truly efficiently recyclable catalyst with high stability, are as follows. The post-reaction X-ray pattern (Fig. 9a) looks the

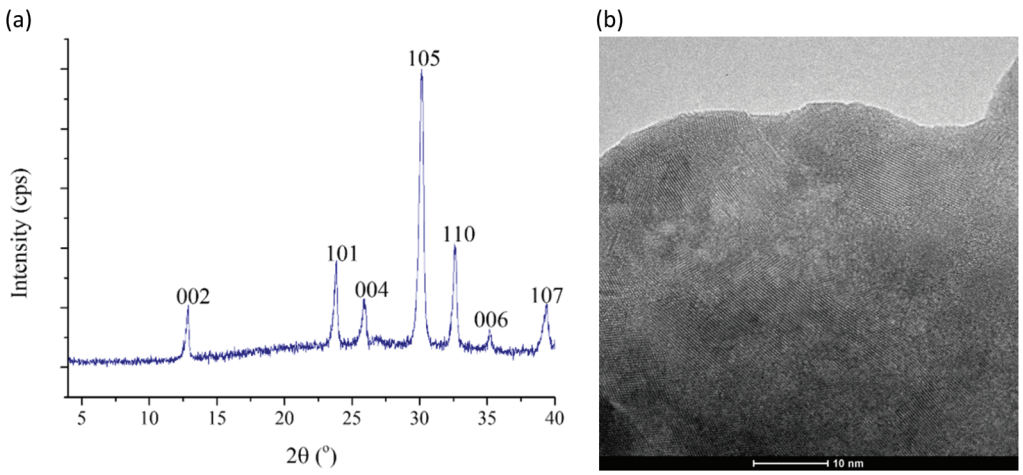

Fig. 9 The X-ray pattern (a) and high-resolution TEM image (b) of the used catalyst sample. (TEM – transmission electron microscopy.)

same as trace C in Fig. 2. Indexing may even be attempted using that of beyerite as a known close analog. The Raman spectra of the freshly-made and the used samples are also very similar (compare trace C in Fig. 3 to the spectrum in Fig. S9†) indicating that the structure did not change, the anionic component (the carbonate ion), and the silver ion attachment to the carbonate oxygen all remained the same. The ICP–AES measurement performed on the used catalyst gave a formula of $Ag_{0.17}Bi_{0.91}O_2CO_3$ (Table S3,† last row), which is practically the same as the freshly-made one, *i.e.*, the sample survived the recycling test without losing any of its components. The XPS spectra revealed that there was no change in the oxidation states of any of the cationic components (Fig. S10†). The high-resolution TEM image indicates (Fig. 9b) that the layered structure is preserved in the used catalyst sample as well. Taking into account all the characterization data of the used sample, we can conclude that the hybrid material proved to be a highly robust heterogeneous catalyst preserving its structure even after extended use.

Conclusions

An Ag(I)Bi(III)-containing hybrid material ($Ag_{0.17}Bi_{0.88}O_2CO_3$) was synthesized as inspired by a naturally occurring mineral and on the analogy of layered double hydroxides. It proved to be a robust, efficiently recyclable, highly active catalyst in the direct synthesis of organic nitriles from terminal alkynes. The most important reaction conditions determining the reaction rate and the product selectivity were carefully optimized in order to achieve high-yielding nitrile formation and minimal waste generation. A diverse set of aromatic as well as aliphatic alkynes were successfully transformed into the corresponding nitriles with small amounts of triazole as the only unwanted product. The heterogeneous nature of the reaction was demonstrated by the completion of the hot filtration test. Importantly, the solid catalyst could be recycled and reused ten times without loss of activity and without detectable structural degradation. To the best of our knowledge, the first example of a heterogeneous noble metal catalyzed nitrile synthesis *via* alkyne activation has been presented herein. Due to its outstanding activity, selectivity, reusability and robustness, the catalyst reported may contribute towards the development of sustainable silver-mediated processes, and may find applications in the synthesis of valuable organic compounds.

Conflicts of interest

There are no conflicts to declare.

Acknowledgements

This work was supported by the National Science Fund of Hungary through grants OTKA NKFI K 115731 and GINOP-2.3.2-15-2016-00013. SBÖ acknowledges the Premium Post Doctorate Research Program of the Hungarian Academy of Sciences. RM and GV were supported by the UNKP-17-3 New National Excellence Program of the Ministry of Human Capacities. The financial help is highly appreciated. Bertalan Oszkó (University of Szeged) and László Korecz (Research Center for Natural Sciences of the Hungarian Academy of Sciences, Budapest) are thanked for registering the X-ray photoelectron and the electron paramagnetic spectra, respectively.

Notes and references

1 (*a*) Q.-Z. Zheng and N. Jiao, *Chem. Soc. Rev.*, 2016, **45**, 4590–4627; (*b*) K. Sekine and T. Yamada, *Chem. Soc. Rev.*, 2016, **45**, 4524–4532; (*c*) R. Karmakar and D. Lee, *Chem. Soc. Rev.*, 2016, **45**, 4459–4470; (*d*) H. Pellissier, *Chem. Rev.*, 2016, **116**, 14868–14917; (*e*) Y. Wang, R. K. Kumar and X. Bi, *Tetrahedron Lett.*, 2016, **57**, 5730–5741; (*f*) V. K.-Y. Lo, A. O.-Y. Chan and C.-M. Che, *Org. Biomol. Chem.*, 2015, **13**, 6667–6680; (*g*) G. Fang and X. Bi, *Chem. Soc. Rev.*, 2015, **44**, 8124–8173; (*h*) G. Abbiati and E. Rossi, *Beilstein J. Org. Chem.*, 2014, **10**, 481–513; (*i*) T. Xu and G. Liu, *Synlett*, 2012, 955–958; (*j*) Y. Yamamoto, *Chem. Rev.*, 2008, **108**, 3199–3222; (*k*) M. Naodovic and H. Yamamoto, *Chem. Rev.*, 2008, **108**, 3132–3148; (*l*) M. Álvarez-Corral, M. Muñoz-Dorado and I. Rodríguez-García, *Chem. Rev.*, 2008, **108**, 3174–3198; (*m*) J.-M. Weibel, A. Blanc and P. Pale, *Chem. Rev.*, 2008, **108**, 3149–3173.

2 (*a*) X. E. Verykios, F. P. Stein and R. W. Coughlin, *Catal. Rev.*, 1980, **22**, 197–234; (*b*) C. Wen, A. Yin and W.-L. Dai, *Appl. Catal., B*, 2014, **160–161**, 730–741.

3 *Silver in organic chemistry*, ed. M. Harmata, John Wiley & Sons Inc., 2010.

4 X.-Y. Dong, Z.-W. Gao, K.-F. Yang, W.-Q. Zhang and L.-W. Xu, *Catal. Sci. Technol.*, 2015, **5**, 2554–2574.

5 S. F. Cai, H. P. Rong, X. F. Yu, X. W. Liu, D. S. Wang, W. He and Y. D. Li, *ACS Catal.*, 2013, **3**, 478–486.

6 A. K. Clarke, M. J. James, P. O'Brien, R. J. K. Taylor and W. P. Unsworth, *Angew. Chem., Int. Ed.*, 2016, **55**, 13798–13802.

7 X. Y. Toy, I. I. B. Roslan, G. K. Chuah and S. Jaenicke, *Catal. Sci. Technol.*, 2014, **4**, 516–523.

8 J. Safari and S. Gandomi-Ravandi, *RSC Adv.*, 2014, **4**, 11654–11660.

9 T. Mitsudome, Y. Mikami, H. Funai, T. Mizugaki, K. Jitsukawa and K. Kaneda, *Angew. Chem., Int. Ed.*, 2008, **47**, 138–141.

10 N. Salam, A. Sinha, A. S. Roy, P. Mondal, N. R. Jana and S. M. Islam, *RSC Adv.*, 2014, **4**, 10001–10012.

11 J. D. Kim, T. Palani, M. R. Kumar, S. Lee and H. C. Choi, *J. Mater. Chem.*, 2012, **22**, 20665–20670.

12 (*a*) C. T. Campbell, *Acc. Chem. Res.*, 2013, **46**, 1712–1719; (*b*) G. Prieto, J. Zečević, H. Friedrich, K. P. de Jong and P. E. de Jongh, *Nat. Mater.*, 2013, **12**, 34–39; (*c*) R. J. White, R. Luque, V. L. Budarin, J. H. Clark and D. J. Macquarrie, *Chem. Soc. Rev.*, 2009, **38**, 481–494.

13 (*a*) B. Ballarin, D. Barreca, E. Boanini, M. C. Cassani, P. Dambruoso, A. Massi, A. Mignani, D. Nanni, C. Parise and A. Zaghi, *ACS Sustainable Chem. Eng.*, 2017, **5**, 4746–4756; (*b*) R. Ricciardi, J. Huskens and W. Verboom, *ChemSusChem*, 2015, **8**, 2586–2605; (*c*) L. D. Pachón and G. Rothenberg, *Appl. Organomet. Chem.*, 2008, **22**, 288–299.

14 (*a*) J. Cao, G. Xu, P. Li, M. Tao and W. Zhang, *ACS Sustainable Chem. Eng.*, 2017, **5**, 3438–3447; (*b*) X. Tang, C. Qi, H. He, H. Jiang, Y. Ren and G. Yuan, *Adv. Synth. Catal.*, 2013, **355**, 2019–2028; (*c*) M. Jeganathan, A. Dhakshinamoorthy and K. Pitchumani, *ACS Sustainable Chem. Eng.*, 2014, **2**, 781–787; (*d*) A. H. Jadhav, A. Chinnappan, R. H. Patil, W.-J. Chung and H. Kim, *Chem. Eng. J.*, 2014, **236**, 300–305; (*e*) K. T. Venkateswara Rao, P. S. Sai Prasad and N. Lingaiah, *Green Chem.*, 2012, **14**, 1507–1514; (*f*) K. Mohan Reddy, N. Seshu Babu, I. Suryanarayana, P. S. Sai Prasad and N. Lingaiah, *Tetrahedron Lett.*, 2006, **47**, 7563–7566.

15 *Modern Alkyne Chemistry: Catalytic and Atom-Economic Transformations*, ed. B. M. Trost and C.-J. Li, Wiley-VCH Verlag GmbH & Co. KGaA, 2014.

16 (*a*) F. Chen, T. Wang and N. Jiao, *Chem. Rev.*, 2014, **114**, 8613–8661; (*b*) X. Zeng, *Chem. Rev.*, 2013, **113**, 6864–6900; (*c*) V. A. Peshkov, O. P. Pereshivko and E. V. Van der Eycken, *Chem. Soc. Rev.*, 2012, **41**, 3790–3807; (*d*) R. Chinchilla and C. Najera, *Chem. Soc. Rev.*, 2011, **40**, 5084–5121.

17 M. Meldal and C. W. Tornøe, *Chem. Rev.*, 2008, **108**, 2952–3015.

18 R. K. Kumar and X. Bi, *Chem. Commun.*, 2016, **52**, 853–868.

19 Z. Zhou, C. He, L. Yang, Y. Wang, T. Liu and C. Duan, *ACS Catal.*, 2017, **7**, 2248–2256.

20 *The Chemistry of the Cyano Group*, ed. Z. Rappoport, John Wiley & Sons Ltd, 1970.

21 (*a*) L.-G. Xie, S. Niyomchon, A. J. Mota, L. González and N. Maulide, *Nat. Commun.*, 2016, **7**, 10914; (*b*) Y. Wang, L.-J. Song, X. Zhang and J. Sun, *Angew. Chem., Int. Ed.*, 2016, **55**, 9704–9708; (*c*) B. Gutmann, J.-P. Roduit, D. Roberge and C. O. Kappe, *Angew. Chem., Int. Ed.*, 2010, **49**, 7101–7105.

22 (*a*) F. F. Fleming, L. Yao, P. C. Ravikumar, L. Funk and B. C. Shook, *J. Med. Chem.*, 2010, **53**, 7902–7917; (*b*) F. F. Fleming, *Nat. Prod. Rep.*, 1999, **16**, 597–606.

23 H. H. Hodgson, *Chem. Rev.*, 1947, **40**, 251–277.

24 (*a*) G. P. Ellis and T. M. Romney-Alexander, *Chem. Rev.*, 1987, **87**, 779–794; (*b*) J. Kim, H. J. Kim and S. Chang, *Angew. Chem., Int. Ed.*, 2012, **51**, 11948–11959; (*c*) N. Kurono and T. Ohkuma, *ACS Catal.*, 2016, **6**, 989–1023.

25 (*a*) W. E. Dennis, *J. Org. Chem.*, 1970, **35**, 3253–3255; (*b*) M. K. Singh and M. K. Lakshman, *J. Org. Chem.*, 2009, **74**, 3079–3084.

26 A. Martin and B. Lücke, *Catal. Today*, 2000, **57**, 61–70.

27 B. V. Rokade and K. R. Prabhu, *J. Org. Chem.*, 2012, **77**, 5364–5370.

28 (*a*) T. Shen, T. Wang, C. Qin and N. Jiao, *Angew. Chem., Int. Ed.*, 2013, **52**, 6677–6680; (*b*) P. Bisseret, G. Duret and N. Blanchard, *Org. Chem. Front.*, 2014, **1**, 825–833.

29 *Handbook of Heterogeneous Catalysis*, ed. G. Ertl, H. Knözinger and J. Weitkamp, Wiley-VCH Verlag GmbH, 2nd edn, 2008.

30 (*a*) A. Primo and H. Garcia, *Chem. Soc. Rev.*, 2014, **43**, 7548–7561; (*b*) J. Li, A. Corma and J. Yu, *Chem. Soc. Rev.*, 2015, **44**, 7112–7127.

31 (*a*) G. Fan, F. Li, D. G. Evans and X. Duan, *Chem. Soc. Rev.*, 2014, **43**, 7040–7066; (*b*) J. Feng, Y. He, Y. Liu, Y. Du and D. Li, *Chem. Soc. Rev.*, 2015, **44**, 5291–5319.

32 Z. P. Xu, J. Zhang, M. O. Adebajo, H. Zhang and C. Zhou, *Appl. Clay Sci.*, 2011, **53**, 139–150.

33 (*a*) J. Qu, Q. Zhang, X. Li, X. He and S. Song, *Appl. Clay Sci.*, 2016, **119**, 185–192; (*b*) F. L. Theiss, G. A. Ayoko and R. L. Frost, *Appl. Surf. Sci.*, 2016, **383**, 200–213.

34 (*a*) K. Yan, Y. Liu, Y. Lu, J. Chai and L. Sun, *Catal. Sci. Technol.*, 2017, **7**, 1622–1645; (*b*) V. Prevot and Y. Tokudome, *J. Mater. Sci.*, 2017, **52**, 11229–11250.

35 C. H. Zhou, *Appl. Clay Sci.*, 2011, **53**, 87–96.

36 Z. Wang, G. Chen and K. Ding, *Chem. Rev.*, 2009, **109**, 322–359.

37 S. He, Z. An, M. Wei, D. G. Evans and X. Duan, *Chem. Commun.*, 2013, **49**, 5912–5920.

38 P. Sipos and I. Pálinkó, *Catal. Today*, DOI: 10.1016/j.cattod.2016.12.004, in press.

39 D. Srankó, A. Pallagi, E. Kuzmann, S. E. Canton, M. Walczak, A. Sápi, Á. Kukovecz, Z. Kónya, P. Sipos and I. Pálinkó, *Appl. Clay Sci.*, 2010, **48**, 214–217.

40 (*a*) G. Varga, Á. Kukovecz, Z. Kónya, L. Korecz, S. Muráth, Z. Csendes, G. Peintler, S. Carlson, P. Sipos and I. Pálinkó, *J. Catal.*, 2016, **335**, 125–134; (*b*) G. Varga, Z. Timár, S. Muráth, Z. Kónya, Á. Kukovecz, S. Carlson, P. Sipos and I. Pálinkó, *Catal. Today*, DOI: 10.1016/j.cattod.2016.12.005, in press; (*c*) G. Varga, S. Ziegenheim, S. Muráth, Z. Csendes, Á. Kukovecz, Z. Kónya, S. Carlson, L. Korecz, E. Varga, P. Pusztai, P. Sipos and I. Pálinkó, *J. Mol. Catal. A: Chem.*, 2016, **423**, 49–60; (*d*) M. Szabados, R. Mészáros, S. Erdei, Z. Kónya, Á. Kukovecz, P. Sipos and I. Pálinkó, *Ultrason. Sonochem.*, 2016, **31**, 409–416.

41 (*a*) S. B. Ötvös, Á. Georgiádes, R. Mészáros, K. Kis, I. Pálinkó and F. Fülöp, *J. Catal.*, 2017, **348**, 90–99; (*b*) S. B. Ötvös, Á. Georgiádes, M. Ádok-Sipiczki, R. Mészáros, I. Pálinkó, P. Sipos and F. Fülöp, *Appl. Catal., A*, 2015, **501**, 63–73.

42 A. Inayat, M. Klumpp and W. Schwieger, *Appl. Clay Sci.*, 2011, **51**, 452–459.

43 A. Rockenbauer and L. Korecz, *Appl. Magn. Reson.*, 1996, **10**, 29–43.

44 S. Brunauer, P. H. Emmett and E. Teller, *J. Am. Chem. Soc.*, 1938, **60**, 309–319.

45 (*a*) R. Huisgen, *Angew. Chem., Int. Ed. Engl.*, 1963, **2**, 565–598; (*b*) Y. Tanaka, S. R. Velen and S. I. Miller, *Tetrahedron*, 1973, **29**, 3271–3283.

46 Z. Liu, P. Liao and X. Bi, *Org. Lett.*, 2014, **16**, 3668–3671.

47 A. F. Cotton and G. Wilkinson, *Advanced inorganic chemistry*, John Wiley & Sons, 5th edn, 1988, p. 940.

48 A. V. Besserguenev, A. M. Fogg, R. J. Francis, S. J. Price, D. O'Hare, V. P. Isupov and B. P. Tolochko, *Chem. Mater.*, 1997, **9**, 241–247.

49 A. F. Cotton and G. Wilkinson, *Advanced inorganic chemistry*, John Wiley & Sons, 5th edn, 1988, p. 383.

50 A. F. Cotton and G. Wilkinson, *Advanced inorganic chemistry*, John Wiley & Sons, 5th edn, 1988, p. 1387.
51 V. Malik, M. Pokhriyal and S. Uma, *RSC Adv.*, 2016, **6**, 38252–38262.
52 T. Selvamani, A. M. Asiri, A. O. Al-Youbi and S. Anandan, *Mater. Sci. Forum*, 2013, **764**, 169–193.
53 (*a*) H. Xia and G. Yang, *J. Mater. Chem.*, 2012, **22**, 18664–18670; (*b*) H. Xu, J. Zhu, Y. Song, W. Zhao, Y. Xu, Y. Song, H. Ji and H. Li, *RSC Adv.*, 2014, **4**, 9139–9147.
54 C.-B. Wang, G. Deo and I. E. Wachs, *J. Phys. Chem. B*, 1999, **103**, 5645–5656.
55 G. Zhao, Y. Tian, H. Fan, J. Zhang and L. Hu, *J. Mater. Sci. Technol.*, 2013, **29**, 209–214.
56 F. Chen, B. Song, C. Lin, S. Dai, J. Cheng and J. Heo, *Mater. Chem. Phys.*, 2012, **135**, 73–79.
57 F. Dong, S. C. Lee, Z. Wu, Y. Huang, M. Fu, W.-K. Ho, S. Zou and B. Wang, *J. Hazard. Mater.*, 2011, **195**, 346–354.
58 P. Dararutana, S. Pongkrapan, N. Sirikulrat, M. Thawornmongkolkij and P. Wathanakul, *Spectrochim. Acta, Part A*, 2009, **73**, 440–442.
59 B. M. Gatehouse, S. E. Livingstone and R. S. Nyholm, *J. Chem. Soc.*, 1958, 3137–3142.
60 W. Wang, Y. Liu, H. Zhang, Y. Qian and Z. Guo, *Appl. Surf. Sci.*, 2017, **396**, 102–109.
61 T. B. Phan and H. Mayr, *J. Phys. Org. Chem.*, 2006, **19**, 706–713.
62 K. Alfonsi, J. Colberg, P. J. Dunn, T. Fevig, S. Jennings, T. A. Johnson, H. P. Kleine, C. Knight, M. A. Nagy, D. A. Perry and M. Stefaniak, *Green Chem.*, 2008, **10**, 31–36.
63 M. B. T. Thuong, A. Mann and A. Wagner, *Chem. Commun.*, 2012, **48**, 434–436.
64 T. U. Connell, C. Schieber, I. P. Silvestri, J. M. White, S. J. Williams and P. S. Donnelly, *Inorg. Chem.*, 2014, **53**, 6503–6511.

II

Molecular Catalysis 498 (2020) 111263

Contents lists available at ScienceDirect

Molecular Catalysis

journal homepage: www.journals.elsevier.com/molecular-catalysis

A mineralogically-inspired silver–bismuth hybrid material: Structure, stability and application for catalytic benzyl alcohol dehydrogenations under continuous flow conditions

Rebeka Mészáros [a], Sándor B. Ötvös [b,c,*], Gábor Varga [d,e], Éva Böszörményi [d,e], Marianna Kocsis [d,e], Krisztina Karádi [e], Zoltán Kónya [f,g], Ákos Kukovecz [f], István Pálinkó [d,e,**], Ferenc Fülöp [a,b,*]

[a] Institute of Pharmaceutical Chemistry, University of Szeged, Eötvös u. 6, Szeged, H-6720 Hungary
[b] MTA-SZTE Stereochemistry Research Group, Hungarian Academy of Sciences, Eötvös u. 6, Szeged, H-6720 Hungary
[c] Institute of Chemistry, University of Graz, NAWI Graz, Heinrichstrasse 28, Graz, A-8010 Austria
[d] Department of Organic Chemistry, University of Szeged, Dóm tér 8, Szeged, H-6720 Hungary
[e] Material and Solution Structure Research Group and Interdisciplinary Excellence Centre, Institute of Chemistry, University of Szeged, Aradi Vértanúk tere 1, Szeged, H-6720 Hungary
[f] Department of Applied and Environmental Chemistry, University of Szeged, Rerrich Béla tér 1, Szeged, H-6720 Hungary
[g] MTA-SZTE Reaction Kinetics and Surface Chemistry Research Group, Rerrich Béla tér 1, Szeged, H-6720 Hungary

ARTICLE INFO

Keywords:
Benzylic alcohols
Continuous flow dehydrogenation
Silver-containing hybrid catalyst
Structural characterization

ABSTRACT

In the present contribution, we are reporting our findings on the structure, stability and synthetic applicability of a silver-containing hybrid material, which has recently been introduced by our research groups as a mineralogically-inspired novel heterogeneous catalyst. To determine how silver ions can be fixed into the structure of the catalyst, a set of experiments was designed with modification of the interlayer gallery under hydrothermal conditions. Subsequently, the stability of the material was examined in various solvents under demanding continuous flow conditions with the aim of achieving a clear picture of its applicability in organic syntheses. On the basis of the useful data obtained during the stability tests, a continuous flow methodology was developed for catalytic dehydrogenation of diversely substituted benzylic alcohols. As far as selectivity is concerned the catalyst performed superbly, while the conversions were varied from fair to extremely good.

1. Introduction

In recent years, silver has gained significant importance as catalyst in organic reactions [1–8]. Silver catalysts are environmentally benign and more economical than other commonly used transition metal catalysts, such as gold, palladium and platinum. Thus, silver-catalysed transformations are gaining importance not only in academic research but also in industry. In most cases, silver complexes [9–12] and commercially available silver salts [13–16] are employed as homogeneous catalytic sources. Since the robustness and reusability of such catalysts are extremely beneficial as concerns process simplicity and sustainability, heterogeneous silver catalysts are also known; however, in most cases active silver species, such as nanoparticles, are immobilized *via* weak forces, which often involves inadequate catalyst stability, particularly under demanding reaction conditions [17–20]. Heterogeneous catalysts containing silver play key role not only in organic syntheses but also in environmental applications, such as catalytic elimination of pollutants [21]. Numerous quick and simple methods can be found in the literature for the heterogenization of the transition metal ions as well as nanoparticles [22–28]. Some of them proved to be useful tools to carry out complex organic oxidations or multicomponent reactions [29–33]. Nevertheless, silver-containing heterogeneous catalysts are still less represented than their soluble counterparts [34–36].

Continuous flow reaction technology has become an important tool for the synthetic and medicinal chemistry fields [37–42], and has been extensively investigated to improve the synthesis of active

* Corresponding authors at: MTA-SZTE Stereochemistry Research Group, Hungarian Academy of Sciences, Eötvös u. 6, Szeged, H-6720 Hungary.
** Corresponding author at: Department of Organic Chemistry, University of Szeged, Dóm tér 8, Szeged, H-6720 Hungary.
E-mail addresses: sandor.oetvoes@uni-graz.at (S.B. Ötvös), palinko@chem.u-szeged.hu (I. Pálinkó), fulop@pharm.u-szeged.hu (F. Fülöp).

https://doi.org/10.1016/j.mcat.2020.111263
Received 17 August 2020; Received in revised form 23 September 2020; Accepted 12 October 2020
Available online 1 November 2020

pharmaceutical ingredients [43–49], nanomaterials [50–52] or other complex substances [53–55]. Transition metal-catalysed reactions under flow chemistry conditions have been shown to have many advantages over traditional batch methods [56–61]. However, such reactions frequently require harsh conditions, such as high temperature and high pressure, and the continuous flow of the reaction medium exert a pronounced mechanical stress for solid materials, which together often contribute to limited applicability and stability of heterogeneous transition metal catalysts in flow reactors [62].

It is well-known that different solvents may exert significant effects on the performance of homogeneous as well as heterogeneous catalysts [63]. Therefore, in the course of a catalytic reaction, it is crucial to choose the appropriate solvent [64,65], and this is especially true for flow conditions to ensure reaction homogeneity and to avoid clogging in reactor channels. One of the most important limitations of heterogeneous materials being employed as catalysts in flow systems is their incompatibility with certain solvents [66]. In these cases, temperature-dependent solvent interactions result in irreversible structural changes, which significantly reduce catalyst robustness and performance. For example, amide type solvents delaminate the layers of layered double hydroxides, which leads to the collapse of catalyst structure and leaching under flow conditions [67].

Recently, we reported on a silver–bismuth hybrid, beyerite-like [68] material (AgBi-HM) with structurally-bound silver catalytic centres, and successfully employed it for heterogeneous catalytic C≡C bond activation to yield organic nitriles directly from terminal alkynes under batch reaction conditions [69]. Although the as-prepared material was completely characterized, the actual position of silver ions in the catalyst lattice remained unresolved. In the present contribution, we report our new findings on the structure of the AgBi-HM, and also on the stability of the material in different solvents under a variety of continuous flow conditions. Finally, aided by the data acquired in elaborate stability tests, we aimed for a simple continuous flow methodology for catalytic dehydrogenation of benzylic alcohols to the corresponding aldehydes as valuable substances; the results are presented herein.

2. Experimental

2.1. General information

All fine chemicals, materials and reagents used were commercially available, and were applied as received without further purification. The benzyl alcohol substrates (with purity of ≥98 %) and the solvents used for catalyst stability experiments and also for dehydrogenation reactions were purchased from Sigma-Aldrich (Merck) and VWR. Analytical thin-layer chromatography was performed on Merck silica gel 60 F254 plates and flash column chromatography on Merck silica gel 60. Compounds were visualized by means of UV or $KMnO_4$. NMR spectra were recorded on a Bruker Avance DRX 500 spectrometer, in $CDCl_3$ as solvent, with TMS as internal standard, at 500.1 and 125 MHz, respectively. GC–MS analyses were performed on a Thermo Scientific Trace 1310 Gas Chromatograph coupled with a Thermo Scientific ISQ QD Single Quadrupole Mass Spectrometer using a ThermoScientific TG-SQC column (15 m × 0.25 mm ID × 0.25 μ film). Measurement parameters were as follows. Column oven temperature: from 50 to 300 °C at 15 °C/min, injection temperature: 240 °C, ion source temperature: 200 °C, electrospray ionization: 70 eV, carrier gas: He at 1.5 mL min^{-1}, injection volume: 2 μL, split ratio: 1:33.3, mass range: 50–500 *m/z*.

2.2. Synthesis and characterization of the AgBi-HM

AgBi-HM was prepared by using the urea hydrolysis method following our previously reported procedure [70]. In this way, the pH could precisely be controlled through the temperature of the co-hydrolysis. In a typical synthesis, the adequate amounts of $AgNO_3$ (3.73 g) and $Bi(NO_3)_3{\cdot}5H_2O$ (5.36 g) were dissolved in 50–50 mL 5 wt% nitric acid. After mixing, urea (7.05 g) dissolved in 100 mL of deionized water was added to the solution and stirred for 72 h at 130 °C. As an alternative way of the synthesis, after addition of the urea solution to the mixture of the required salts, the reaction mixture was placed into an oven for 24 h at 105 °C. The obtained material was next filtrated, washed with aqueous thiosulfate solution, water and ethanol four times, and dried at 60 °C to obtain the final product.

AgBi-HM was fully characterized by means of diverse instrumental techniques as detailed earlier [59]. In the present study, the as-prepared and the treated samples of the material were checked by X-ray diffractometry (XRD), Raman and IR spectroscopies as well as SEM-EDX measurements. Powder XRD patterns were registered in the 2θ = 4°–60° range on a Rigaku Miniflex II instrument using Cu Kα (λ = 1.5418 Å) radiation. FT-IR spectra were measured on a BIO-RAD Digilab Division FTS-65A/896 spectrophotometer with 4 cm^{-1} resolution. 256 scans were collected for each spectrum. The spectra of each sample were recorded with diffuse reflection technique by fixing the incident angle in 45° position. Raman spectra were measured with a Thermo Scientific™ DXR™ Raman microscope at an excitation wavelength of 635 nm applying 10 mW laser power and averaging 20 spectra with an exposure time of 6 s. The actual silver-bismuth molar ratios in the samples before and after treatment were determined by performing SEM-EDX measurements with an S-4700 scanning electron microscope (SEM, Hitachi, Japan) with accelerating voltage of 10–18 kV coupled with a Röntec QX2 energy dispersive microanalytical system.

2.3. Anion-exchange experiments under hydrothermal conditions

For hydrothermal treatment of the AgBi-HM, highly concentrated iodide (c_{NaI} = 4 M), chloride (c_{NaCl} = 4 M) and carbonate (c_{Na2CO3} = 3 M) aqueous solutions were prepared and used. The direct anion-exchange tests were carried out in a Teflon-lined stainless steel autoclave at 120 °C for 2 days. The obtained slurries were filtered, washed with water several times and dried at 80 °C overnight. Treated samples were characterized by XRD, Raman and IR spectroscopies, as well as SEM-EDX measurements.

2.4. Procedure for investigating the solvent compatibility of AgBi-HM under flow conditions

To examine the stability of the as-prepared AgBi-HM, a simple continuous flow set-up was assembled (Fig. 1). The system consisted of an HPLC pump (JASCO PU-2085), a stainless steel cartridge with internal dimensions of 30 × 2.1 mm and a 10-bar backpressure regulator (BPR; IDEX) to enable overheating of the solvents. The column was charged with approximately 50 mg of the AgBi-HM, and was sealed with compatible frits (0.5 μm pore size). Parts of the system were connected with stainless steel capillary tubing (internal diameter 250 μm). The catalyst bed was immersed into an oil bath for heating purposes. In each

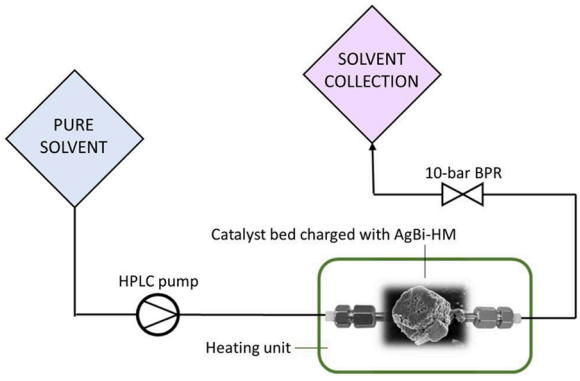

Fig. 1. Experimental setup for the continuous flow experiments.

test, the selected solvent was continuously pumped through the column for 90 min under the appropriate conditions. The treated hybrid material sample was then removed from the cartridge, and was examined by XRD and IR spectroscopy.

2.5. Procedure for AgBi-HM-catalysed alcohol dehydrogenations under flow conditions

The silver-catalysed dehydrogenation reactions were carried out by using the same flow system as the one used for the solvent compatibility tests (Fig. 1). As catalyst bed, a stainless steel cartridge with internal dimensions of 100 × 4.6 mm was used, which encompassed approximately 2 g of AgBi-HM. For each reaction, the corresponding benzyl alcohol (c = 0.075 M) was dissolved in toluene, and the solution was pumped continuously under the selected conditions. In each run, 4 mL of product solution was collected. Between two experiments, the system was washed for 20 min by pumping toluene at a flow rate of 0.5 mL min^{-1}. The crude products were checked by NMR spectroscopy, to determine the conversions and the selectivities. If necessary, column chromatographic purification was carried out with mixture of hexane and EtOAc as eluent. The reaction products were characterized by NMR and MS techniques. The characterization data can be found in the *Supporting Information (SI)* file.

3. Results and discussion

3.1. Indirect proof of the structure of the AgBi-HM

From our earlier investigations [70], it was clear that the AgBi-HM contained Ag(I) and Bi(III) cationic and carbonate anionic components with silver ion as the minor cationic component. The material exhibited layered structure resembling that of a mineral called beyerite ($CaBi_2O_2(CO_3)_2$) [69], which contains Ca(II) ions fixed between $BiO(CO)_3$ layers. In the hybrid material, Bi(III) ions are connected *via* one of the oxygen atoms of the carbonate ions and they are constituents of the layers. At that point, we speculated that Ag(I) ions as minor cationic component are residing among the Bi(III)-containing layers, and are strongly coordinated to the carbonate ions. As concerns the catalytic applicability of the hybrid material, this structural information is of crucial importance. For example, it is essential to know how leaching of the active component can occur, and whether it takes place in a way that the lamellar structure remains intact. On the other hand, the inserted lamellar (Aurivillius) structure may not only be formed by intercalating silver cations among the bismutite layers, but also via incorporating those into the framework of the structure [71]. Accordingly, the removal of silver content without definitive termination of the long-range order of the lamellar structure is only possible from the interlayer-modified bismutite.

To prove the presence or absence of exchangeable interlayer anions of silver species, anion exchange reactions were attempted in the presence of highly concentrated 'entry' anions under hydrothermal conditions. As-prepared AgBi-HM samples were thus treated with concentrated NaI, NaCl or Na_2CO_3 aqueous solutions at 120 °C for 2 days, and the treated samples were compared to the as-prepared one.

As can be seen in Fig. 2, the XRD patterns of the treated samples showed large differences from the as-prepared material. The significant shifts in the characteristic peaks as well as the change in the intensities of the reflections indicated that notable anion exchange took place. Moreover, by finding perfect agreement in the JCPDS (Joint Committee of Powder Diffraction Standards – International Centre for Diffraction Data) database, the produced structures could be undoubtedly identified as bismuth oxyiodide (P(owder)D(iffraction)F(ile) #73-2062) and oxychloride (PDF#06-0249) with tetragonal matlockite crystal phase, which is a layered structure. The framework consists of fluorite-like $[M_2O_2]$ layers sandwiched between double halogen layers upon applying iodide and chloride anions, respectively, as entry anions.

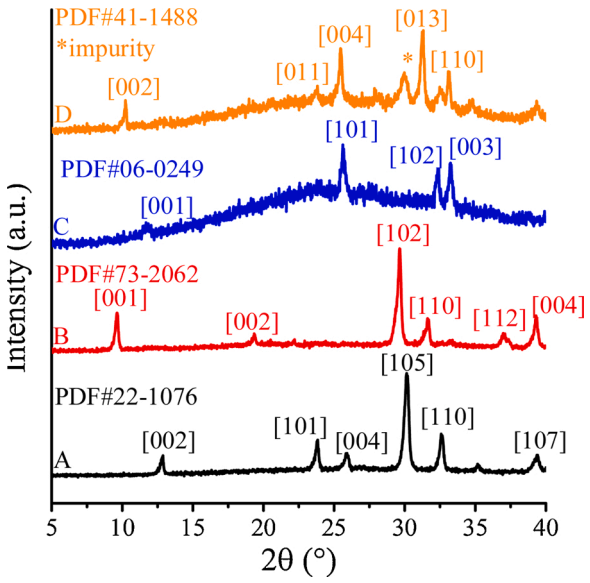

Fig. 2. XRD patterns of AgBi-HM samples: as-prepared material (A), material treated with iodide- (B), chloride- or (C) carbonate-containing solutions (D).

Additionally, by using carbonate as guest anions, pure bismutite (PDF#41-1488) was obtained. It could be assigned to orthorhombic crystal structure similarly to the AgBi-HM. However, because of the theoretical reasons, more expanded interlayer gallery was detected for bismuth subcarbonate without silver ions, which was indicated by the shift of the [002] Bragg reflection into lower 2θ values.

Furthermore, neither the FT-IR nor the Raman spectra of bismuth oxyiodide and oxychloride contained any relevant vibrational bands related to the carbonate species of the raw material (Fig. 3) [72]. In the halogen-containing systems, the broadened stretching vibrations at around 1040 cm^{-1} may be attributed to the Bi–I/Cl band in the BiOI/Cl structure [73]. In addition, the Raman spectra confirmed that the treated materials had oxyiodide/oxychloride structure with the same Raman peaks as in the literature. The characteristic Raman bands at around 180 and 150 cm^{-1} could be associated with A_{1g} internal Bi–Cl stretching and E_g external Bi–Cl stretching modes of bismuth oxychloride upon intercalation of chloride anions [74]. Moreover, two incisive characteristic bands at 160 and 81 cm^{-1} of the iodine-treated samples were assigned to A_{1g} and E_g stretching modes of bismuth oxyiodide [75]. Additionally, by means of SEM-EDX measurements, the loss of the silver cations from the treated structures could also be illustrated (Fig. 4).

These results lead to the conclusion that by performing hydrothermal heat treatment on the Aurivillius structures in the presence of highly concentrated anions, partial or complete anion exchange could be achieved. At the same time, the silver content also diminished. Consequently, it has been proven that silver cations are fixed among the bismutite-like layers of the hybrid material in the form of silver-containing anionic species.

3.2. Investigating the stability and solvent-compatibility of the AgBi-HM under continuous flow conditions

To obtain valuable data on the applicability of the AgBi-HM for organic synthesis in continuous flow mode, the effects of various solvents and reaction conditions on the structure of the material were examined. A simple flow reactor set-up was assembled as detailed in the *Experimental* section. A comprehensive list of solvents was compiled for the stability tests comprising polar, non-polar, protic and aprotic ones. This included CH_2Cl_2, $CHCl_3$, EtOAc, acetone, diethyl ether, MeOH, EtOH, *i*PrOH, H_2O, MeCN, tetrahydrofuran (THF), *N*-methyl-2-

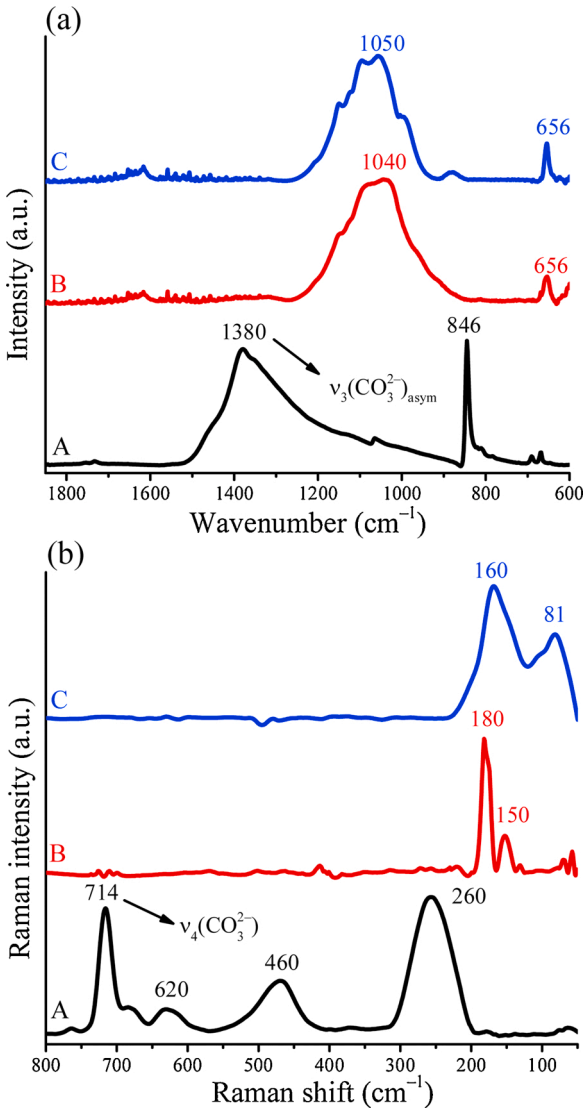

Fig. 3. (a) IR and (b) Raman spectra of AgBi-HM samples: as-prepared material (A), material treated with iodide- (B) or chloride-containing solutions (C).

pyrrolidone (NMP), *n*-hexane, toluene, *N*,*N*-dimethylformamide (DMF), dimethyl sulfoxide (DMSO) and *N*,*N*-dimethylacetamide (DMA). In each test, the appropriate solvent was pumped for 90 min at 0.5 mL min^{-1} flow rate through a catalyst bed encompassing a sample of AgBi-HM. The tests were carried out at 25, 50, 100, 150 and 200 °C as temperatures typically used in catalytic flow reactions. It should be noted that according to TG and DTG measurements, the structure of the hybrid material is thermally stable until 380 °C [70].

The XRD patterns of the treated AgBi-HM samples verified that none of the tested conditions caused collapse or even damage of the structure of the as-prepared material. This was also found for DMF and DMA, which are known as delaminating solvents for certain layered materials [67]. For toluene, DMSO, H_2O, MeCN and EtOAc, the XRD patterns of the treated samples were analogous with that of the as-prepared material at most of the temperatures investigated (Fig. 5, diffractograms B and C as examples). The calculated basal spacings related to the lamellar structures were exactly the same before and after the solvent treatment. In certain solvents, such as acetone, CH_2Cl_2, diethyl ether and alcohols, the XRD patterns were still typical of the beyerite-like hybrid material with basal reflections in the 2θ = 9–38° region, but doubling of characteristic reflections appeared on their diffractograms at different temperatures (Fig. 5, diffractograms D and E as examples). This observation

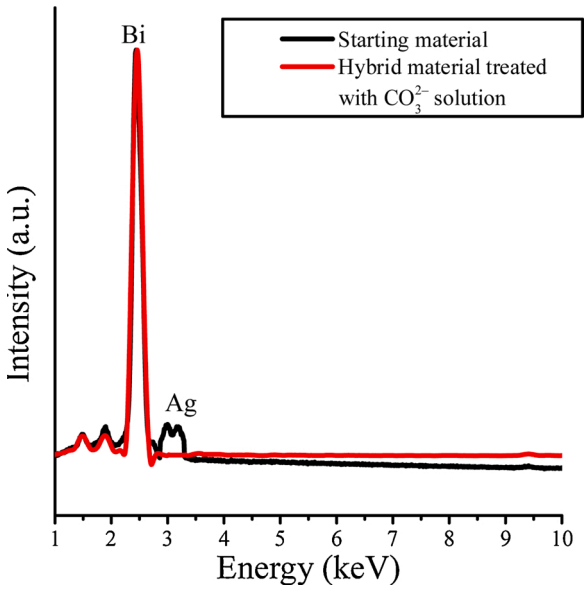

Fig. 4. EDX spectra of the as-prepared AgBi-HM and the one treated with carbonate-containing solution.

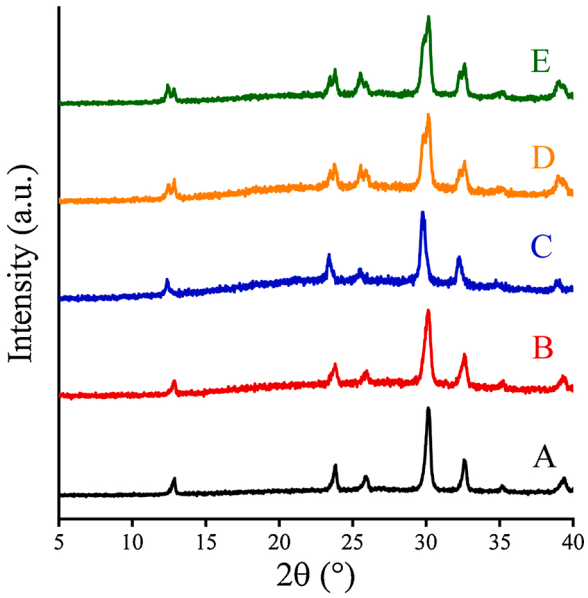

Fig. 5. XRD patterns of AgBi-HM samples: as-prepared material (A), sample treated with toluene at 25 °C (B), sample treated with H_2O at 150 °C (C), sample treated with *i*PrOH at 50 °C (D) and sample treated with diethyl ether at 25 °C (E).

is very similar to the well-known staging effect of lamellar structures [76], and may be explained by partial recrystallization and the formation of a new phase with increased interlayer distances. IR spectra of samples with doubled reflections showed the typical characteristics of the non-treated material, the new absorption bands appeared at around 2900 cm^{-1} can be identified as C—H stretching vibrations of organic solvent traces (Fig. S18) [77]. The results of the stability tests are summarized in Table 1, and the complete collection of diffractograms is presented in the *SI* file.

3.3. Catalytic dehydrogenation of benzylic alcohols under flow conditions

Encouraged by the promising results on the stability of the AgBi-HM

Table 1
Summary of the results of the AgBi-HM stability tests under flow conditions. (A: XRD patterns analogous with that of the as-prepared material, B: doubled characteristic reflections.).

Entry	Solvent	25 °C	50 °C	100 °C	150 °C	200 °C
1	acetone	A	B	B	B	B
2	DMA*	A	A	A	B	B
3	toluene	A	A	A	A	A
4	THF*	A	A	B	B	B
5	DMSO*	A	A	A	A	A
6	$CHCl_3$	B	B	A	A	A
7	*i*PrOH	A	B	B	B	A
8	CH_2Cl_2	B	B	B	B	B
9	MeOH	B	B	B	B	B
10	NMP*	B	B	A	B	A
11	diethyl ether	B	B	B	B	B
12	EtOH	B	B	B	B	A
13	H_2O	B	A	A	A	A
14	MeCN	A	A	A	A	A
15	hexane	B	B	A	A	A
16	DMF*	B	B	A	B	A
17	EtOAc	A	A	A	A	A

* tetrahydrofuran (THF), N-methyl-2-pyrrolidone (NMP), N,N-dimethylformamide (DMF), dimethyl sulfoxide (DMSO), N,N-dimethylacetamide (DMA).

under demanding conditions, we next turned our attention to potential synthetic applications in continuous flow mode. As a consequence of the ubiquity of carbonyl compounds, catalytic oxidation/dehydrogenation of alcohols are of fundamental importance in synthetic organic chemistry and, accordingly, in the fine chemical and pharmaceutical industries [78–82]. Oxidant-free dehydrogenation processes are cleaner, more atom-efficient, and due to the lack of over-oxidation, generally more selective than catalytic oxidations [83–85]. However, such reactions typically require harsh conditions, and hence pose a significant synthetic challenge. In fact, besides well-established industrial processes for gas-phase alcohol dehydrogenations [86,87], liquid-phase catalytic methodologies are quite limited, and often suffer from significant drawbacks, such as low activity, limited substrate scope and the necessity of various additives [88–91]. Inspired by these factors, we selected catalytic dehydrogenation of benzylic alcohols as a benchmark to evaluate the synthetic capability of the AgBi-HM catalyst under demanding flow conditions.

To investigate the effects of reaction conditions on the catalytic dehydrogenation, 4-methylbenzyl alcohol was selected as a model substrate. Initially, the AgBi-HM catalyst was tested under batch conditions and, in parallel, another reaction was performed under the same conditions using $AgNO_3$ as catalyst (Scheme 1). After stirring for 24 h in refluxing toluene (110 °C), 62 % conversion was detected with the hybrid material, whereas $AgNO_3$ gave only 15 % conversion (selectivity was 100 % in both reactions). No conversion was detected without the presence of catalyst. The enhanced activity of the catalyst – compared to silver nitrate salt – may be assigned to the promoter roles of the bismuth centres and the oxide surface. A possible reaction mechanism was suggested accordingly (Scheme S1). Moreover, in our opinion, the exclusive selectivity is the contribution not only of Ag(I) centres but the shape-selective effect of the layered structure.

The promising preliminary results encouraged us to explore the reaction further under continuous flow conditions using a simple fixed-bed system as shown in Fig. 1. Considering that the AgBi-HM was proven to be compatible with wide variety of solvents even at high temperatures (Table 1), extensive solvent screening was carried out at 180 °C (Table 2). The reaction outcome proved to be strongly dependent on the solvent applied. In acetone, CH_2Cl_2, EtOAc and MeCN, conversions of 20–46 % were detected; however, selectivity was very low (entries 1–4). Contrarily, in DMSO, MeOH, THF or toluene, selective aldehyde formation was observed (entries 5–8). The highest conversion was achieved in toluene (92 %, entry 8), which was therefore chosen as solvent for further parameter optimization.

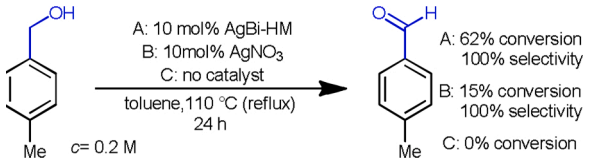

Scheme 1. Catalytic dehydrogenation of 4-methylbenzyl alcohol under batch conditions.

The reaction temperature was found to have significant role on the conversion and the selectivity (Fig. 6a). For example, at 100 °C, conversion of merely 13 % occurred, which was improved remarkably upon gradual increase of the temperature. Gratifyingly, at 180 °C, 92 % conversion and 100 % selectivity were observed. However, further increase to 200 °C triggered the benzylation of toluene with the substrate as competing side reaction, and thus provoked a momentous decrease in selectivity to 62 % (besides a marginal increase in conversion). Such benzylations are known from the literature, and can be accessed in the presence of various metal catalysts typically at higher temperatures [92, 93]. The residence time also had significant effects on the reaction outcome. Upon decreasing the flow rate from 150 μL min^{-1}, the conversion gradually improved from 64 % until it finally reached 100 % at 20 μL min^{-1} (Fig. 6b), which corresponded to a residence time of approximately 75 min. However, at 20 μL min^{-1} flow rate, the competing benzylation appeared as side reaction, and reduced the selectivity to 56 %. As optimum flow rate, 30 μL min^{-1} was selected (corresponding to 50 min residence time), which ensured an excellent conversion of 92 % and fully selective aldehyde formation. The effects of substrate concentration were also examined (Table S1), and 0.075 M was found to be the best as higher concentrations led to lower selectivity due to side product formation.

Based on the findings of the parameter optimization, the reaction was operated most efficiently at 30 μL min^{-1} flow rate and 180 °C reaction temperature with a substrate concentration of 0.075 M. With these conditions in hand, we finally set out to investigate the substrate scope of the process (Table 3). Excellent conversions were found for substituted benzyl alcohol derivatives containing methyl, methoxy, bromo and nitro groups in the *para* position. The reactions also worked well with meta-substituted benzyl alcohols, and furnished conversions in the range of 36–82 %. The multisubstituted 3-methyl-4-nitrobenzyl alcohol gave an acceptable conversion of 40 %. Dehydrogenation of 2-bromobenzyl alcohol was also attempted, but due to the significant steric hindrance generated by the *ortho* bromo moiety, the conversion of the substrate was merely 18 %. It is remarkable that in all reactions, fully selective aldehyde formation was observed, side products were not detected.

Table 2
Investigating the effects of various solvents on the dehydrogenation reaction of 4-methylbenzyl alcohol under continuous flow conditions.

Entry	Solvent	Conv.[a] (%)	Sel.[a] (%)
			
1	acetone	20	traces
2	CH_2Cl_2	36	traces
3	EtOAc	46	25
4	MeCN	27	40
5	DMSO	8	100
6	MeOH	4	100
7	THF	22	100
8	toluene	92	100

[a] Determined by ^{1}H NMR analysis of the crude product.

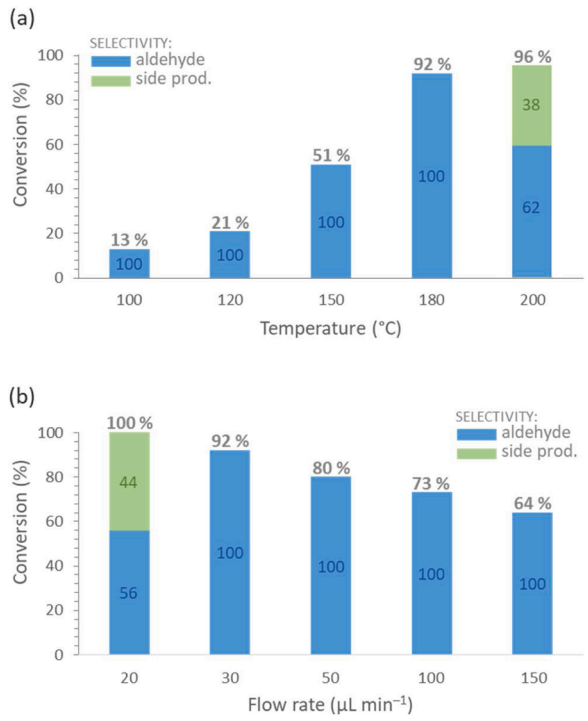

Fig. 6. Investigating the effects of temperature (a) and flow rate (b) on the AgBi-HM-catalysed dehydrogenation of 4-methylbenzyl alcohol under continuous flow conditions. (Reaction conditions: $c = 0.075$ M, toluene as solvent, 30 µL min^{-1} flow rate for the temperature study, 180 °C temperature for the flow rate study.).

Table 3
AgBi-HM-catalyzed dehydrogenation of diversely substituted benzyl alcohols under continuous flow conditions.

Entry	Substrate	Conv.[a] (%)	Sel.[a] (%)
	180 °C, 30 µL min^{-1}, toluene; AgBi-HM; c= 0.075 M		
1	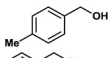	92	100
2	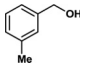	82	100
3	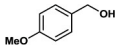	95	100
4	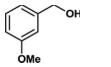	36	100
5	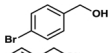	70	100
6	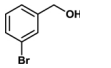	59	100
7	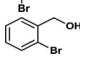	18	100
8	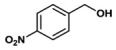	73	100
9	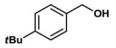	43	100
10	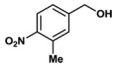	40	100

[a] Determined by ^{1}H NMR analysis of the crude product.

4. Conclusions

By strategic anion-exchange reactions under hydrothermal conditions, the modification of the interlayer gallery of the AgBi-HM was successfully achieved, which indirectly proved that silver cations were fixed among the layers of the material as silver-containing anionic species. The stability of the material was investigated in a wide variety of organic solvents under continuous flow conditions to aid potential synthetic applications. It was found that none of the tested solvents resulted in the collapse or even damage of the structure of the material, even at temperatures as high as 200 °C. As proof of concept, a novel continuous flow protocol was established for catalytic dehydrogenation of benzylic alcohols using the hybrid material as catalyst. The effects of reaction temperature, residence time, substrate concentration and various solvents were explored to achieve high conversions and selective aldehyde formation without the need for any additives. The scope and applicability of the flow protocol was also demonstrated.

CRediT authorship contribution statement

Rebeka Mészáros: Investigation, Data curation, Writing - original draft. **Sándor B. Ötvös:** Conceptualization, Supervision, Writing - review & editing. **Gábor Varga:** Investigation, Data curation. **Éva Böszörményi:** Investigation. **Marianna Kocsis:** Investigation. **Krisztina Karádi:** Investigation. **Zoltán Kónya:** Methodology. **Ákos Kukovecz:** Methodology. **István Pálinkó:** Conceptualization, Supervision, Validation, Writing - review & editing. **Ferenc Fülöp:** Supervision, Resources.

Declaration of Competing Interest

The authors report no competing interest.

Acknowledgements

Financial support was obtained from the ÚNKP-19-3 New National Excellence Program of the Ministry for Innovation and Technology (Hungary). SBÖ acknowledges the Premium Post Doctorate Research Program of the Hungarian Academy of Sciences. All these supports are highly appreciated.

Appendix A. Supplementary data

Supplementary material related to this article can be found, in the online version, at doi:https://doi.org/10.1016/j.mcat.2020.111263.

References

[1] Z. Chen, N. Ren, X. Ma, J. Nie, F.-G. Zhang, J.-A. Ma, Silver-catalyzed [3 + 3] dipolar cycloaddition of trifluorodiazoethane and glycine imines: access to highly functionalized trifluoromethyl-substituted triazines and pyridines, ACS Catal. 9 (2019) 4600–4608.
[2] J. George, H.Y. Kim, K. Oh, Silver-catalyzed asymmetric desymmetrization of cyclopentenediones via [3 + 2] cycloaddition with α-substituted isocyanoacetates, Org. Lett. 20 (2018) 2249–2252.
[3] A.K. Clarke, J.M. Lynam, R.J.K. Taylor, W.P. Unsworth, "Back-to-Front" indole synthesis using silver(I) catalysis: unexpected C-3 pyrrole activation mode supported by DFT, ACS Catal. 8 (2018) 6844–6850.
[4] Z.-Z. Zhou, M. Liu, L. Lv, C.-J. Li, Silver(I)-catalyzed widely applicable aerobic 1,2-diol oxidative cleavage, Angew. Chem. Int. Ed. 57 (2018) 2616–2620.
[5] Y. Ning, Q. Ji, P. Liao, E.A. Anderson, X. Bi, Silver-catalyzed stereoselective aminosulfonylation of alkynes, Angew. Chem. Int. Ed. 56 (2017) 13805–13808.
[6] K. Sekine, T. Yamada, Silver-catalyzed carboxylation, Chem. Soc. Rev. 45 (2016) 4524–4532.
[7] H. Pellissier, Enantioselective silver-catalyzed transformations, Chem. Rev. 116 (2016) 14868–14917.
[8] V.K.-Y. Lo, A.O.-Y. Chan, C.-M. Che, Gold and silver catalysis: from organic transformation to bioconjugation, Org. Biomol. Chem. 13 (2015) 6667–6680.
[9] A. Yanagisawa, N. Yang, K. Bamba, Asymmetric allylation of carbonyl compounds catalyzed by a chiral phosphine–silver complex, Eur. J. Org. Chem. (2017) 6614–6618.
[10] A. Koizumi, M. Harada, R. Haraguchi, S.-I. Fukuzawa, Chiral silver complex-catalyzed diastereoselective and enantioselective Michael addition of 1-Pyrroline-5-carboxylates to α-enones, J. Org. Chem. 82 (2017) 8927–8932.
[11] S. Ghorai, D. Lee, Aryne formation via the hexadehydro Diels-Alder reaction and their Ritter-type transformations catalyzed by a cationic silver complex, Tetrahedron 73 (2017) 4062–4069.

[12] A. Yanagisawa, Y. Lin, A. Takeishi, K. Yoshida, Enantioselective nitroso aldol reaction catalyzed by a chiral phosphine–silver complex, Eur. J. Org. Chem. (2016) 5355–5359.
[13] R.J. Scamp, B. Scheffer, J.M. Schomaker, Regioselective differentiation of vicinal methylene C–H bonds enabled by silver-catalysed nitrene transfer, Chem.Commun. 55 (2019) 7362–7365.
[14] M. Dell'Acqua, V. Pirovano, S. Peroni, G. Tseberlidis, D. Nava, E. Rossi, G. Abbiati, Silver-catalysed domino approach to 1,3-dicarbo-substituted isochromenes, Eur. J. Org. Chem. (2017) 1425–1433.
[15] S. Guo, F. Cong, R. Guo, L. Wang, P. Tang, Asymmetric silver-catalysed intermolecular bromotrifluoromethoxylation of alkenes with a new trifluoromethoxylation reagent, Nat. Chem. 9 (2017) 546–551.
[16] X. Zhou, C. Huang, Y. Zeng, J. Xiong, Y. Xiao, J. Zhang, Silver-catalysed tandem hydroamination and cyclization of 2-trifluoromethyl-1,3-enynes with primary amines: modular entry to 4-trifluoromethyl-3-pyrrolines, Chem. Commun. 53 (2017) 1084–1087.
[17] J. An, G. Sun, H. Xia, Aerobic oxidation of 5-hydroxymethylfurfural to high-yield 5-hydroxymethyl-2-furancarboxylic acid by poly(vinylpyrrolidone)-capped Ag nanoparticle catalysts, ACS Sustainable Chem. Eng. 7 (2019) 6696–6706.
[18] W.-J. Chen, B.-H. Cheng, Q.-T. Sun, H. Jiang, Preparation of MOF confined Ag nanoparticles for the highly active, size selective hydrogenation of olefins, ChemCatChem 10 (2018) 3659–3665.
[19] B. Ballarin, D. Barreca, E. Boanini, M.C. Cassani, P. Dambruoso, A. Massi, A. Mignani, D. Nanni, C. Parise, A. Zaghi, Supported gold nanoparticles for alcohols oxidation in continuous-flow heterogeneous systems, ACS Sustainable Chem. Eng. 5 (2017) 4746–4756.
[20] X.-Y. Dong, Z.-W. Gao, K.-F. Yang, W.-Q. Zhang, L.-W. Xu, Nanosilver as a new generation of silver catalysts in organic transformations for efficient synthesis of fine chemicals, Catal. Sci. Technol. 5 (2015) 2554–2574.
[21] C. Wen, A. Yin, W.-L. Dai, Recent advances in silver-based heterogeneous catalysts for green chemistry processes, Appl. Catal. B 160-161 (2014) 730–741.
[22] M.S. Esmaeili, Z. Varzi, R. Eivazzadeh-Keihan, A. Maleki, H. Ghafuri, Design and development of natural and biocompatible raffinose-Cu_2O magnetic nanoparticles as a heterogeneous nanocatalyst for the selective oxidation of alcohols, Mol. Catal. 492 (111037) (2020) 1–12.
[23] R. Eivazzadeh-Keihan, F. Radinekiyan, A. Maleki, M.S. Bani, Z. Hajizadeh, S. Asgharnasl, A novel biocompatible core-shell magnetic nanocomposite based on cross-linked chitosan hydrogels for in vitro hyperthermia of cancer therapy, Int. J. Biol. Macromol. 140 (2019) 407–414.
[24] J. Rahimi, R. Taheri-Ledari, M. Niksefat, A. Maleki, Enhanced reduction of nitrobenzene derivatives: effective strategy executed by Fe_3O_4/PVA-10% Ag as a versatile hybrid nanocatalyst, Catal. Commun. 134 (105850) (2020) 1–6.
[25] A. Maleki, K. Valadi, S. Gharibi, R. Taheri-Ledari, Convenient and fast synthesis of various chromene pharmaceuticals assisted by highly porous volcanic micro-powder with nanoscale diameter porosity, Res. Chem. Intermed. 46 (2020) 4113–4128.
[26] A. Maleki, T. Kari, Novel leaking-free, green, double core/shell, palladium-loaded magnetic heterogeneous nanocatalyst for selective aerobic oxidation, Catal. Lett. 148 (2018) 2929–2934.
[27] M. Azizi, A. Maleki, F. Hakimpoor, Solvent, metal and halogen-free synthesis of sulfoxides by using a recoverable heterogeneous urea-hydrogen peroxide silica-based oxidative catalytic system, Catal. Commun. 100 (2017) 62–65.
[28] R. Firouzi-Haji, A. Maleki, L-proline-functionalized Fe_3O_4 nanoparticles as an efficient nanomagnetic organocatalyst for highly stereoselective one-pot two-step tandem synthesis of substituted cyclopropanes, ChemistrySelect 4 (2019) 853–857.
[29] Z. Hajizadeh, A. Maleki, Poly (ethylene imine)-modified magnetic halloysite nanotubes: a novel, efficient and recyclable catalyst for the synthesis of dihydropyrano [2, 3-c] pyrazole derivatives, Mol. Catal. 460 (2018) 87–93.
[30] A. Maleki, M. Rabbani, S. Shahrokh, Preparation and characterization of a silica-based magnetic nanocomposite and its application as a recoverable catalyst for the one-pot multicomponent synthesis of quinazolinone derivatives, Appl. Organomet. Chem. 29 (2015) 809–814.
[31] A. Maleki, Green oxidation protocol: selective conversions of alcohols and alkenes to aldehydes, ketones and epoxides by using a new multiwall carbon nanotube-based hybrid nanocatalyst via ultrasound irradiation, Ultrason. Sonochem. 40 (2018) 460–464.
[32] A. Maleki, R. Rahimi, S. Maleki, Efficient oxidation and epoxidation using a chromium (VI)-based magnetic nanocomposite, Environ. Chem. Lett. 14 (2016) 195–199.
[33] A. Shaabani, A. Maleki, Green and efficient synthesis of quinoxaline derivatives via ceric ammonium nitrate promoted and in situ aerobic oxidation of α-hydroxy ketones and α-keto oximes in aqueous media, Chem. Pharm. Bull. 56 (2008) 79–81.
[34] A. Zuliani, P. Ranjan, R. Luque, E.V. Van der Eycken, Heterogeneously catalyzed synthesis of imidazolones via cycloisomerizations of propargylic ureas using Ag and Au/Al SBA-15 systems, ACS Sustainable Chem. Eng. 7 (2019) 5568–5575.
[35] E. Plessers, J.E. van den Reijen, P.E. de Jongh, K.P. de Jong, M.B.J. Roeffaers, Origin and abatement of heterogeneity at the support granule scale of silver on silica catalysts, ChemCatChem 9 (2017) 4562–4569.
[36] Z. Zhou, C. He, L. Yang, Y. Wang, T. Liu, C. Duan, Alkyne activation by a porous silver coordination polymer for heterogeneous catalysis of carbon dioxide cycloaddition, ACS Catal. 7 (2017) 2248–2256.
[37] A.R. Bogdan, A.W. Dombrowski, Emerging trends in flow chemistry and applications to the pharmaceutical industry, J. Med. Chem. 62 (2019) 6422–6468.
[38] L. Rogers, K.F. Jensen, Continuous manufacturing – the green chemistry promise? Green Chem. 21 (2019) 3481–3498.
[39] R. Gerardy, N. Emmanuel, T. Toupy, V.-E. Kassin, N.N. Tshibalonza, M. Schmitz, J.-C.M. Monbaliu, Continuous flow organic chemistry: successes and pitfalls at the interface with current societal challenges, Eur. J. Org. Chem. (2018) 2301–2351.
[40] M.B. Plutschack, B. Pieber, K. Gilmore, P.H. Seeberger, The hitchhiker's guide to flow chemistry, Chem. Rev. 117 (2017) 11796–11893.
[41] R. Porta, M. Benaglia, A. Puglisi, Flow chemistry: recent developments in the synthesis of pharmaceutical products, Org. Process Res. Dev. 20 (2016) 2–25.
[42] I.M. Mándity, S.B. Ötvös, F. Fülöp, Strategic application of residence-time control in continuous-flow reactors, ChemistryOpen 4 (2015) 212–223.
[43] S.B. Ötvös, M.A. Pericàs, C.O. Kappe, Multigram-scale flow synthesis of the chiral key intermediate of (−)-paroxetine enabled by solvent-free heterogeneous organocatalysis, Chem. Sci. 10 (2019) 11141–11146.
[44] V.-E.H. Kassin, R. Gerardy, T. Toupy, D. Collin, E. Salvadeo, F. Toussaint, K. van Hecke, J.-C.M. Monbaliu, Expedient preparation of active pharmaceutical ingredient ketamine under sustainable continuous flow conditions, Green Chem. 21 (2019) 2952–2966.
[45] R.E. Ziegler, B.K. Desai, J.-A. Jee, B.F. Gupton, T.D. Roper, T.F. Jamison, 7-step flow synthesis of the HIV integrase inhibitor Dolutegravir, Angew. Chem. Int. Ed. 57 (2018) 7181–7185.
[46] H. Ishitani, K. Kanai, Y. Saito, T. Tsubogo, S. Kobayashi, Synthesis of (±)-Pregabalin by utilizing a three-step sequential-flow system with heterogeneous catalysts, Eur. J. Org. Chem. (2017) 6491–6494.
[47] M.O. Kitching, O.E. Dixon, M. Baumann, I.R. Baxendale, Flow-assisted synthesis: a key fragment of SR 142948A, Eur. J. Org. Chem. (2017) 6540–6553.
[48] S. Borukhova, T. Nöel, V. Hessel, Continuous-flow multistep synthesis of Cinnarizine, Cyclizine, and a Buclizine derivative from bulk alcohols, ChemSusChem 9 (2016) 67–74.
[49] B. Gutmann, D. Cantillo, C.O. Kappe, Continuous-flow technology—a tool for the safe manufacturing of active pharmaceutical ingredients, Angew. Chem. Int. Ed. 54 (2015) 6688–6728.
[50] F.J. Martin-Martinez, K. Jin, D. López Barreiro, M.J. Buehler, The rise of hierarchical nanostructured materials from renewable sources: learning from nature, ACS Nano 12 (2018) 7425–7433.
[51] M.P. Tsang, G. Philippot, C. Aymonier, G. Sonnemann, Supercritical fluid flow synthesis to support sustainable production of engineered nanomaterials: case study of titanium dioxide, ACS Sustainable Chem. Eng. 6 (2018) 5142–5151.
[52] J.J. Pagano, T. Bánsági Jr., O. Steinbock, Bubble-templated and flow-controlled synthesis of macroscopic silica tubes supporting zinc oxide nanostructures, Angew. Chem. Int. Ed. 47 (2008) 9900–9903.
[53] S. Fuse, Y. Otake, H. Nakamura, Peptide synthesis utilizing micro-flow technology, Chem. Asian J. 13 (2018) 3818–3832.
[54] J. Britton, C.L. Raston, Multi-step continuous-flow synthesis, Chem. Soc. Rev. 46 (2017) 1250–1271.
[55] S.B. Ötvös, F. Fülöp, Flow chemistry as a versatile tool for the synthesis of triazoles, Catal. Sci. Technol. 5 (2015) 4926–4941.
[56] J.C. Pastre, D.L. Browne, S.V. Ley, Flow chemistry syntheses of natural products, Chem. Soc. Rev. 42 (2013) 8849–8869.
[57] Y. Deng, X.-J. Wei, X. Wang, Y. Sun, T. Noël, Iron-catalyzed cross-coupling of alkynyl and styrenyl chlorides with alkyl Grignard reagents in batch and flow, Chem. Eur. J. 25 (2019) 14532–14535.
[58] F. Ferlin, P.M. Luque Navarro, Y. Gu, D. Lanari, L. Vaccaro, Waste minimized synthesis of pharmaceutically active compounds via heterogeneous manganese catalysed C–H oxidation in flow, Green Chem. 22 (2020) 397–403.
[59] L.J. Durndell, M.A. Isaacs, C. Li, C.M.A. Parlett, K. Wilson, A.F. Lee, Cascade aerobic selective oxidation over contiguous dual-catalyst beds in continuous flow, ACS Catal. 9 (2019) 5345–5352.
[60] S.B. Ötvös, Á. Georgiádes, R. Mészáros, K. Kis, I. Pálinkó, F. Fülöp, Continuous-flow oxidative homocouplings without auxiliary substances: exploiting a solid base catalyst, J. Catal. 348 (2017) 90–99.
[61] D.C. Crowley, D. Lynch, A.R. Maguire, Copper-mediated, heterogeneous, enantioselective intramolecular buchner reactions of α-diazoketones using continuous flow processing, J. Org. Chem. 83 (2018) 3794–3805.
[62] T. Noel, S.L. Buchwald, Cross-coupling in flow, Chem. Soc. Rev. 40 (2011) 5010–5029.
[63] D. Cantillo, C.O. Kappe, Immobilized transition metals as catalysts for cross-couplings in continuous flow—a critical assessment of the reaction mechanism and metal leaching, ChemCatChem 6 (2014) 3286–3305.
[64] N. Yan, C. Xiao, Y. Kou, Transition metal nanoparticle catalysis in green solvent, Coord. Chem. Rev. 254 (2010) 1179–1218.
[65] L. Vaccaro, M. Curini, F. Ferlin, D. Lanari, A. Marrocchi, O. Piermatti, V. Trombettoni, Definition of green synthetic tools based on safer reaction media, heterogeneous catalysis, and flow technology, Pure Appl. Chem. 90 (2018) 21–33.
[66] D. Prat, A. Wells, J. Hayler, H. Sneddon, C.R. McElroy, S. Abou-Shehada, P.J. Dunn, CHEM21 selection guide of classical- and less classical-solvents, Green Chem. 18 (2016) 288–296.
[67] R. Mészáros, S.B. Ötvös, Z. Kónya, Á. Kukovecz, P. Sipos, F. Fülöp, I. Pálinkó, Potential solvents in coupling reactions catalyzed by Cu(II)Fe(III)-layered double hydroxide in a continuous-flow reactor, React. Kinet. Mech. Cat. 121 (2017) 345–351.
[68] S.B. Ötvös, I. Pálinkó, F. Fülöp, Catalytic use of layered materials for fine chemical syntheses, Catal. Sci. Technol. 9 (2019) 47–60.
[69] V. Malik, M. Pokhriyal, S. Uma, Single step hydrothermal synthesis of beyerite, $CaBi_2O_2(CO_3)_2$ for the fabrication of UV-visible light photocatalyst BiOI/$CaBi_2O_2(CO_3)_2$, RSC Adv. 6 (2016) 38252–38262.
[70] S.B. Ötvös, R. Mészáros, G. Varga, M. Kocsis, Z. Kónya, Á. Kukovecz, P. Pusztai, P. Sipos, I. Pálinkó, F. Fülöp, A mineralogically-inspired silver–bismuth hybrid

material: an efficient heterogeneous catalyst for the direct synthesis of nitriles from terminal alkynes, Green Chem. 20 (2018) 1007–1019.
[71] S. Sun, Y. Huang, G. Wang, J. Wang, Z. Fu, R. Peng, R.J. Knize, Y. Lu, Nanoscale structural modulation and enhanced room-temperature multiferroic properties, Nanoscale 6 (2014) 13494–13500.
[72] G. Zhao, Y. Tian, H. Fan, J. Zhang, L.J. Hu, Properties and structures of Bi_2O_3–B_2O_3–TeO_2 glass, J. Mater. Sci. Technol. 29 (2013) 209–214.
[73] L. Li, M. Zhang, Z. Zhao, B. Sun, X. Zhang, Visible/near-IR-light-driven TNFePc/BiOCl organic–inorganic heterostructures with enhanced photocatalytic activity, Dalton Trans. 45 (2016) 9497–9505.
[74] Y. Myung, J. Choi, F. Wu, S. Banerjee, E.H. Majzoub, J. Jin, S.U. Son, P.V. Braun, P. Banerjee, Cationically substituted $Bi_{0.7}Fe_{0.3}OCl$ nanosheets as Li ion battery anodes, ACS Appl. Mater. Interfaces 9 (2017) 14187–14196.
[75] H. Li, Z. Yang, J. Zhang, Y. Huang, H. Ji, Y. Tong, Indium doped BiOI nanosheets: preparation, characterization and photocatalytic degradation activity, Appl. Surf. Sci. 423 (2017) 1188–1197.
[76] K.K. Bardhan, G. Kirczenow, G. Jackle, J.C. Irwin, Staging structures of the intercalation compounds Ag_xTiS_2, Phys. Rev. B 33 (1986) 4149–4159.
[77] H. Masood, R. Yunus, T.S. Choong, U. Rashid, Y.H.T. Yap, Synthesis and characterization of calcium methoxide as heterogeneous catalyst for trimethylolpropane esters conversion reaction, Appl. Catal. A 425 (2012) 184–190.
[78] V.V. Torbina, A.A. Vodyankin, S. Ten, G.V. Mamontov, M.A. Salaev, V.I. Sobolev, O.V. Vodyankina, Ag-based catalysts in heterogeneous selective oxidation of alcohols: a review, Catalysts 8 (2018) 447.
[79] C. Parmeggiani, C. Matassinia, F. Cardona, A step forward towards sustainable aerobic alcohol oxidation: new and revised catalysts based on transition metals on solid supports, Green Chem. 19 (2017) 2030–2050.
[80] J.K. Mobley, M. Crocker, Catalytic oxidation of alcohols to carbonyl compounds over hydrotalcite and hydrotalcite-supported catalysts, RSC Adv. 5 (2015) 65780–65797.
[81] R. Ciriminna, V. Pandarus, F. Béland, Y.-J. Xu, M. Pagliaro, Heterogeneously catalyzed alcohol oxidation for the fine chemical industry, Org. Process Res. Dev. 19 (2015) 1554–1558.
[82] S.E. Davis, M.S. Ide, R.J. Davis, Selective oxidation of alcohols and aldehydes over supported metal nanoparticles, Green Chem. 15 (2013) 17–45.
[83] J. Zheng, J. Qu, H. Lin, Q. Zhang, X. Yuan, Y. Yang, Y. Yuan, Surface composition control of the binary Au–Ag catalyst for enhanced oxidant-free dehydrogenation, ACS Catal. 6 (2016) 6662–6669.
[84] K. Kon, S.M.A.H. Siddiki, K. Shimizu, Size- and support-dependent Pt nanocluster catalysis for oxidant-free dehydrogenation of alcohols, J. Catal. 304 (2013) 63–71.
[85] T. Mitsudome, Y. Mikami, H. Funai, T. Mizugaki, K. Jitsukawa, K. Kaneda, Oxidant-free alcohol dehydrogenation using a reusable hydrotalcite-supported silver nanoparticle catalyst, Angew. Chem. Int. Ed. 47 (2008) 138–141.
[86] F. Liu, H. Wang, A. Sapi, H. Tatsumi, D. Zherebetskyy, H.-L. Han, L.M. Carl, G. A. Somorjai, Molecular orientations change reaction kinetics and mechanism: a review on catalytic alcohol oxidation in gas phase and liquid phase on size-controlled Pt nanoparticles, Catalysts 8 (2018) 226.
[87] J.V. Ochoa, F. Cavani, Transition Metal Catalysis in Aerobic Alcohol Oxidation, The Royal Society of Chemistry, 2015, pp. 203–230.
[88] D.K. Kurhe, T.A. Fernandes, T.S. Deore, R.V. Jayaram, Oxidant free dehydrogenation of alcohols using chitosan/polyacrylamide entrapped Ag nanoparticles, RSC Adv. 5 (2015) 46443–46447.
[89] A. Bayat, M. Shakourian-Fard, N. Ehyaei, M. Mahmoodi Hashemi, Silver nanoparticles supported on silica-coated ferrite as magnetic and reusable catalysts for oxidant-free alcohol dehydrogenation, RSC Adv. 5 (2015) 22503–22509.
[90] V.L. Sushkevich, I.I. Ivanova, E. Taarning, Mechanistic study of ethanol dehydrogenation over silica-supported silver, ChemCatChem 5 (2013) 2367–2373.
[91] K. Shimizu, K. Sugino, K. Sawabe, A. Satsuma, Oxidant-free dehydrogenation of alcohols heterogeneously catalyzed by cooperation of silver clusters and acid–base sites on alumina, Chem. Eur. J. 15 (2009) 2341–2351.
[92] A.K. Maity, P.N. Chatterjee, S. Roy, Multimetallic Ir–Sn_3-catalyzed substitution reaction of π-activated alcohols with carbon and heteroatom nucleophiles, Tetrahedron 69 (2013) 942–956.
[93] J. Choudhury, S. Podder, S. Roy, Cooperative Friedel−crafts catalysis in heterobimetallic regime: alkylation of aromatics by π-activated alcohols, J. Am. Chem. Soc. 127 (2005) 6162–6163.

III

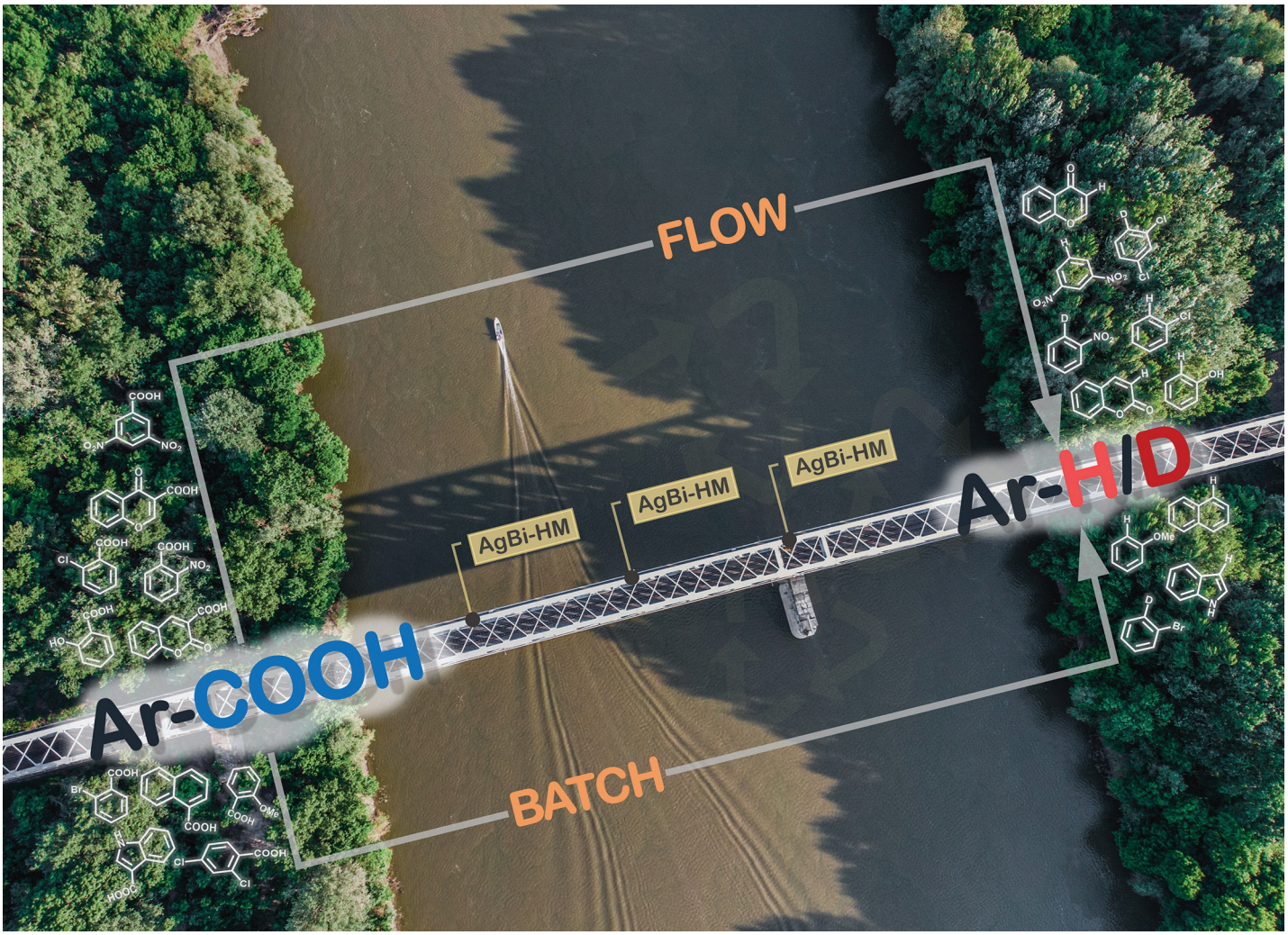

A collaborative research presented by groups of Prof. Ferenc Fülöp, Prof. István Pálinkó (University of Szeged, Hungary) and Dr. Sándor B. Ötvös (University of Graz, Austria).

Exploiting a silver–bismuth hybrid material as heterogeneous noble metal catalyst for decarboxylations and decarboxylative deuterations of carboxylic acids under batch and continuous flow conditions

A silver-containing hybrid material with structurally-bound catalytic centers has been exploited as an efficiently recyclable and highly active heterogenous noble metal catalyst for protodecarboxylations and decarboxylative deuterations of carboxylic acids. After an initial batch method development, a chemically intensified continuous flow process was established in a simple packed-bed system which enabled gram-scale protodecarboxylations without detectable structural degradation of the catalyst.

As featured in:

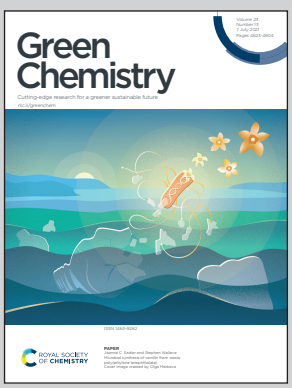

See Sándor B. Ötvös *et al.*, *Green Chem.*, 2021, **23**, 4685.

ROYAL SOCIETY OF CHEMISTRY

rsc.li/greenchem

Registered charity number: 207890

Green Chemistry

PAPER

View Article Online
View Journal | View Issue

Cite this: *Green Chem.*, 2021, **23**, 4685

Exploiting a silver–bismuth hybrid material as heterogeneous noble metal catalyst for decarboxylations and decarboxylative deuterations of carboxylic acids under batch and continuous flow conditions†‡

Rebeka Mészáros,[a] András Márton,[b] Márton Szabados,[b,c] Gábor Varga,[*c,d] Zoltán Kónya,[e,f] Ákos Kukovecz,[e] Ferenc Fülöp,[*a,g] István Pálinkó[§b,c] and Sándor B. Ötvös[*g,h]

Herein, we report novel catalytic methodologies for protodecarboxylations and decarboxylative deuterations of carboxylic acids utilizing a silver-containing hybrid material as a heterogeneous noble metal catalyst. After an initial batch method development, a chemically intensified continuous flow process was established in a simple packed-bed system which enabled gram-scale protodecarboxlyations without detectable structural degradation of the catalyst. The scope and applicability of the batch and flow processes were demonstrated through decarboxylations of a diverse set of aromatic carboxylic acids. Catalytic decarboxylative deuterations were achieved on the basis of the reaction conditions developed for the protodecarboxylations using D_2O as a readily available deuterium source.

Received 14th March 2021,
Accepted 17th May 2021

DOI: 10.1039/d1gc00924a

rsc.li/greenchem

1. Introduction

Carboxylic acids are of outstanding importance as inexpensive and easily accessible intermediates for the synthesis of an array of value-added products.[1] Among carboxylic acid transformations, protodecarboxylations and related decarboxylative couplings play a crucial role in the formation of C–C, C–X and C–H bonds, and hence they are appealing for the generation of molecular diversity.[2,3] The most common catalysts for protodecarboxylations contain copper, silver, gold, palladium or rhodium metals, typically as homogeneous sources in combination with various bases or ligands.[4–6] For example, in copper- and rhodium-catalyzed examples, well-defined complexes are predominant over reusable heterogeneous sources.[7–10] Palladium-catalyzed protodecarboxylations generally require high catalyst loading which severely limits their practical applicability.[11–13] In addition, various hexaaluminate catalysts proved useful for decarboxylation of biomass-derived carboxylic acids.[14–17] Due to the high costs involved, only a few studies have been reported for gold-catalyzed protodecarboxylations.[18–20] Silver-catalyzed reactions have also emerged in the field of protodecarboxylations and decarboxylative transformations, such as decarboxylative allylations and azidations, and exhibited a highly beneficial reactivity trend, comparable to that of the more costly gold-catalyzed protocols.[21–24] However, with a few exceptions,[25] such reactions are promoted by soluble silver salts as non-reusable catalytic sources,[26,27] typically in the presence of various ligands, which can be regarded as a considerable drawback from an environmental point of view.[28–30]

Due to economic and environmental reasons, there is a continuously growing need for heterogeneous noble metal cat-

[a]*Institute of Pharmaceutical Chemistry, University of Szeged, Eötvös u. 6, Szeged, H-6720 Hungary*
[b]*Department of Organic Chemistry, University of Szeged, Dóm tér 8, Szeged, H-6720 Hungary*
[c]*Material and Solution Structure Research Group and Interdisciplinary Excellence Centre, Institute of Chemistry, University of Szeged, Aradi Vértanúk tere 1, Szeged, H-6720 Hungary*
[d]*Department of Physical Chemistry and Materials Science, University of Szeged, Rerrich Béla tér 1, Szeged, H-6720 Hungary. E-mail: gabor.varga5@chem.u-szeged.hu*
[e]*Department of Applied and Environmental Chemistry, University of Szeged, Rerrich Béla tér 1, Szeged, H-6720 Hungary*
[f]*MTA-SZTE Reaction Kinetics and Surface Chemistry Research Group, Hungarian Academy of Sciences, Rerrich Béla tér 1, Szeged, H-6720 Hungary*
[g]*MTA-SZTE Stereochemistry Research Group, Hungarian Academy of Sciences, Eötvös u. 6, Szeged, H-6720 Hungary. E-mail: fulop@pharm.u-szeged.hu*
[h]*Institute of Chemistry, University of Graz, NAWI Graz, Heinrichstrasse 28, Graz, A-8010 Austria. E-mail: sandor.oetvoes@uni-graz.at*

† Dedicated to the memory of our friend and colleague Prof. István Pálinkó.

‡ Electronic supplementary information (ESI) available. See DOI: 10.1039/d1gc00924a

§ Deceased.

alysts.[31] However, immobilization of metal catalysts on various prefabricated supports is often accompanied by reduced selectivity or loss of activity, and in the case of inadequate catalyst-support interactions, leaching of the metal component may lead to substantial environmental concerns.[32,33] Nowadays, in organic synthesis silver catalysis is considered as a significant methodology, which is due to its wide applicability, environmentally-benign nature and its lower costs compared with other precious noble metals such as gold, platinum or palladium.[34,35] Typical synthetic applications of silver catalysis rely on Ag(I) salts or complexes as homogeneous sources for the catalytically active metal.[36–38] As concerns heterogeneous silver sources, supported nanoparticles (nanosilver) are the most widely applied.[33,39,40] Such heterogeneous materials are easily obtained *via* immobilization on various surfaces, however their main limitation is weak catalyst-support interactions which give rise to unsatisfactory stability and limits their practical synthetic utilities, especially under demanding reaction conditions, such as high-temperature continuous flow conditions or in the presence of coordinating ligands. On the basis of a naturally occurring mineral, called beyerite, we recently developed a heterogeneous silver–bismuth hybrid material (AgBi-HM) with structurally-bound silver catalytic centers.[41] The material exhibited a layered structure and contained Ag(I) and Bi(III) cationic and carbonate anionic components with silver ion as the minor cationic component. As compared with traditionally immobilized catalysts, structurally-bound catalytic centres imply increased thermodynamic stability and robustness, and exhibit an increased tolerance against challenging reaction conditions and improved compatibility with various reactants and solvents.[42]

Continuous flow reaction technology in combination with heterogeneous catalysis have attracted significant attention in recent years,[43–48] and now comprise a powerful methodology for the synthesis of an array of useful products.[49–56] Heterogeneous catalysts can easily be handled, recycled and reused in packed-bed reactors, moreover, unlike in traditional batch processes, separation from the reaction products is really straightforward.[57] Due to the enhanced control over the most important reaction conditions (*e.g.* residence time and temperature),[58–60] reaction selectivity can easily be improved while less waste is generated.[61,62] Moreover, in loaded catalyst columns, the continuous stream of reactants interacts with a superstoichiometric amount of catalyst species, which improves reaction rates significantly.[63–65] On the downside, with increasing reactor dimensions scale-up may involve difficulties, such as insufficient intraparticle heat transfer rates, intraparticle diffusion limitations as well as susceptibility to liquid maldistribution.[66] However, if catalyst deactivation and leaching can be eliminated, the scale of production becomes a direct function of the process time without modifying the reactor geometry (*i.e.* scale-out).[67–69] In spite of these obvious benefits, there are very few precedents for heterogeneous silver-catalysts being utilized in continuous flow processes,[70,71] which may be explained by the fact that stable and robust heterogeneous silver catalyst are at scarce.[41,42,72,73]

To the best of our knowledge, protodecarboxylations promoted by heterogeneous noble metal catalysts have not yet been achieved under efficient continuous flow conditions. We speculated that our silver-containing hybrid material may act as a ligand-free heterogeneous silver catalyst for protodecarboxylations, and because of its stability and robustness, not only under batch but also under more demanding flow conditions. We intended to investigate the flow reactions in a high-temperature packed-bed reactor system to exploit extended parameter spaces, and to study the possibility of chemical intensification as compared with the batch process. Considering the outstanding significance of deuterated compounds in chemistry, biochemistry, environmental sciences and also in pharmacological research,[74,75] we were intrigued to explore not only protodecarboxylations but also decarboxylative deuterations as facile and site-specific access to valuable deuterium-labelled compounds.[76,77] Our results are presented herein.

2. Experimental

2.1. General information

All chemicals used were analytical grade and were applied without further purification. Reaction products were characterized by NMR spectroscopy and mass spectrometry. ^{1}H NMR and ^{13}C NMR spectra were recorded on a Bruker Avance NEO 500 spectrometer, in $CDCl_3$ as solvent, with tetramethylsilane as internal standard at 500.1 and 125 MHz, respectively. GC-MS analyses were performed on a Thermo Scientific Trace 1310 Gas Chromatograph coupled with a Thermo Scientific ISQ QD Single Quadrupole Mass Spectrometer using a Thermo Scientific TG-SQC column (15 m × 0.25 mm ID × 0.25 μm film). Measurement parameters were as follows. Column oven temperature: from 50 to 300 °C at 15 °C min^{-1}; injection temperature: 240 °C; ion source temperature: 200 °C; electrospray ionization: 70 eV; carrier gas: He at 1.5 mL min^{-1} injection volume: 2 μL; split ratio: 1 : 33.3; and mass range: 25–500 *m*/*z*.

2.2. Synthesis and characterization of the AgBi-HM

AgBi-HM was synthesized by using the urea hydrolysis method according to a modified version of our procedure reported previously.[42] $AgNO_3$ (3.73 g) and $Bi(NO_3)_3{\cdot}5H_2O$ (5.36 g) were dissolved in 50–50 mL 5 wt% nitric acid and the solutions were combined. Urea (7.05 g) dissolved in 100 mL of deionized water was next added to the mixture which was then placed into an oven for 24 h at 105 °C. The obtained material was next filtrated, washed with aqueous thiosulfate solution, water and ethanol four times, and dried at 60 °C to obtain the final product.

The as-prepared material was fully characterized by means of diverse instrumental techniques as detailed earlier.[40,41] The X-ray diffraction (XRD) patterns were recorded on a Rigaku XRD-MiniFlex II instrument applying CuKα radiation (λ = 0.15418 nm), 40 kV accelerating voltage at 30 mA. The morphology of the as-prepared and treated samples were studied

by scanning electron microscopy (SEM). The SEM images were registered on an S-4700 scanning electron microscope (Hitachi, Japan) with accelerating voltage of 10–18 kV. The actual Ag/Bi metal ratios in the samples were determined with energy dispersive X-ray analysis (EDX) measurements (Röntec QX2 spectrometer equipped with Be window coupled to the microscope). More detailed images, both of the as-prepared and the used samples, were taken by transmission electron microscopy (TEM). For these measurements, an FEI Tecnai™ G2 20 X-Twin type instrument was applied, operating at an acceleration voltage of 200 kV. The thermal behaviour of the catalyst samples were investigated by thermogravimetry (TG) and differential thermogravimetry (DTG) using a Setaram Labsys derivatograph operating in air at 5 °C min^{-1} heating rate. For the measurements, 20–30 mg of the samples were applied. The amount of metal ions was measured by ICP–AES on a Thermo Jarell Ash ICAP 61E instrument. Before measurements, a few milligrams of the samples measured with analytical accuracy were digested in 1 mL cc. nitric acid; then, they were diluted with distilled water to 50 mL and filtered.

2.3. General procedure for the batch reactions

A typical procedure for the decarboxylation and decarboxylative deuteration reactions is as follows. *N,N*-Dimethylformamide (DMF, 3 mL), the appropriate carboxylic acid (0.45 mmol, 0.15 M, 1 equiv.), KOH (6 mg, 15 mol%) and AgBi-HM as catalyst (60 mg, corresponding to 5 mol% Ag loading) were combined in an oven-dried Schlenk tube equipped with a magnetic stir bar. In case of decarboxylative deuteration, 10 equiv. of D_2O (90 μL) was also added to the reaction mixture. After stirring for 24 h at 110 °C, the reaction mixture was cooled to room temperature, and the catalyst was filtered off. The crude products were diluted with diethyl ether and were washed with aqueous $NaHCO_3$ and brine. The combined organic layers were dried over Na_2SO_4, and concentrated under reduced pressure. The crude products were checked by NMR spectroscopy to determine conversion and selectivity. The products of the batch reactions were characterized by NMR and GC-MS techniques. In case deuterondecarboxylations, deuterium contents were determined from the relative intensities of the ^1H NMR indicator signals. Characterization data can be found in the ESI.‡

2.4. Investigation of the catalyst reusability under batch conditions

For investigation of catalyst reusability, the decarboxylation of 2-nitrobenzoic acid was carried out multiple times utilizing a single portion of catalyst. DMF (3 mL), 2-nitrobenzoic acid (0.45 mmol, 0.15 M, 1 equiv.), KOH (6 mg, 15 mol%) and AgBi-HM as catalyst (60 mg, corresponding to 5 mol% Ag loading) were combined in an oven-dried Schlenk tube equipped with a magnetic stir bar. The reaction mixture was stirred for 24 h at 110 °C. The mixture was next cooled to room temperature, and the solid material was removed by centrifugation. The liquid phase was extracted, dried and evaporated as detailed in section 2.3. The removed catalyst was washed with DMF (four times) and was dried in nitrogen flow before the next reaction cycle. Conversion and selectivity were determined after each cycle by using ^1H NMR.

2.5. General procedure for the flow reactions

To carry out the decarboxylation and decarboxylative deuteration reactions under flow conditions, a simple continuous flow set-up was assembled as shown in Fig. 1. The system consisted of an HPLC pump (JASCO PU-2085), a stainless steel HPLC column with internal dimensions of 4.6 × 100 mm as catalyst bed and a 5-bar backpressure regulator (BPR) from IDEX to prevent solvent boil over. The column encompassed 2 g of AgBi-HM as catalyst. For each reaction, the corresponding carboxylic acid (c = 0.1 M) and 15 mol% KOH were dissolved in acetonitrile (MeCN) or DMF. In order to achieve a clear solution, 20 equiv. of H_2O was also added to the reaction mixture. In case of deuterodecarboxylation reactions, 20 equiv. D_2O was added to the reaction mixture as deuterium source. In each run, 4 mL of product solution was collected under steady-state conditions. Between two experiments, the system was washed for 20 min by pumping the appropriate solvent at a flow rate of 0.5 mL min^{-1}. When DMF was used as solvent, the crude product was worked-up similarly as detailed in section 2.3. In case of MeCN as solvent, the reaction mixture was simply evaporated. Samples were checked by NMR spectroscopy to determine conversion and selectivity. For scale-out, 2-nitrobenzoic acid (c = 0.1 M) and 15 mol% KOH was dissolved in MeCN together with 20 equiv. of H_2O to achieve a clear solution. The reaction mixture was pumped continuously at 100 μL min^{-1} through the heated catalyst bed at 170 °C. The product solution was collected for 20 h under steady state conditions, and samples were taken in every hour to determine conversion and selectivity. The products of the flow reactions were characterized by NMR and GC-MS techniques. In case deuterondecarboxylations, deuterium contents were determined from the relative intensities of the ^1H NMR indicator signals. Characterization data can be found in the ESI.‡ The residence time on the catalyst bed was determined experimentally by pumping a dye solution. The elapsed time between the first

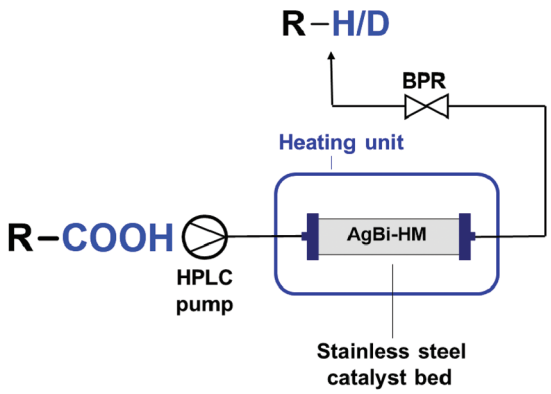

Fig. 1 Experimental setup for the continuous flow experiments.

contact of the dye with the column and the moment when the coloured solution appeared at column the outlet was measured.

3. Results and discussion

3.1. Decarboxylation of carboxylic acids under batch conditions

In order to achieve an initial picture on the catalytic activity of the silver-containing hybrid material in decarboxylation of carboxylic acids, batch reactions were explored first. The decarboxylation of 2-nitrobenzoic acid was chosen as model reaction to demonstrate the performance of the AgBi-HM in comparison with various commercially available silver and copper salts as the most typical homogeneous catalytic sources for this reaction type (Fig. 2). Based on literature data,[25,78] DMF was selected as solvent, and the reaction mixture containing the substrate (0.15 M) together with 5 mol% of the appropriate catalyst and 15 mol% of KOH as base was stirred for 24 h at 110 °C.

It was corroborated, that product formation was not occurring without any catalyst present. Gratifyingly, the application of the hybrid material as catalyst resulted quantitative and selective decarboxylation to nitrobenzene. AgOAc, Ag_2O, Ag_2CO_3 and $AgNO_3$ as catalyst gave slightly lower conversions (95–97%) and 100% selectivity in each cases. In contrast to silver catalysts, copper salts performed poorer. In the presence of CuOAc and $Cu(NO_3)_2$, conversion was 68% and 70%, respectively, whereas $CuBr_2$ was proven even less effective with a conversion of merely 39%. In all the copper-catalyzed reactions, potassium 2-nitrobenzoate appeared in the reaction mixture. Considering that the reaction is initiated by deprotonation of the carboxylic acid, the presence of the corresponding potassium salt as side product therefore indicates the incompleteness of the reaction.[25] As corroborated by a test reaction carried out in the presence of 5 mol% of $Bi(NO_3)_3{\cdot}5H_2O$, the Bi(III) component of the hybrid material is inactive in decarboxylation of 2-nitrobenzoic acid.

After achieving promising preliminary results, the effects of the major reaction conditions were next explored. Upon investigation of solvent effects (Table 1), the best results were achieved by using DMF (entry 1). MeCN and *N*,*N*-dimethylacetamide (DMA) also gave acceptable conversions (85% and 62%, respectively) and high selectivities (100% and 85%, respectively; entries 2 and 3). In EtOAc and toluene only trace amounts of nitrobenzene formation was detected (entries 4 and 5), whereas in *N*-methyl-2-pyrrolidone (NMP) and dimethyl sulfoxide (DMSO), no decarboxylation occurred (entries 6 and 7).

As concerns reaction time, 24 h was required for completion, lower reaction times gave incomplete transformations (Fig. S1‡). As was expected, decarboxylation was not taking place at temperatures ≤50 °C, however conversion started to increase at 80 °C and reached completion at 110 °C (Fig. S1‡). The reaction gave the best results with substrate concentrations of 0.1 or 0.15 M (Table S1‡) The optimum value of the catalyst loading was 5 mol% as lower amounts resulted in decrease of the conversion (Table 2, entries 1–4). Upon investigation of the effects of the amount of the extraneous KOH (Table 2, entries 5–9), it was observed that without base the reaction gives only traces of the decarboxylated product; however only catalytic amounts are required for completion (*e.g.* 100% conversion was achieved with 15 mol% KOH). This is in accordance with the mechanistic proposal of Jaenicke and co-workers suggesting a negatively charged aryl–silver intermediate upon decarboxylation which is responsible for deprotonation after the base-promoted initiation of the reaction.[25] In our study, KOH was selected as base as it involved no precipitation and ensured a pumpable clear solution when

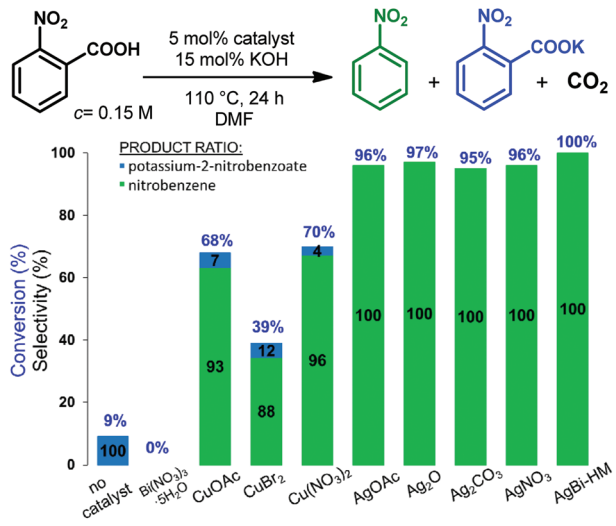

Fig. 2 Investigation of various catalysts in the decarboxylation of 2-nitrobenzoic acid.

Table 1 Investigation of various solvents in the AgBi-HM-catalyzed decarboxylation of 2-nitrobenzoic acid under batch conditions

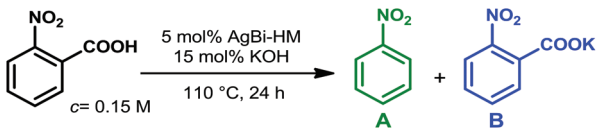

Entry	Solvent	Conversion[a] (%)	Selectivity[a] (%) A	B
1	DMF	100	100	0
2	MeCN	85	100	0
3	DMA	62	85	15
4	EtOAc	11	100	0
5	Toluene	3	100	0
6	NMP	7	0	100
7	DMSO	8	0	100

[a] Determined by ^{1}H NMR analysis of the crude product.

Table 2 Investigation of the effects various catalyst and base amounts in the AgBi-HM-catalyzed decarboxylation of 2-nitrobenzoic acid under batch conditions

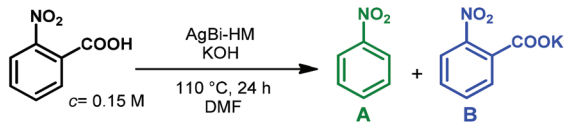

Entry	Catalyst (mol%)	KOH (mol%)	Conv.[a] (%)	Selectivity[a] (%) A	B
1	1	15	25	100	0
2	3	15	69	93	7
3	5	15	100	100	0
4	10	15	100	100	0
5	5	—	8	100	0
6	5	5	80	100	0
7	5	10	85	100	0
8	5	15	100	100	0
9	5	20	100	100	0

[a] Determined by ^{1}H NMR analysis of the crude product.

being combined with the substrate which is crucial when considering the upcoming continuous flow experiments.

Having established an optimal set of conditions for the decarboxylation of the model compound (5 mol% catalyst loading, 15 mol% KOH as base, DMF as solvent, 0.15 M substrate concentration, 110 °C temperature and 24 h reaction time), we set out to investigate the scope and applicability of the batch process (Table 3). Besides 2-nitrobenzoic acid (entry 1), its 5-methoxy-substituted derivative as well as 3,5-dinitrobenzoic acid underwent quantitative and selective protodecarboxylations (entries 2 and 3). The reaction tolerated well the replacement of the *ortho*-nitro substituent with bromine or methoxy groups, and gave good conversions (80% and 74%, respectively) and 100% selectivities in reactions of the corresponding benzoic acid derivatives (entries 4 and 5). Despite the higher steric hindrance, decarboxylation of 2,6-dimethoxybenzoic acid was also successful, although conversion was somewhat lower (65%) than in the case of the mono-substituted derivative (entry 6 *vs.* entry 5). Interestingly, decarboxylation of 2-chlorobenzoic acid and 2-hydroxybenzoic acid (salicylic acid) were not successful (entries 7 and 8), however 2,4-dichlorobenzoic acid proved as an excellent substrate and gave the corresponding dichlorobenzene with 92% conversion and 100% selectivity (entry 9). Selective decarboxylation of 1-naphtolic acid to naphthalene was also possible, however only with a moderate conversion of 49% (entry 10). To our delight, selective decarboxylation of heteroaromatic carboxylic acids, such as thiophene-2-carboxylic acid and nicotinic acid, proceeded with excellent conversions (100% and 86%, respectively; entries 11 and 12). Similarly high conversions (97–100%) and selectivities were achieved in decarboxylations of fused heteroaromatic substrates, such as indole-3-carboxylic acid, coumarin-3-carboxylic acid and chromone-3-carboxylic (entries 13–15). Decarboxylations of *metha*- and *para*-monosubstituted

Table 3 Exploring the AgBi-HM-catalyzed decarboxylation of various aromatic carboxylic acids under batch conditions

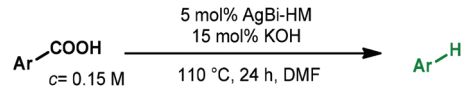

Entry	Substrate	Conversion[a,b] (%)	Selectivity[a] (%)
1	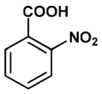	100 (98)	100
2	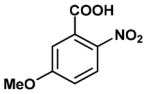	100	100
3	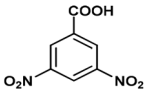	100 (97)	100
4		80	100
5	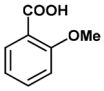	74	100
6	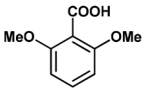	65	100
7		Traces	—
8		Traces	—
9	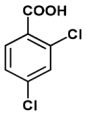	92	100
10	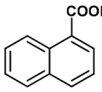	49	100
11	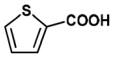	100	100
12	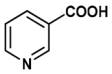	86	100
13	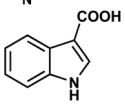	100 (97)	100
14	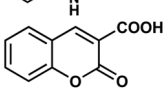	100	100
15	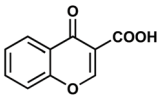	97	100

[a] Determined by ^{1}H NMR analysis of the crude product. [b] For representative examples, isolated yields are shown in parentheses.

benzoic acid derivates, such as 3- and 4-nitrobenzoic acid, were also attempted, however in these cases no reaction occurred. These results are in accordance with earlier literature

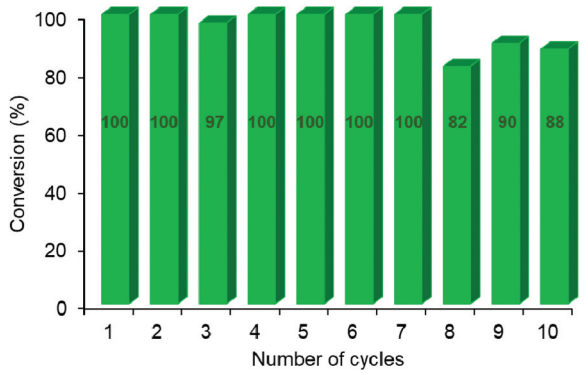

Fig. 3 Testing the reusability of the AgBi-HM catalyst in the decarboxylation of 2-nitrobenzoic acid. Selectivity was 100% in all reactions. (Reaction conditions: 0.15 M substrate concentration, 5 mol% catalyst, 15 mol% of KOH as base, DMF as solvent, 110 °C, 24 h reaction time.).

findings suggesting the formation of a metal-centered carboxylate intermediate which is stabilized by the electronic effects of the substituent(s) on the aromatic rings.[79,80] Moreover, decarboxylation of aliphatic carboxylic acids, such as hexanoic acid and levulinic acid, was proven unsuccessful using this methodology. Note that isolated yield was determined in some representative instances.

One of the main benefits of heterogeneous catalysis is the ability to reuse and recycle the catalytic material. In order to evaluate this sustainable feature of the AgBi-HM, protodecarboxylation of 2-nitrobenzoic acid was performed repeatedly under optimized conditions utilizing the same portion of catalyst for each reactions. The used hybrid material was removed between each cycle by centrifugation and after washing and drying, it was simply reused. Gratifyingly, no decrease in catalytic activity or selectivity occurred during the first 7 consecutive catalytic cycles, and conversion was around 90% even after the 10th reaction which implies the significant stability and robustness of the catalytic material (Fig. 3).

3.2. Decarboxylation of carboxylic acids under continuous flow conditions

After achieving convincing batch results, we next turned our attention to continuous flow operation with the aim to improve the efficacy and sustainability of the catalytic process. As detailed in the Experimental, AgBi-HM was employed in a simple packed-bed reactor setup (see also Fig. 1). Similarly as in the batch study, the effects of the reaction conditions were investigated again using the decarboxylation of 2-nitrobenzoic acid as a model reaction. The effects of solvents which gave good results in the batch reactions were explored again under flow conditions. For this, the catalyst bed was heated to 170 °C, and the solution of the substrate together with 15mol% KOH was pumped continuously at 50 μL min^{-1} flow rate. Gratifyingly, under these conditions, MeCN performed superior compared to DMF and DMA, and resulted selective decarboxylation with conversions of 100% and 96% at 0.1 M and 0.15 M substrate concentrations, respectively (Table 4). This is a remarkable improvement considering that MeCN is much more acceptable from environmental aspects than DMF which performed best under batch conditions (Table 1, entry 1).[81]

Table 4 Investigation of various solvents in the AgBi-HM-catalyzed decarboxylation of 2-nitrobenzoic acid under flow conditions

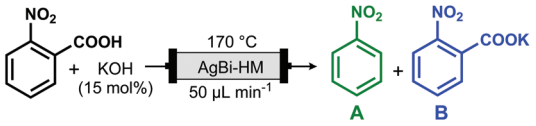

Entry	Solvent	c (M)	Conversion[a] (%)	Selectivity[a] (%) A	B
1	DMA	0.1	81	100	0
2	DMF	0.1	90	89	11
3	MeCN	0.1	100	100	0
4	MeCN	0.15	96	100	0

[a] Determined by ^{1}H NMR analysis of the crude product.

Upon investigation of the effects of the residence time and reaction temperature, it was verified that a significant chemical intensification is possible under flow conditions. Due to the backpressure applied, it was possible to easily overheat the reaction mixture and to study the effects of temperatures far above the boiling point of MeCN. As shown in Fig. 4, quantitat-

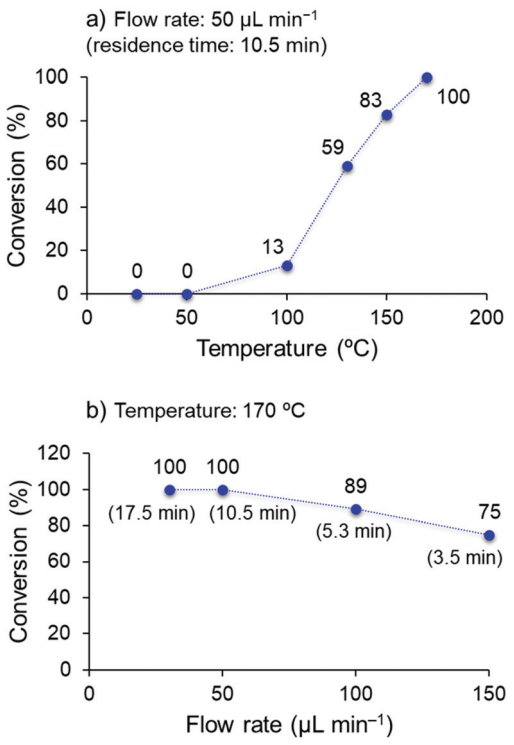

Fig. 4 Investigation of the effects of the reaction temperature (a) and residence time (b) in the AgBi-HM-catalyzed decarboxylation of 2-nitrobenzoic acid in a continuous flow reactor. (Reaction conditions: 0.1 M substrate concentration, 15 mol% of KOH as base, MeCN as solvent.).

ive and selective decarboxylation could be achieved at 170 °C while the reaction mixture (containing the substrate in 0.1 M concentration together with 15 mol% KOH) was streamed at 50 μL min^{-1} flow rate. Notably, this corresponded to a residence time of only 10.5 min which is a significant improvement compared to the batch reaction time of 24 h. When residence time was decreased to approximately 3.5 min (150 μL min^{-1} flow rate), the conversion of the decarboxylation was still 75% at 170 °C. When residence time was kept constant at 10.5 min, a rapid decrease of conversion was observed with the temperature; for example at 100 °C conversion was only 13%.

A range of aromatic carboxylic acids exhibiting diverse substitution patterns were next submitted to the optimized flow conditions (Table 5). Similarly as in the batch reactions, quantitative and selective decarboxylation was achieved in cases of 2-nitrobenzoic acid, its 5-methoxy-substituted derivative as well as 3,5-dinitrobenzoic acid (entries 1–3). To our delight, the flow protocol proved more effective in numerous reactions than the batch method. For example, 2-bromo-, 2-methoxy- as well as 2,6-dimethoxybenzoic acid furnished quantitative conversions (entries 4–6), whereas in batch, conversions were much lower. Notably, selective decarboxylations of 2-chloro- and 2-hydroxybenzoic acid were achieved successfully under flow conditions (conversions were 100% and 23%, respectively; entries 7 and 8), whereas these substrates remained inert under batch conditions. 2,4-Dichlorobenzoic acid and 1-naphtolic acid were also successfully decarboxylated and gave similar conversions than in the corresponding batch reactions (entries 9 and 10). Fused heteroaromatic substrates showed excellent reactivity, and gave quantitative conversion and 100% selectivity, similarly as under batch conditions (entries 11–13). Unfortunately, flow reactions of thiophene-2-carboxylic acid and nicotinic acid could not be evaluated due to possible deposition of the substrates and/or the products within the catalyst column. (Isolated yield was also determined for some representative examples.)

In order to investigate the preparative capabilities of the AgBi-HM catalyzed protodecarboxylation under flow conditions, the reaction of 2-nitrobenzoic acid was scaled-out (Fig. 5). With the aim to maximize the productivity of the synthesis, the flow rate was increased to 100 μL min^{-1} (approx. 5 min residence time), all further reaction parameters were kept at the previously optimized values (0.1 M substrate concentration, 15 mol% of KOH as base, MeCN as solvent, 170 °C temperature). A 20 h reaction window was explored, with conversion and selectivity being determined in every hour to obtain a clear view of the actual catalyst activity. Gratifyingly, the packed-bed system proved highly stable. No decrease in activity or selectivity occurred in the first 18 h of the experiment: conversion remained steady around 80–85% and no side product formation occurred. In the last two hours, a slight loss of catalytic activity was detected, however after 20 h, at the end of the experiment, a satisfying conversion of 71% could still be achieved. Finally, as the result of the scale-out, 1.207 g of nitrobenzene was isolated which corresponded to an overall yield of 82%.

Table 5 Exploring the AgBi-HM-catalyzed decarboxylation of various aromatic carboxylic acids under continuous flow conditions

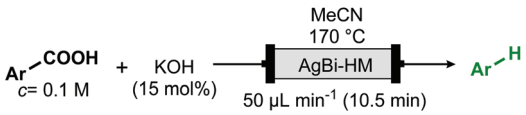

Entry	Substrate	Conversion[a,b] (%)	Selectivity[a] (%)
1	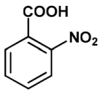	100 (99)	100
2	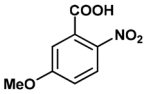	100	100
3	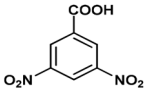	100	100
4	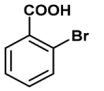	100 (98)	100
5[c]	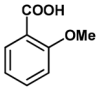	100	100
6	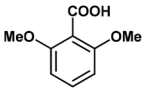	100	100
7	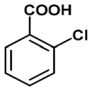	100	100
8	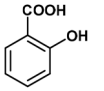	23	100
9[c]	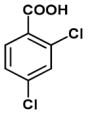	87	100
10	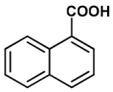	48	100
11[c]	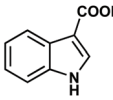	100	100
12[c]	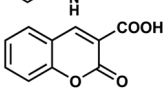	100	100
13[c]	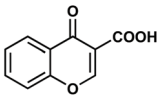	100 (97)	100

[a] Determined by ^{1}H NMR analysis of the crude product. [b] For representative examples, isolated yields are shown in parentheses. [c] DMF was used as solvent due to solubility issues.

3.3. Characterization of used AgBi-HM samples

With the aim to evaluate catalyst stability and robustness, AgBi-HM samples previously used in batch recycling experiments as well as in flow scale-out were examined extensively by various instrumental techniques. The materials were character-

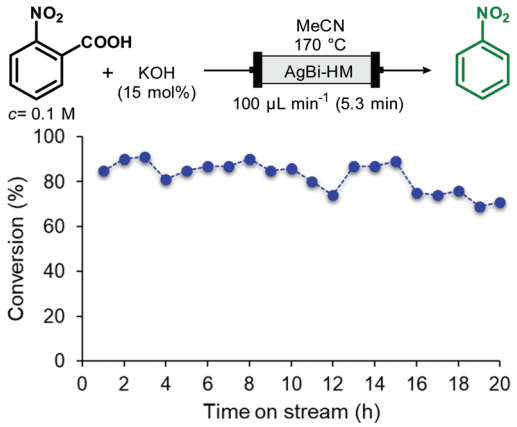

Fig. 5 Scaling-out of the AgBi-HM-catalyzed decarboxylation of 2-nitrobenzoic acid in a continuous flow reactor. (Selectivity of the reaction was 100% in all points investigated.).

ized by TG, SEM (SEM-EDX), TEM and XRD measurements, and the structure of the used catalyst samples was compared to that of the as-prepared material (Fig. 6).

Thermal analysis revealed that the original structure was kept up to 380 °C, and weight losses occurred in three endothermic steps which was also observed in both used catalyst samples (Fig. 6a). In the case of the AgBi-HM sample used in the batch recycling experiment, slightly greater weight loss could be observed at lower temperatures which may be explained by trace amounts of organic deposition on the surface. The X-ray patterns of both used samples seemed to be the same as was experienced in case of the as-prepared sample

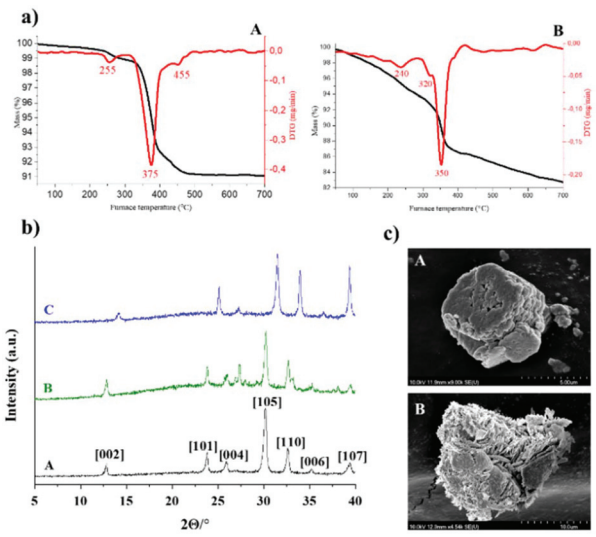

Fig. 6 (a) Thermal behaviour of used AgBi-HM samples: sample used in flow scale-out (A), sample used in batch recycling experiment (B). (b) Comparison of the X-ray patterns of various AgBi-HM samples: as-prepared sample (A), sample used in batch recycling experiments (B), sample used in flow scale-out (C). (c) SEM images: as-prepared AgBi-HM sample – micrograph taken from ref. 41 (A), AgBi-HM sample used in flow scale-out (B).

(Fig. 6b), there was no evidence of structural degradation visible. Identification of the X-ray patterns were accomplished on the basis of our previous work.[42] These results provided some further information about primer crystallite size of the composite calculated by using the well-known Scherrer equation. This resulted in an average primer crystallite size of 20.98 nm, not only for the as-prepared catalyst but also for the used ones. As shown earlier,[41] the SEM image of the freshly-made catalyst displayed a lamellar (plate-like) morphology which was also observed in the used material (Fig. 6c). Additionally, this observation was also strengthened by TEM images, in which well-aggregated plates with a secondary particle size of around 100 nm could be seen for the as-prepared as well as for the used catalyst sample (Fig. S2‡). The SEM images also confirmed that organic contaminants in the form of larger aggregates (up to 10 µm) remained on the surface which makes more difficult to identify the original morphology. The SEM-EDX elemental maps demonstrated that the silver and bismuth ions are located evenly in the used sample as well (Fig. S3‡). ICP-AES measurements confirmed that the quantity of silver and bismuth ions are in arrangement with the as-prepared sample considering errors of measurements.[41]

Taking into account all the characterization data, it can be ascertained that the AgBi-HM is a highly robust heterogeneous catalyst which proved to be invariable in a structural point of view after extensive and demanding use under batch or flow conditions.

3.4. Decarboxylative deuterations

Due to its relatively good availability and also because of the considerably large isotope effect, deuterium is of outstanding importance among stable isotopes used for labelling studies.[82,83] Synthetic protocols that incorporate deuterium into various organic substances have therefore many applications in medicinal, analytical or pharmaceutical chemistry.[74] Deuterium-labelled compounds are typically applied as analytical standards, for the evaluation of the metabolic pathways or in tracer studies to investigate pharmacokinetics, catalytic cycles and reaction pathways.[84–86] As exemplified by Austedo®, the first deuterated drug marketed, pharmaceutical ingredients may also be potentiated by deuterium exchange.[87,88] In contrast to deuterations of C–C or C–X (X = hetero atom) multiple bonds,[89–93] synthetic processes for the site-specific incorporation of a single deuterium into an aromatic ring are more challenging.[74,76,77,94,95] In most cases, these methods involve halogen/D exchange and are commonly mediated by strong bases which severely limits the functional group tolerance.[96] Furthermore, catalytic and acid- or base-mediated H/D exchange reactions are also available, however, unlike halogen/D exchange reactions, these often involve selectivity issues.[97–99]

Inspired by these limitations, we were intrigued to explore decarboxylative deuterations of benzoic acid derivatives in the presence of the silver-containing hybrid material as catalyst. Initially, reactions were investigated in batch (Table 6), under

Table 6 Exploring AgBi-HM-catalyzed decarboxylative deuterations under batch conditions

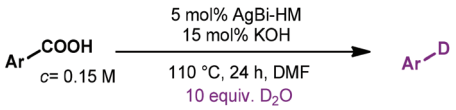

Entry	Product	Conv.[a] (%)	Selectivity[a] (%)	$D^{a,b}$ (%)
1		100	100	98
2	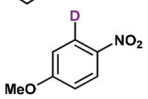	100	100	86
3	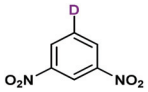	100	100	100
4	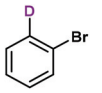	88	100	100
5	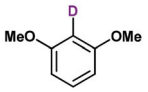	79	100	76
6	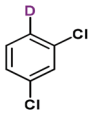	100	100	100

[a] Determined by ^{1}H NMR analysis of the crude product. [b] Deuterium content (represent deuterium incorporation rate over incidental hydrogen incorporation).

Table 7 Exploring AgBi-HM-catalyzed decarboxylative deuterations under continuous flow conditions

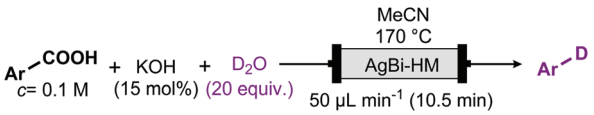

Entry	Product	Conv.[a] (%)	Selectivity[a] (%)	$D^{a,b}$ (%)
1[c]		100	100	31
2		100	100	100
3	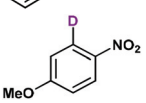	100	100	71
4	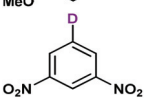	100	100	100
5	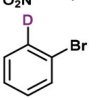	100	100	100
6	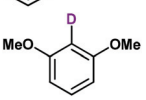	100	100	100

[a] Determined by ^{1}H NMR analysis of the crude product. [b] Deuterium content (represent deuterium incorporation rate over incidental hydrogen incorporation). [c] 10 equiv. of D_2O was used as deuterium source.

conditions optimized for the protodecarboxylations earlier (0.15 M substrate concentration, 5 mol% AgBi-HM as catalyst, 15 mol% of KOH as base, DMF as solvent, 110 °C temperature and 24 h reaction time). As deuterium source, 10 equiv. of D_2O was added to the reaction mixture. We were satisfied to find that with this simple protocol, deuterodecarboxylations of various nitrobenzoic acids as well as 2-bromo-, 2,6-dimethoxy- and 2,4-dichlorobenzoic acid went smoothly. Excellent conversions (79–100%) and 100% chemoselectivity were achieved in all cases. In all reactions, deuteration was highly favoured over incidental hydrogen incorporation as indicated by deuterium contents of 76–100%.

Continuous flow deuterodecarboxylations were next attempted in a packed bed reactor charged with AgBi-HM. Reaction conditions were simply taken from the protodecarboxylation experiments (0.1 M substrate concentration, 15 mol% of KOH as base, MeCN as solvent, 170 °C temperature, 50 µL min^{-1} flow rate, 10.5 min residence time). In these cases, 20 equiv. of D_2O was used as deuterium source to achieve high deuterium contents. Gratifyingly, in all reactions investigated (Table 7), quantitative conversion and 100% chemoselectivity was achieved, and deuterium incorporation was also perfect in most cases.

4. Conclusion

A silver-containing hybrid material with structurally-bound catalytic centers has been exploited as heterogenous noble metal catalyst for decarboxylations of carboxylic acids under batch and continuous flow conditions. It proved to be a robust, efficiently recyclable and highly active ligand-free catalyst which outperformed the most typical homogeneous catalytic sources in the decarboxylation of 2-nitrobenzoic acid as model reaction. Although, under batch conditions the catalyst performed best in DMF as solvent, the application of a simple packed-bed flow system enabled a solvent switch to the environmentally more acceptable MeCN. After the optimization of the most important reaction conditions, the selective decarboxylation of diversely substituted aromatic carboxylic acids were achieved with high conversions either in batch or in continuous flow mode. Importantly, the application of continuous flow conditions offered a marked chemical intensification as compared with the batch reactions (10 min residence time *vs.* 24 h reaction time) and ensured time-efficient syntheses. The preparative utility of the flow process was verified by a 20 h scale-out run in which the multigram-scale decarboxylation of 2-nitrobenzoic acid was achieved without notable decrease in the activity and without detectable degradation of the structure of catalyst. On the basis of the reaction conditions established for the protodecarboxylations, heterogeneous catalytic batch as well as flow methodologies were developed for decarboxylative

deuterations in the presence of D_2O as a readily available deuterium source.

Conflicts of interest

There are no conflicts to declare.

Acknowledgements

This research was funded by the Hungarian Ministry of National Economy, National Research Development and Innovation Office (GINOP2.3.2-15-2016-00034) and by TKP-2020. We are grateful to the Hungarian Research Foundation (OTKA No. K115731). R. M. was supported by the ÚNKP-19-3 New National Excellence Program of the Ministry for Innovation and Technology (Hungary). S. B. Ö. acknowledges the Premium Post Doctorate Research Program of the Hungarian Academy of Sciences. G. V. thanks for the postdoctoral fellowship under the grant number PD 128189.

References

1 L. J. Gooßen, N. Rodríguez and K. Gooßen, *Angew. Chem., Int. Ed.*, 2008, **47**, 3100–3120.
2 T. Patra and D. Maiti, *Chem. – Eur. J.*, 2017, **23**, 7382–7401.
3 C. Shen, P. Zhang, Q. Sun, S. Bai, T. S. A. Hor and X. Liu, *Chem. Soc. Rev.*, 2015, **44**, 291–314.
4 S. Cadot, N. Rameau, S. Mangematin, C. Pinel and L. Djakovitch, *Green Chem.*, 2014, **16**, 3089–3097.
5 J. S. Dickstein, J. M. Curto, O. Gutierrez, C. A. Mulrooney and M. C. Kozlowski, *J. Org. Chem.*, 2013, **78**, 4744–4761.
6 S. Seo, J. B. Taylor and M. F. Greaney, *Chem. Commun.*, 2012, **48**, 8270–8272.
7 Z. Li, Z. Fu, H. Zhang, J. Long, Y. Song and H. Cai, *New J. Chem.*, 2016, **40**, 3014–3018.
8 M. T. Keßler, C. Gedig, S. Sahler, P. Wand, S. Robke and M. H. G. Prechtl, *Catal. Sci. Technol.*, 2013, **3**, 992–1001.
9 L. J. Gooßen, W. R. Thiel, N. Rodríguez, C. Linder and B. Melzer, *Adv. Synth. Catal.*, 2007, **349**, 2241–2246.
10 N. Chatani, H. Tatamidani, Y. Ie, F. Kakiuchi and S. Murai, *J. Am. Chem. Soc.*, 2001, **123**, 4849–4850.
11 S. Pan, B. Zhou, Y. Zhang, C. Shao and G. Shi, *Synlett*, 2016, **27**, 277–281.
12 M. H. Al-Huniti, M. A. Perez, M. K. Garr and M. P. Croatt, *Org. Lett.*, 2018, **20**, 7375–7379.
13 R. A. Daley and J. J. Topczewski, *Synthesis*, 2020, 365–377.
14 G. J. S. Dawes, E. L. Scott, J. Le Nôtre, J. P. M. Sanders and J. H. Bitter, *Green Chem.*, 2015, **17**, 3231–3250.
15 A. Bohre, U. Novak, M. Grilc and B. Likozar, *Mol. Catal.*, 2019, **476**, 110520.
16 A. Bohre, B. Hočevar, M. Grilc and B. Likozar, *Appl. Catal., B*, 2019, **256**, 117889.
17 A. Bohre, K. Avasthi, U. Novak and B. Likozar, *ACS Sustainable Chem. Eng.*, 2021, **9**, 2902–2911.
18 H. Hikawa, F. Kotaki, S. Kikkawa and I. Azumaya, *J. Org. Chem.*, 2019, **84**, 1972–1979.
19 S. Dupuy, L. Crawford, M. Bühl and S. P. Nolan, *Chem. – Eur. J.*, 2015, **21**, 3399–3408.
20 S. Dupuy and S. P. Nolan, *Chem. – Eur. J.*, 2013, **19**, 14034–14038.
21 R. A. Crovak and J. M. Hoover, *J. Am. Chem. Soc.*, 2018, **140**, 2434–2437.
22 R. Grainger, J. Cornella, D. C. Blakemore, I. Larrosa and J. M. Campanera, *Chem. – Eur. J.*, 2014, **20**, 16680–16687.
23 L. Cui, H. Chen, C. Liu and C. Li, *Org. Lett.*, 2016, **18**, 2188–2191.
24 Y. Zhu, X. Li, X. Wang, X. Huang, T. Shen, Y. Zhang, X. Sun, M. Zou, S. Song and N. Jiao, *Org. Lett.*, 2015, **17**, 4702–4705.
25 X. Y. Toy, I. I. B. Roslan, G. K. Chuah and S. Jaenicke, *Catal. Sci. Technol.*, 2014, **4**, 516–523.
26 L. J. Gooßen, C. Linder, N. Rodríguez, P. P. Lange and A. Fromm, *Chem. Commun.*, 2009, 7173–7175.
27 P. Lu, C. Sanchez, J. Cornella and I. Larrosa, *Org. Lett.*, 2009, **11**, 5710–5713.
28 R. A. Sheldon, *Green Chem.*, 2017, **19**, 18–43.
29 M. C. Bryan, P. J. Dunn, D. Entwistle, F. Gallou, S. G. Koenig, J. D. Hayler, M. R. Hickey, S. Hughes, M. E. Kopach, G. Moine, P. Richardson, F. Roschangar, A. Steven and F. J. Weiberth, *Green Chem.*, 2018, **20**, 5082–5103.
30 H. C. Erythropel, J. B. Zimmerman, T. M. de Winter, L. Petitjean, F. Melnikov, C. H. Lam, A. W. Lounsbury, K. E. Mellor, N. Z. Janković, Q. Tu, L. N. Pincus, M. M. Falinski, W. Shi, P. Coish, D. L. Plata and P. T. Anastas, *Green Chem.*, 2018, **20**, 1929–1961.
31 C. Wen, A. Yin and W.-L. Dai, *Appl. Catal., B*, 2014, **160–161**, 730–741.
32 A. K. Clarke, M. J. James, P. O'Brien, R. J. K. Taylor and W. P. Unsworth, *Angew. Chem., Int. Ed.*, 2016, **55**, 13798–13802.
33 X.-Y. Dong, Z.-W. Gao, K.-F. Yang, W.-Q. Zhang and L.-W. Xu, *Catal. Sci. Technol.*, 2015, **5**, 2554–2574.
34 C.-J. Li and X. Bi, *Silver catalysis in organic synthesis*, Wiley-VCH, Weinheim, 2019.
35 Q.-Z. Zheng and N. Jiao, *Chem. Soc. Rev.*, 2016, **45**, 4590–4627.
36 L. Maestre, R. Dorel, Ó. Pablo, I. Escofet, W. M. C. Sameera, E. Álvarez, F. Maseras, M. M. Díaz-Requejo, A. M. Echavarren and P. J. Pérez, *J. Am. Chem. Soc.*, 2017, **139**, 2216–2223.
37 J. Ozawa and M. Kanai, *Org. Lett.*, 2017, **19**, 1430–1433.
38 S. Guo, F. Cong, R. Guo, L. Wang and P. Tang, *Nat. Chem.*, 2017, **9**, 546–551.
39 N. Salam, A. Sinha, A. S. Roy, P. Mondal, N. R. Jana and S. M. Islam, *RSC Adv.*, 2014, **4**, 10001–10012.
40 J. D. Kim, T. Palani, M. R. Kumar, S. Lee and H. C. Choi, *J. Mater. Chem.*, 2012, **22**, 20665–20670.
41 S. B. Ötvös, R. Mészáros, G. Varga, M. Kocsis, Z. Kónya, Á. Kukovecz, P. Pusztai, P. Sipos, I. Pálinkó and F. Fülöp, *Green Chem.*, 2018, **20**, 1007–1019.

42 R. Mészáros, S. B. Ötvös, G. Varga, É. Böszörményi, M. Kocsis, K. Karádi, Z. Kónya, Á. Kukovecz, I. Pálinkó and F. Fülöp, *Mol. Catal.*, 2020, **498**, 111263.
43 A. Tanimu, S. Jaenicke and K. Alhooshani, *Chem. Eng. J.*, 2017, **327**, 792–821.
44 R. Ciriminna, M. Pagliaro and R. Luque, *Green Energy Environ.*, 2021, DOI: 10.1016/j.gee.2020.09.013, (In Press).
45 X. Liu, B. Unal and K. F. Jensen, *Catal. Sci. Technol.*, 2012, **2**, 2134–2138.
46 C. G. Frost and L. Mutton, *Green Chem.*, 2010, **12**, 1687–1703.
47 R. Munirathinam, J. Huskens and W. Verboom, *Adv. Synth. Catal.*, 2015, **357**, 1093–1123.
48 W.-J. Yoo, H. Ishitani, Y. Saito, B. Laroche and S. Kobayashi, *J. Org. Chem.*, 2020, **85**, 5132–5145.
49 R. Gérardy, N. Emmanuel, T. Toupy, V.-E. Kassin, N. N. Tshibalonza, M. Schmitz and J.-C. M. Monbaliu, *Eur. J. Org. Chem.*, 2018, 2301–2351.
50 R. Porta, M. Benaglia and A. Puglisi, *Org. Process Res. Dev.*, 2016, **20**, 2–25.
51 B. Gutmann, D. Cantillo and C. O. Kappe, *Angew. Chem., Int. Ed.*, 2015, **54**, 6688–6728.
52 M. Baumann and I. R. Baxendale, *Beilstein J. Org. Chem.*, 2015, **11**, 1194–1219.
53 S. B. Ötvös and F. Fülöp, *Catal. Sci. Technol.*, 2015, **5**, 4926–4941.
54 A. Hommes, H. J. Heeres and J. Yue, *ChemCatChem*, 2019, **11**, 4671–4708.
55 R. Gérardy, D. P. Debecker, J. Estager, P. Luis and J.-C. M. Monbaliu, *Chem. Rev.*, 2020, **120**, 7219–7347.
56 D. L. Riley and N. C. Neyt, *Synthesis*, 2018, 2707–2720.
57 K. Masuda, T. Ichitsuka, N. Koumura, K. Sato and S. Kobayashi, *Tetrahedron*, 2018, **74**, 1705–1730.
58 Á. Georgiádes, S. B. Ötvös and F. Fülöp, *Adv. Synth. Catal.*, 2018, **360**, 1841–1849.
59 I. M. Mándity, S. B. Ötvös and F. Fülöp, *ChemistryOpen*, 2015, **4**, 212–223.
60 M. B. Plutschack, B. Pieber, K. Gilmore and P. H. Seeberger, *Chem. Rev.*, 2017, **117**, 11796–11893.
61 F. M. Akwi and P. Watts, *Chem. Commun.*, 2018, **54**, 13894–13928.
62 L. Rogers and K. F. Jensen, *Green Chem.*, 2019, **21**, 3481–3498.
63 A. Puglisi, M. Benaglia and V. Chiroli, *Green Chem.*, 2013, **15**, 1790–1813.
64 C. Rodríguez-Escrich and M. A. Pericàs, *Eur. J. Org. Chem.*, 2015, 1173–1188.
65 T. Tsubogo, T. Ishiwata and S. Kobayashi, *Angew. Chem., Int. Ed.*, 2013, **52**, 6590–6604.
66 V. V. Ranade, R. Chaudhari and P. R. Gunjal, *Trickle bed reactors: Reactor engineering and applications*, Elsevier, Amsterdam, 2011.
67 S. B. Ötvös, M. A. Pericàs and C. O. Kappe, *Chem. Sci.*, 2019, **10**, 11141–11146.
68 S. B. Ötvös, P. Llanes, M. A. Pericàs and C. O. Kappe, *Org. Lett.*, 2020, **22**, 8122–8126.
69 C. De Risi, O. Bortolini, A. Brandolese, G. Di Carmine, D. Ragno and A. Massi, *React. Chem. Eng.*, 2020, **5**, 1017–1052.
70 R. L. Papurello, J. L. Fernández, E. E. Miró and J. M. Zamaro, *Chem. Eng. J.*, 2017, **313**, 1468–1476.
71 L. Zhang, Z. Liu, Y. Wang, R. Xie, X.-J. Ju, W. Wang, L.-G. Lin and L.-Y. Chu, *Chem. Eng. J.*, 2017, **309**, 691–699.
72 J. Cao, G. Xu, P. Li, M. Tao and W. Zhang, *ACS Sustainable Chem. Eng.*, 2017, **5**, 3438–3447.
73 M. Jeganathan, A. Dhakshinamoorthy and K. Pitchumani, *ACS Sustainable Chem. Eng.*, 2014, **2**, 781–787.
74 J. Atzrodt, V. Derdau, W. J. Kerr and M. Reid, *Angew. Chem., Int. Ed.*, 2018, **57**, 1758–1784.
75 S. L. Harbeson and R. D. Tung, *Med. Chem. News*, 2014, **24**, 8–22.
76 R. Grainger, A. Nikmal, J. Cornella and I. Larrosa, *Org. Biomol. Chem.*, 2012, **10**, 3172–3174.
77 M. Rudzki, A. Alcalde-Aragonés, W. I. Dzik, N. Rodríguez and L. J. Gooßen, *Synthesis*, 2012, 184–193.
78 S. Bhadra, W. I. Dzik and L. J. Gooßen, *Angew. Chem., Int. Ed.*, 2013, **52**, 2959–2962.
79 L. J. Gooßen, N. Rodríguez, C. Linder, P. P. Lange and A. Fromm, *ChemCatChem*, 2010, **2**, 430–442.
80 J. Cornella, C. Sanchez, D. Banawa and I. Larrosa, *Chem. Commun.*, 2009, 7176–7178.
81 D. Prat, A. Wells, J. Hayler, H. Sneddon, C. R. McElroy, S. Abou-Shehada and P. J. Dunn, *Green Chem.*, 2016, **18**, 288–296.
82 A. J. Percy, M. Rey, K. M. Burns and D. C. Schriemer, *Anal. Chim. Acta*, 2012, **721**, 7–21.
83 K. Gevaert, F. Impens, B. Ghesquière, P. Van Damme, A. Lambrechts and J. Vandekerckhove, *Proteomics*, 2008, **8**, 4873–4885.
84 H. Wang, A. A. Hussain, J. S. Pyrek, J. Goodman and P. J. Wedlund, *J. Pharm. Biomed. Anal.*, 2004, **34**, 1063–1070.
85 K. Sanderson, *Nature*, 2009, **458**, 269.
86 D. M. Marcus, K. A. McLachlan, M. A. Wildman, J. O. Ehresmann, P. W. Kletnieks and J. F. Haw, *Angew. Chem., Int. Ed.*, 2006, **45**, 3133–3136.
87 P. Chen, S. Ren, H. Song, C. Chen, F. Chen, Q. Xu, Y. Kong and H. Sun, *Bioorg. Med. Chem.*, 2019, **27**, 116–124.
88 C. Schmidt, *Nat. Biotechnol.*, 2017, **35**, 493–494.
89 B. Dong, X. Cong and N. Hao, *RSC Adv.*, 2020, **10**, 25475–25479.
90 M. Espinal-Viguri, S. E. Neale, N. T. Coles, S. A. Macgregor and R. L. Webster, *J. Am. Chem. Soc.*, 2019, **141**, 572–582.
91 R. Mészáros, B.-J. Peng, S. B. Ötvös, S.-C. Yang and F. Fülöp, *ChemPlusChem*, 2019, **84**, 1508–1511.
92 S. B. Ötvös, C.-T. Hsieh, Y.-C. Wu, J.-H. Li, F.-R. Chang and F. Fülöp, *Molecules*, 2016, **21**(318), 1–11.
93 C.-T. Hsieh, S. B. Ötvös, Y.-C. Wu, I. M. Mándity, F.-R. Chang and F. Fülöp, *ChemPlusChem*, 2015, **80**, 859–864.
94 A. Tlahuext-Aca and J. F. Hartwig, *ACS Catal.*, 2021, **11**, 1119–1127.
95 G. Orsy, F. Fülöp and I. M. Mándity, *Green Chem.*, 2019, **21**, 956–961.

96 J. Atzrodt, V. Derdau, T. Fey and J. Zimmermann, *Angew. Chem., Int. Ed.*, 2007, **46**, 7744–7765.
97 G. Erdogan and D. B. Grotjahn, *J. Am. Chem. Soc.*, 2009, **131**, 10354–10355.
98 G. S. Coumbarides, M. Dingjan, J. Eames, A. Flinn and J. Northen, *J. Labelled Compd. Radiopharm.*, 2006, **49**, 903–914.
99 P. S. Kiuru and K. Wähälä, *Steroids*, 2006, **71**, 54–60.